

Effects of Nanoparticle Interfacial Additives on Phase Inversion of Pickering Emulsions

by

Sileola Ogunlaja

A thesis
presented to the University of Waterloo
in fulfillment of the
thesis requirement for the degree of
Doctor of Philosophy
in
Chemical Engineering

Waterloo, Ontario, Canada, 2020

©Sileola Ogunlaja 2020

Author's Declaration

This thesis consists of material all of which I authored or co-authored: see Statement of Contributions included in the thesis. This is a true copy of the thesis, including any required final revisions, as accepted by my examiners.

I understand that my thesis may be made electronically available to the public.

A Statement of Contributions

A portion of the work presented in Chapter 4 has been published in the Canadian Journal of Chemical Engineering 2018 (volume 96, 1089) and Chapter 5 has been published in the Colloids and Interfaces journal 2020 (volume 4, 2). I was the first author, and I conducted all the experimental work presented in the manuscripts.

Abstract

Understanding the effects of interfacial additives such as surface-active nanoparticles on phase inversion of Pickering emulsions is important from a practical point of view. In this work, we studied the effects of surface-active starch nanoparticles on catastrophic phase inversion of Pickering emulsions by continuous addition of a dispersed phase. Two types of experimental grade starch nanoparticles were used: hydrophilic starch nanoparticles (HSNP) and hydrophobic starch nanoparticles (HOSNP). The dynamic oil-water interfacial tension was measured using the pendant drop method at varying starch concentrations in the aqueous phase while the contact angles were measured using the sessile drop method of the Axisymmetric Drop Shape Analysis-Profile (ADSA-P). Both types of starch nanoparticles (HSNP and HOSNP) were effective in delaying the phase inversion of emulsions from water-in-oil (W/O) type to oil-in-water (O/W) type. This delay in phase inversion was directly correlated with the concentration of starch nanoparticles. The interfacial tension decreased as the drop aged at a given starch nanoparticle concentration. The contact angles for both types of starch nanoparticles were within the intermediate wettability range that confirmed the irreversible adsorption of starch nanoparticles at the oil/water interface leading to increased stability of the emulsions.

The stabilization effects of HSNP and HSNP/hydrophilic nanoclay hybrid in non-electrolyte medium was investigated. An interesting inversion behaviour was noticed at HSNP concentrations of 0.2, 0.4 and 1wt.% for pure HSNP only and all HSNP: Nanoclay hybrids. Inversions from W/O to O/W emulsions for these systems seem to occur twice. It was observed that the higher the concentration of the HSNP, the longer the emulsion stayed in the mid-O/W phase. This signifies that the concentrations of the HSNP, the medium in which they are

dispersed and the hybrid formations affect the behaviour of the phase inversion from W/O to O/W.

The effects of unmodified and modified bentonite nanoclays (with various degrees of surfactant modification) on the catastrophic phase inversion of water-in-oil (W/O) emulsion to oil-in-water (O/W) emulsion were determined experimentally. The bentonite nanoclay (NC-Bt) was suspended in the aqueous phase and the critical volume fraction of water where phase inversion of W/O to O/W emulsion took place was determined through conductivity measurements. Cetyl trimethyl ammonium bromide (CTAB) was used as a surfactant to modify the nanoclay. The adsorption of CTAB on nanoclay had a strong influence on the contact angle and the critical volume fraction of water where phase inversion took place. The modification of the nanoclay brought about by the adsorption of CTAB increased the three-phase contact angle (measured through the aqueous phase), thereby making it more hydrophobic, and prolonged the phase inversion point. CTAB alone and CTAB-modified nanoclay delayed the phase inversion process in a similar manner, showing a strong dependence on the CTAB concentration.

The effects of starch nanoparticles (SNPs) in oil recovery from oil sands was investigated using experimental-grade starch nanoparticles in the presence of trace quantities of octanol. Increasing starch concentration from 0.01wt.% to 1wt.% seems to have an effect on the percent oil recovery from oil sand, suggesting a direct relationship between the starch solution concentrations and the percent oil recovered. The presence of octanol as a co-solvent enhanced the oil recovery from oil sands. These results show that there is a potential for the use of these naturally occurring starch nanoparticles in oil recovery. The modification of these biodegradable nanoparticles to replace currently used petroleum-based polymers in the oil industry will further extend its applicability and the promotion of less toxic options in the enhancement of oil recovery from oil sands.

During the experimental procedure to establish a basis for the use of HSNPs for oil recovery from oil sands, mechanisms such as mixing, incubated shaking and temperature variation were explored to enhance oil recovery. In the presence of HSNPs, it was hypothesized that Pickering emulsion will be formed, hence the need to further explore the phase inversion phenomenon and separation behaviour of Pickering emulsion using HSNPs. The relevance of investigating the interfacial characteristics and separation behaviour of Pickering emulsions was further strengthened by the trends observed during the preliminary investigations. Understanding the interfacial behaviour of starch nanoparticle stabilized systems extend beyond the oil sand industry with potential application in other industries such as food, agriculture, pharmaceuticals, and cosmetics.

Acknowledgments

I would like to thank my supervisor, Prof. Rajinder Pal, for selecting me as his student, for the brainstorming sessions and for his assistance in securing the research grant that funded this research work. I am very grateful for the financial support provided by the NSERC Strategic Partnership Grant.

I also appreciate the support of my examining committee members Professors William Anderson, Boxin Zhao and Hind Al-Abadleh for serving on my committee and offering their valuable suggestions and feedbacks. I am grateful to Professor Sean Sanders, of the University of Alberta, for taking the time to be my external examiner and for his feedback.

I would like to thank members of the ECOWIN group for their valuable discussions and constructive criticisms during our review meetings. I am very grateful to Ecosynthetix for providing the experimental grade materials used in this thesis. I would like to thank Professor Jean Duhamel for his assistance and for providing the protocol and resources, for me to be trained by his student, Lu Li, on the oil recovery extraction procedure. Thanks to Ryan Amos and Professor Mario Gauthier for their preparation of the experimental hydrophobic starch samples.

Thanks to Anand Lopez for his help in Professor Lui Juewen's lab to conduct DLS measurements. Dr. Carla Abarca of Professor Robert Pelton's Lab and Oluseye Adeyemi both at McMaster University for their help in conducting surface tension and contact angle measurements. Professor Boxin Zhao for allowing me access to his lab to use his spin coater and oven. Professor William Anderson and Dr. Shazia Tanvir for granting me access to use their

incubated shaker. I thank Dr. Chau Mai for helping with the use of hydraulic press and stirrers on numerous occasions.

My sincere thanks go to the technical staff of the chemical engineering department Bert Habicher, Ravindra Singh and Ronald Neill of the Department of Chemical Engineering for their valuable support during this journey. Ralph Dickhout for his assistance with equipment training and access to the analytical laboratory resources. I sincerely appreciate the friendship and administrative support of Judy Caron, Rose Guderian and Ingrid Sherrer for their help during my time at the Chemical Engineering department. My former colleagues in Dr. Pal's research group, Yifan Wu, Arshdeep Singh, Upinder Bains, and Sima Lashkari are kindly acknowledged.

To the love of my life, the chosen one, Dr. Olumuyiwa Omotola Ogunlaja, you indeed complete me, thank you for being the voice of reason in my head and standing behind me through the depths of uncertainties and standing right there until the very end. Thank you for believing in my out-of-this-world dreams and aspirations. Your reassurance gave me the hopes that despite all I have been through; my dreams are still valid. And that I too can achieve my dream of earning a doctorate degree in chemical engineering. You have sacrificed too much for us. I look forward to all that God has prepared for us beyond this phase of our lives. Iwo ni igi leyin ogba mi.

To my sunshine, Daniel and angel, Victoria, thank you for always believing in your mother. You both have inspired me in unimaginable ways, you stood with me through the thick and thin, through the late nights, late dinners, constant birthday postponements, non-existent summer vacation and the lonely weekends when I have to be in the laboratory overnight. You have shown an unfathomable level of maturity and understanding. I remember the times you say "mummy, it is okay, we can wait". You are the reason why I couldn't give up on this dream. I

hope this journey has taught you that you can achieve anything your heart truly desires if you never give up. You both make my equation complete.

I would like to thank Pastor (Dr.) Mrs. Victoria Adepate Akinsiku, you are more than a mother, you are my assigned angel. You have been there since I gave my first breath, fighting all manner of battles on your knees for me, never fainting, never giving up. Staying in that war room of prayer all through my many trials and triumphs, Angeli mi ni yin. I thank God for allowing you to live to see the fruit of your labour of love.

To the blessed memory of my father Otunba Matthew Omosola Akinsiku, I only wish you were alive to see this day. Your blessings and confessions over me are coming to pass. I am sure you are looking down from heaven and smiling on this day. I didn't give up on that dream I told you about before you left us. Here it is Dad. You will never be forgotten.

To my siblings, Foluke Oni, Dr. Omolabake Fakunle, Adewale Omoregie, Damilare Matthew-Akinsiku, Babatomide Akinsiku, although continents apart, thirteen years not seeing each other, yet, never deterred in your love and support for me all through these years. You have shown your unwavering support and loudest cheers in every way possible, thank you for your love.

To the memory of my sister Oluwabanke Akinsiku, although your time with us was suddenly cut short, the thought of you is evergreen in my memory. Thank you for believing in Muyiwa and me. The times we shared together, your many jokes and songs have left an indelible mark, you are a true shining star.

All my friends turned family, Oluwaseun Olajumoke, Funke Olambo, Tina Adeleye, Tolu Olumuyiwa, Kemi Akinsiku, Pastor Bukky Osagie, Verlisa Tang, Rose Oriowo, Yinka Okusaga,

Udeme Anosike, Titi Adedeji, Margaret Lucas, Heather Card, Tola Komaiya and Bolaji Olawoye. Thank you all for your support and prayers.

Finally, I give all the glory to God, my maker and my saviour Jesus Christ. The author of life himself, to whom I owe all that I am and all that I can ever be. The sustainer of life himself. The one who owns knowledge, without whom I am nothing and this life would have been an endless search for meaning. I cannot imagine me without you, Lord. Thank you for your presence and the strength to go through this journey, without you, I am indeed undone.

Dedication

This thesis is dedicated to my loving and ever-supportive husband, Dr. Olumuyiwa Omotola Ogunlaja and my children, Daniel Ireoluwa Ogunlaja and Victoria Aanuoluwa Ogunlaja for their sacrifices and never-ending support.

Table of Contents

Examining Committee Membership	ii
Author’s Declaration.....	iii
A Statement of Contributions	iv
Abstract	v
Acknowledgments.....	viii
Dedication.....	xii
List of Tables.....	xvii
List of Figures	xviii
List of Abbreviations.....	xxiii
List of Symbols.....	xxiv
Chapter 1 : Introduction.....	1
1.1 BACKGROUND	1
1.2 RESEARCH AIMS AND OBJECTIVES	4
1.3 DISSERTATION OUTLINE.....	5
Chapter 2 : Literature Review	6
2.1 EMULSIONS	6
2.1.1 Emulsion Stability	6
2.1.2 Emulsion Destabilization Pathways	7
2.2 PICKERING EMULSION	9
2.3 ROLES OF PARTICLES AS PICKERING EMULSION STABILIZER	10
2.3.1 Colloidal Stabilization Basics.....	11
2.3.2 Particle type and size	15
2.3.3 Particle concentration	15

2.3.4 Particle wettability	16
2.4 PHASE INVERSION OF EMULSIONS	19
2.4.1 Phase Inversion Phenomenon.....	19
2.4.2 Phase Inversion Occurrence	21
Chapter 3 : Materials and Experimental Methodology	23
3.1 INTRODUCTION.....	23
3.2 MATERIALS	23
3.2.1 Interfacial Additives - Starch.....	23
3.2.2 Interfacial Additives - Nanoclay.....	23
3.2.3 Water	26
3.2.4 Oil	26
3.2.5 Surfactant.....	26
3.2.6 Other Materials	26
3.3 EXPERIMENTAL METHODS	27
3.3.1 Sample Preparation-Dispersion	27
3.3.2 Preparation of Emulsions.....	30
3.3.3 Measurements	32
Chapter 4 : Effects of Starch Nanoparticles on Phase Inversion of Pickering Emulsions	37
4.1 INTRODUCTION.....	37
4.2 MATERIALS AND METHODOLOGY	39
4.2.1 Materials	39
4.3 EXPERIMENTAL METHODOLOGY	41
4.3.1 Preparation of nanoparticle dispersion	41
4.3.2 Emulsion preparation and characterization	41
4.3.3 Phase inversion experiments	42
4.3.4 Stability experiments	43
4.3.5 Interfacial tension measurements	44
4.3.6 Contact Angle measurements	46

4.4 STATISTICAL ANALYSIS	47
4.5 RESULTS AND DISCUSSIONS	47
4.5.1 Phase Inversion.....	47
4.5.2 Separation Behaviour	52
4.5.3 Interfacial Tension (IFT)	55
4.5.4 Contact Angle.....	58
4.5.5 Synergistic effect of HSNP-CTAB system on the phase inversion.....	59
4.5.6 Synergistic effects of HSNP and Nanoclay in Non-electrolyte medium.....	65
4.6 CONCLUSIONS	68
Chapter 5 : Effects of Bentonite Nanoclay and Cetyltrimethyl Ammonium Bromide Modified Bentonite on Phase Inversion of Water-In-Oil Emulsions	71
5.1 INTRODUCTION.....	71
5.2 MATERIALS AND METHODOLOGY	73
5.2.1 Materials	73
5.2.2 Methodology.....	74
5.3 STATISTICAL ANALYSIS	78
5.4 RESULTS AND DISCUSSIONS	78
5.4.1 Material Characterization	78
5.5 CONCLUSIONS	91
Chapter 6 : Preliminary Investigation of the Extraction of Oil from Oil Sands using Starch Nanoparticles	93
6.1 INTRODUCTION.....	93
6.2 MATERIALS AND METHODOLOGY	95
6.2.1 Materials	95
6.2.2 Methodology.....	95
6.3 STATISTICAL ANALYSIS	98
6.4 RESULTS AND DISCUSSIONS	99

6.5 CONCLUSION	101
6.6 LIMITATION OF STUDY AND FUTURE RECOMMENDATIONS	101
Chapter 7 : Summary and Recommendations	102
7.1 SUMMARY	102
7.2 RECOMMENDATIONS FOR FUTURE WORK	104
Letter of Copyright Permission	106
References	111
Appendix A	125
Appendix B.....	127
Appendix C	184

List of Tables

	Page
Table 3-1: Properties of CTAB.....	26
Table 3-2: Materials and sources	27
Table 4-1: Source and Purity of Mineral Oil Used.	40
Table 4-2: Characteristics of Hydrophilic and Hydrophobic Starch Nanoparticles	40

List of Figures

	Page
Figure 2-1: Processes involved in the breakdown of an unstable emulsion. Reproduced with permission of [28] through PLSclear.....	7
Figure 2-2: Schematic of nanoparticle self-assembly at the water-oil interface[34]. Reproduced by permission of the Royal Society of Chemistry.	10
Figure 2-3: Diagram of the DLVO interaction showing the interaction energy versus interparticle separation distance. Reprinted with permission[23] Copyright John Wiley & Sons.	13
Figure 2-4: Schematic of zeta potential definition. Reprinted with permission[48] from Particle Technology Labs.....	14
Figure 2-5: Schematic diagram of a spherical solid particle at an oil-water interface showing the various interfacial energies and the three-phase contact angle measured into the water phase. Adapted with permission from [59] Copyright 2002 American Chemical Society. .	17
Figure 2-6: Variation in wettability of solid particle at the oil-water interface at contact angles $> 90^\circ$ and $<90^\circ$ respectively[34]. Reproduced by permission of the Royal Society of Chemistry.....	18
Figure 2-7 Diagrammatic representation of W/O to O/W phase inversion process. Reprinted with permission of [77] Copyright Elsevier.....	21
Figure 3-1: Montmorillonite Layered Structure. Reprinted with permission [83] from Elsevier.	24
Figure 3-2: Molecular Structure of CTAB.....	26
Figure 3-3: Picture showing Gifford-Wood homogenizer used for the experiment.....	31
Figure 3-4: Picture showing the set-up employed for the phase inversion experiment.....	31
Figure 3-5: Axisymmetric Drop Shape Analysis-Profile experimental set-up.....	34
Figure 4-1: Schematic representation of the catastrophic phase inversion by emulsification. The starch solution is sequentially added to the W/O emulsion until a phase inversion occurs with the formation of an O/W emulsion	42
Figure 4-2: Size and distribution of Hydrophilic Starch Nanoparticles determined using DLS ..	44

Figure 4-3: Size and distribution of Hydrophobic Starch Nanoparticles determined using DLS 44

Figure 4-4: A typical pendant drop image of the aqueous phase in mineral oil 45

Figure 4-5: Schematic of the Pendant Drop Method for Measuring Interfacial Tension 46

Figure 4-6: Schematic of the Sessile Drop Method for Measuring Contact Angle 47

Figure 4-7: Conductivity of water-mineral oil emulsions stabilized by hydrophilic starch nanoparticles as a function of the volume fraction of water; The [HSNP] are 0 (filled circle), 0.1 (filled square), 0.2 (filled diamond), 0.4 (open circle), 1 (open diamond) and 2 (filled triangle) % by weight based on the aqueous phase..... 49

Figure 4-8: Conductivity of water-mineral oil emulsions stabilized by hydrophobic starch nanoparticle as a function of the volume fraction of water; The [HOSNP] are 0 (filled circle), 0.1 (filled square), 0.2 (filled diamond), 0.4 (open circle), 0.6 (open square), 0.8 (filled triangle), 1 (open diamond) and 2 (open triangle) % by weight based on the aqueous phase. 50

Figure 4-9: Comparison between conductivity data for catastrophic phase inversion from W/O to O/W emulsion as a function of the volume fraction of water by the addition of water to the oil phase. Emulsions are stabilized by hydrophilic starch nanoparticles (HSNP) in (a) Oil A – 15 cSt @ 40°C/104°F and (b) Oil B – 36.1 cSt @ 40°C/104°F. Particle concentrations are 0 (filled circle), 0.1 (filled square), 0.2 (filled diamond), 0.4 (open circle), 1 (open diamond) and 2 (filled triangle) % by weight based on the aqueous phase. 51

Figure 4-10: Critical Volume Fraction of Water vs HSNP concentration..... 52

Figure 4-11: Normalized volume of coalesced aqueous phase against time for W/O Emulsion using HSNP. The [HSNP] are 0 (filled circle), 0.1 (filled square), 0.2 (filled diamond), 0.4 (open circle), 1 (open diamond) and 2 (filled triangle) % by weight based on the aqueous phase. 53

Figure 4-12: Normalized volume of coalesced aqueous phase against time for W/O Emulsion using HOSNP. The [HOSNP] are 0 (filled circle), 0.1 (filled square), 0.2 (filled diamond), 0.4 (open circle), 0.6 (open square), 0.8 (filled triangle), 1 (open diamond) and 2 (open triangle) % by weight based on the aqueous phase..... 54

Figure 4-13: Time at 50% phase separation as a function of starch concentration for 0, 0.1, 0.2, 0.4, 1 and 2% by weight based on the aqueous phase (pre-inversion) respectively. [HOSNP] - Filled circle and [HSNP] - filled square.	55
Figure 4-14: Dynamic interfacial tension measurements at mineral oil-water interface containing HSNP solutions in concentrations 0.1 (open circle) and 1 (open square) % by weight dispersed in (a) 0.01M NaCl and 0.15% biocide (b) Pure water.	56
Figure 4-15: Dynamic Interfacial Tension measurements at mineral oil-water interface containing HOSNP solutions in concentrations 0.1 (filled square) and 1 (filled circle) % by weight.	57
Figure 4-16: Images of Sessile Drop on Pelletized Starch Immersed in the Oil Phase	58
Figure 4-17: Conductivity data for W/O to O/W phase inversions of CTAB in an electrolyte medium (0.01M NaCl/Ac) at varying concentrations.	59
Figure 4-18: Critical Volume Fraction of water versus CTAB concentration (0, 0.01, 0.02, 0.03, 0.04, 0.05, 0.25 and 0.5 wt%)	60
Figure 4-19: Conductivity data for W/O to O/W phase inversions of HSNP-CTAB mixture at fixed 1wt.% HSNP concentration and varying CTAB concentrations.	61
Figure 4-20: Critical Volume Fraction of water at fixed 1wt.% HSNP against CTAB concentration (0, 0.01, 0.02, 0.03, 0.04, 0.05, 0.25, 0.5 and 1wt%).	61
Figure 4-21: Volume of coalesced aqueous phase against time for W/O emulsion for HSNP - CTAB mixture at fixed 1wt% HSNP and varying CTAB concentration at a fixed ϕ_w of 0.25	62
Figure 4-22: Time for 50% phase separation with constant 1wt.% HSNP as a function of CTAB concentrations of 0, 0.01, 0.02, 0.03, 0.04 and 0.05wt.% by weight based on the aqueous phase (pre-inversion) and a fixed volume fraction of water, ϕ_w of 0.25 respectively.	63
Figure 4-23: Comparison of Critical Volume Fraction of water against CTAB concentration in wt.% for HSNP/CTAB (Orange) and CTAB only (Blue) W/O emulsions.	64
Figure 4-24: Surface tension measurements of water droplets containing 1wt% HSNP with and without CTAB (concentrations of 0.01, 0.03 and 0.05wt%) versus the drop age.	65

Figure 4-25: Conductivity of water-mineral oil emulsions stabilized by HSNP as a function of the volume fraction of water.	66
Figure 4-26: Bright-field (BF) and confocal laser scanning microscopy (CLSM) images of mineral oil-in-water (1:1 by volume) emulsions stabilized by 1wt.% HSNP. A water-soluble fluorescent dye, Nile blue, which binds to HSNP was used to stain the starch and is coded red; the oil phase was stained Nile Red and is coded green. The scale bar corresponds to 50 μ m.	67
Figure 4-27: Conductivity of water-mineral oil emulsions stabilized by 1wt% HSNP: 1wt% Clay hybrid as a function of the volume function of water	68
Figure 5-1: Schematic of a multiscale W/O emulsion system with an emphasis on water droplet stabilized by surfactant modified nanoclay.....	73
Figure 5-2: Confocal fluorescence microscopy images of mineral oil-water emulsions stabilized by 1wt% nanoclay modified with 0.05 wt.% CTAB Scale Bar = 50 μ m	75
Figure 5-3: Schematic of the Sessile Drop Method for Measuring Contact Angle	76
Figure 5-4: Nanoclay coated with immobilized dispersing aqueous film	77
Figure 5-5: SEM Images of dried 1wt% aqueous dispersions of NC-Bt in the presence of (a) 0wt%, (b) 0.05wt% and (c) 0.1wt% CTAB. Scale Bar = 40 μ m.	79
Figure 5-6: Particle size distribution of 0.1wt% and 1wt.% nanoclay dispersion using DLS. 0.1 (blue circle), 1 (red square).....	80
Figure 5-7: Variation of zeta potential and 1wt.% nanoclay dispersion as a function of CTAB concentration.....	81
Figure 5-8: Variation of contact angle measured of a water drop in air (squares) and under oil (circles) as a function of the concentrations CTAB concentration in 1wt% nanoclay dispersions.....	82
Figure 5-9: Images of sessile drop on glass slides coated with 1wt% nanoclay with CTAB concentration of (a) 0, (b) 0.01, (c) 0.03 and (d) 0.05 respectively immersed in the oil phase	83

Figure 5-10: Conductivity of water-mineral oil emulsions stabilized by Nanoclay Solutions (0, 0.25, 0.5, 1, 1.75, 2.5 and 5 wt.%) as a function of the volume fraction of water (VF in the legend refers to the volume fraction of water where phase inversion is observed)	84
Figure 5-11: Critical volume fraction of water versus nanoclay concentration.....	85
Figure 5-12: Conductivity of water-mineral oil emulsions stabilized by pure CTAB solutions (0, 0.01, 0.02, 0.03, 0.04, 0.05, 0.25, and 0.5 wt.%) as a function of the volume fraction of water.....	86
Figure 5-13: Critical volume fraction of water versus CTAB concentration	87
Figure 5-14: Aqueous phase critical volume fraction as a function of normalized concentration for CTAB and nanoclay.....	88
Figure 5-15: Conductivity of water-mineral oil emulsions stabilized by 1wt% Nanoclay at varying CTAB concentration as a function of the volume fraction of water.....	89
Figure 5-16: Critical volume fraction of water versus CTAB concentration in 1wt% Nanoclay-CTAB mixture	90
Figure 5-17: Comparison between plots of Critical volume fraction of water versus varying CTAB concentration for pure CTAB and 1wt% Nanoclay + CTAB mixture respectively..	91
Figure 6-1: Vials containing Oil Sand + Starch Solution + Organic thinner before transfer into an Incubated Shaker.....	96
Figure 6-2: Vials in the incubated shaker	96
Figure 6-3: Vials after incubated shaking for 24hrs	97
Figure 6-4: Post extraction – (a) Top layer of oil extracted (b) Mid-layer emulsion (c) Loose bottom oil layer on sand grain (d) Residual sand after extraction	98
Figure 6-5: Starch concentration with respect to percent oil recovery	100
Figure 6-6: Extraction Efficiency as a function of PEG ₁₁₃ -b-PMEO ₂ MA ₈₀ concentration when the extraction is conducted with 65 mg of toluene. Adapted with permission from [151]. Copyright (2015) American Chemical Society.....	100

List of Abbreviations

ADSA-P	Axisymmetric Drop Shape Analysis-Profile
BF	Bright-field
CTAB	Cetyl Trimethyl Ammonium Bromide
CLSM	Confocal Laser Scanning Microscopy
CMC	Critical Micelle Concentration
CNP	Clay Nanoparticle
CSS	Cyclic Steam Simulation
DLVO	Derjaguin and Landau, Verwey, and Overbeek
DLS	Dynamic Light Scattering
HSNP	Hydrophilic Starch Nanoparticle
HOSNP	Hydrophobic Starch Nanoparticle
SEM	Scanning Electron Microscope
SNP	Starch Nanoparticle
ST	Surface Tension
THF	Tetrahydrofuran
W/O	Water-in-oil
O/W	Oil-in-water
IFT	Interfacial Tension
MMT	Montmorillonite Clay
NC-Bt-CTAB	CTAB-Modified Bentonite Nanoclay
NC-Bt	Bentonite Nanoclay
SAGD	Steam Assisted Gravity Drainage

List of Symbols

ϕ	Contact angle
t_{50}	Time at 50% coalesced aqueous phase
V_s	Creaming velocity
r	Radius of the particle
g	Gravitational constant
ρ	Density of fluid
x	Fluid 1 and 2 - Continuous and Dispersed fluid
η	Viscosity
V_T	Total interaction energy
V_{VA}	Sum of van der Waals attraction forces
V_{ER}	Electrostatic repulsion forces
θ	Contact angle
E	Energy of attachment
γ	Interfacial tension
ΔG	Gibbs free energy
H_o	Interparticle distance

Chapter 1: Introduction

1.1 Background

An emulsion is formed by two immiscible liquid phases, a dispersed phase as droplets within a continuous phase of the other liquid. Examples of emulsions include vinaigrette – an emulsion of vegetable oil in vinegar, milk, cod liver oil and polyspirin. There are three different types of emulsions, oil-in-water - when oil droplets are formed in an aqueous phase, water-in-oil - when the dispersed phase is water and complex or multiple emulsion - when the droplets themselves contain an emulsion.

When droplets coalesce spontaneously in an emulsion, it is said to be unstable. For an emulsion to be stable, the droplets of the dispersed phase must be prevented from coalescing. In order to make droplets resistant to coalescence, interfacial additives which act as a barrier at the interface between the two liquids are used to promote stabilization. Interfacial particles have been known to enhance emulsion stability by providing steric hindrance, influencing the contact area of the emulsion droplet and interfacial hydrodynamic properties. Characteristics of interfacial particles such as size, shape, concentration, wettability, and inter-particle interactions affect their effectiveness in stabilizing emulsions[1].

Process operations in the pharmaceutical industry, oil sand industry, hydrometallurgy, wastewater treatment, and bio remedial processes encounter intended or fortuitous solid-stabilized emulsions. The stability of water-in-oil emulsions stabilized with particles depends on the formation of complex structures at the oil-water interface[2]–[4]. Such structures have been known to effectively sustain the particles in the aforementioned industrial fields. They give rise to complex systems that have been known to undergo increased difficulty in achieving the

desired phase separation due to the unpredictable nature of the embedding solids [5]. Several investigations have indicated that fine solids and surface-active species have a complex effect on the interfacial activity of water-in-oil emulsion[6]–[9]. Various studies have also reported on the roles of charged fine solids in interfacial transfer enhanced by the adsorption of surface-active agents at the interfaces[6]–[10]. The overall effect of solids on the surface and emulsion stability depends on the type of chemical or combination of the chemical species present [11], [12]. Hence, investigating the phase inversion and interfacial behaviour of particle-stabilized emulsions will add to the literature knowledge base with respect to these systems.

Several surfactants have been used to stabilize emulsions, including amphiphilic surfactants, commonly used in biological systems[13]. The wettability of particulate interfacial additives has been altered by the adsorption of suitable surfactants [12]. Quaternary ammonium surfactants have a high affinity for clay surfaces and treatment with a surfactant can render clay surfaces very hydrophobic [13]. A recent study compared the behaviour of three hydrophilic quaternary amine surfactants pre-treated clay minerals to stabilize emulsions[13][14]. Examples of these surfactants previously used in the literature are cetyltrimethylammonium bromide (CTAB), quaternary C₁₂₋₁₄ alkylamine ethoxylate chloride (Berol R648) and cocobis (2-hydroxyethyl) methylammonium chloride (Ethoquad C₁₂).

A Pickering emulsion, which is an emulsion stabilized by solid particles located at the interface of oil and water, was discovered over a century ago[15]. The term “Pickering” was the name of the author considered to be the first to report on oil-in-water emulsion stabilized by solid particles adsorbed at the surface of oil droplets. The re-emergence of interest in Pickering emulsions within the last decade has been significant due to their wide applicability in pharmaceutical, food and energy industries. Some of the advantages of Pickering emulsion

include providing superior stability, low toxicity, and wide applicability in terms of modification possibilities of various solid particles of interest. Over the years, scientific progress has been made in the world of Pickering emulsions and these cut across disciplines and areas of research including but not limited to chemistry, chemical engineering, material science, physics, metallurgy, pharmaceutical, and medicine[16]-[18].

Pickering emulsions have been a focus of a wide range of research in recent years and most of the particles or interfacial additives used are synthetic or not biodegradable[19], [20]. The main focus of this thesis involves the investigation of Pickering emulsions and the effects of selected particulate interfacial additives such as starch nanoparticles and nanoclay, as well as a non-particulate interfacial additive, cetyltrimethylammonium bromide (CTAB). The uniqueness of this work is the biodegradability of the starch nanoparticles (SNPs) and the natural occurrence of the clays used as emulsion stabilizers. Specifically, this research work was conducted in two phases. Phase I investigated the effect of starch nanoparticles, while Phase II investigated the effects of clay and surfactant-modified nanoclay, in stabilizing a model water-in-oil emulsion system consisting of mineral oil as the oil phase and water as the aqueous phase.

When an oil-water system is agitated, the oil becomes dispersed as oil drops that form an oil-in-water (O/W) dispersion. Further addition of oil to the resultant emulsion leads to the instability of the system at a certain high concentration of oil. This instability results in the formation of a water-in-oil emulsion (W/O), a process called phase inversion. Conversely, dispersion of water in oil phase eventually leads to the opposite inversion, that is, initial W/O emulsion inverts to form O/W emulsion. Another area of focus of this work involves the investigation of how starch nanoparticle, nanoclays, and surfactants delay or enhance the phenomenon of phase inversion.

1.2 Research Aims and Objectives

The aims of this research work are:

1. To investigate the effects of hydrophilic starch nanoparticles (HSNP) and hydrophobic starch nanoparticles (HOSNP) on the interfacial properties and catastrophic phase inversion of W/O to O/W Pickering emulsions.
2. To investigate the synergistic effects of HSNP and surfactant on phase inversion of W/O to O/W Pickering emulsions.
3. To investigate the effects of nanoclay on the phase inversion of W/O to O/W Pickering emulsions.
4. To investigate the effect of CTAB on the phase inversion of W/O to O/W Pickering emulsions.
5. To investigate the synergistic effects of nanoclay and CTAB on phase inversion of W/O to O/W Pickering emulsions.
6. To investigate the synergistic effects of HSNP and nanoclay on phase inversion of W/O to O/W Pickering emulsions.
7. To investigate the effects of HSNP in oil recovery from oil sands.

The primary objective of this study is to investigate the effects of different concentrations of selected nanoparticulate additives on the catastrophic phase inversion points and to identify the triggering factors for the phase inversion. Examining the effects of nanoparticles on phase inversion illuminates their role in the stabilization of water-in-oil emulsions which helps to explain their stability mechanisms and interfacial behaviours, thereby contributing to the body of knowledge for potential application in pharmaceutical, food and oil and gas industries.

1.3 Dissertation Outline

This dissertation is written in chapters as described below;

- a) Chapter 2 presents a general literature review on Pickering emulsions, emulsion stability, and phase inversion.
- b) Chapter 3 presents the materials and experimental methodologies employed in this work.
- c) Chapter 4, written in a paper format (abridged version) as published in the Canadian Journal of Chemical Engineering.
- d) Chapter 5, written in a paper format (abridged version) as published in the Colloids and Interfaces journal.
- e) Chapter 6 presents the preliminary investigation of the effects of starch nanoparticles in oil recovery from oil sands.
- f) Chapter 7 presents the overall conclusions and recommendations for future work.

Chapter 2: Literature Review

2.1 Emulsions

An emulsion is formed when there is a colloidal dispersion of one liquid in another liquid. Pure liquids cannot form a stable emulsion because of the interfacial area between the two liquid [21]. Hence, an emulsion is a heterogeneous system in which one immiscible liquid is dispersed in another in the form of droplets [14], [15]. Such a system possesses minimum stability which can be enhanced by additives that form a film around the dispersed droplets such as surface-active agents including particles and surfactants[13], [22].

Two phases are present in an emulsion, the phase that forms the finely divided droplets, called the dispersed phase and the phase forming the medium in which the droplets are suspended, referred to as the continuous phase[21]. Upon the formation of the droplets, the coalescence of the dispersed phase tends to occur, leading to macroscopic phase separation. Hence, the two liquids will separate into their minimum energy state[23].

2.1.1 Emulsion Stability

Emulsions are stabilized to prevent coalescence using interfacial additives such as amphiphilic solid particles and molecular surfactants. The stability of an emulsion is determined by the interfacial additives used because some additives are often affected by factors such as temperature, which in turn affects the emulsion properties. The stability of an emulsion is the resistance to physical changes over time. Some conditions that lead to emulsion instability as described in the next section are flocculation, coalescence, sedimentation, and creaming of the emulsion drops. These conditions can affect an emulsion's stability and can occur simultaneously or consecutively in the emulsion.

2.1.2 Emulsion Destabilization Pathways

There are several physical processes that can induce the destabilization of emulsions. Some of these mechanisms are presented in **Figure 2-1**. Several factors that affect the stability of emulsions have previously been discussed in the literature [15]. These factors include oil to water ratio, the concentration of particles and the particle wettability. Additional effects such as oil polarity and sample pH impact the dispersion of particles in either the continuous or dispersed fluid phase, [24], [25]. It is believed that the main stabilization mechanism for particle-stabilized emulsions happens through the formation of a steric barrier, created by the organization of the particles in a closely packed network at the interface[26], [27].

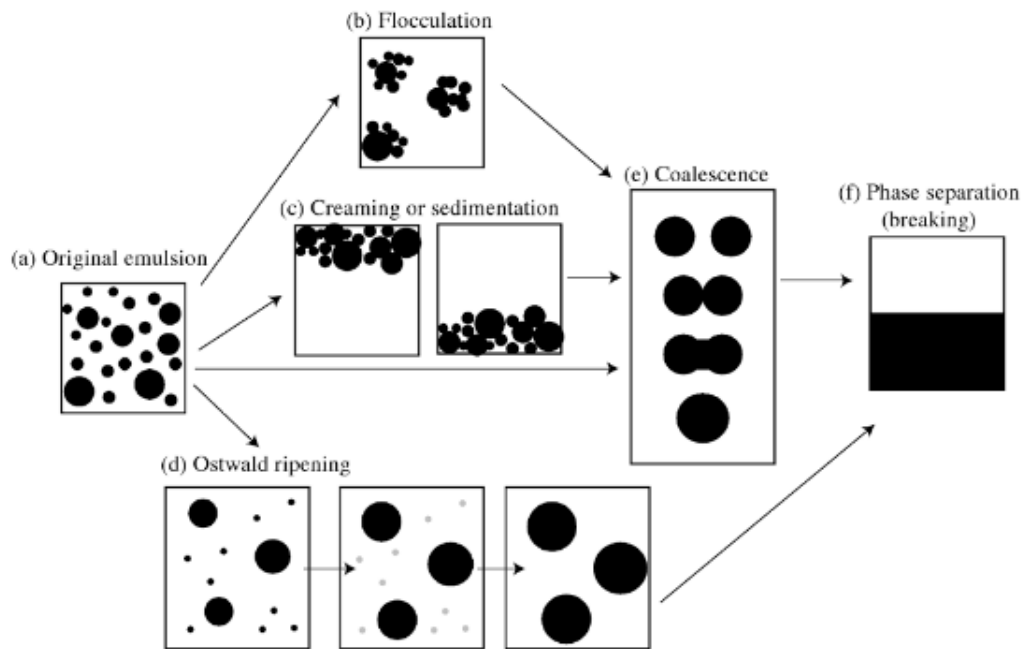


Figure 2-1: Processes involved in the breakdown of an unstable emulsion. *Reproduced with permission of [28] through PLSclear.*

Breakdown of an emulsion that occurs by the merging of two droplets to form a larger droplet is referred to as coalescence. Particle layers residing on droplets prevent coalescence of the two

colliding droplets. The formation of inter droplet networks can also slow down or prevent the destabilization of the emulsion by changing its rheological properties[17].

Destabilization by flocculation occurs when attractive interactions occur between droplets. This is a reversible process that can be easily restored upon shaking. Flocculation is sometimes referred to as aggregation or coagulation. In aggregation, two or more droplets clump together, touching only at certain points, and with virtually no change in the total surface area[29].

In coalescence, two or more droplets fuse together to form a single larger unit with a reduced total surface area. In aggregation, the species retain their identity but lose their kinetic independence because the aggregates move as a single unit. Aggregation of droplets may lead to coalescence and the formation of larger droplets until the phases become separated. In coalescence, on the other hand, the original droplet loses their identity and become part of a larger droplet[29]. Ostwald ripening involves the growth of a large droplet at the expense of a smaller one until the latter disappears completely[30].

Creaming and sedimentation are due to gravitational separations usually indicated by the emergence of a distinct clearer phase at the top or the bottom of the system. The term creaming comes from the familiar separation of cream from raw milk. The density difference between the dispersed and continuous phases causes a vertical concentration gradient in the system. Although the two separate layers produced have different dispersed phase concentrations, gravitation separation is not necessarily destabilization of the emulsion as a gentle agitation of the system totally reverses the separation. However high levels of sedimentation or creaming can be promoted by flocculation and coalescence[31].

Mathematical models applying Stokes' Law (Equation 2.1) can be used to predict the rate at which an isolated drop (described as a rigid spherical particle) creams in an ideal liquid[29]:

$$v_s = -\frac{2gr^2(\rho_2 - \rho_1)}{9\eta} \text{----- (2.1)}$$

where V_s is the creaming velocity in m/s, r is the radius of the particle in m, g is the acceleration due to gravity in m/s^2 , ρ is the density of fluid in kg/m^3 , 1 and 2 refer to the continuous and dispersed fluid, respectively, η is the shear viscosity of fluid in $kg/s.m$. The sign of V_s establishes the movement of the drop in the surrounding fluid: the drop creams for positive values and sediments for negative values. Equation 2.1 highlights that gravitational separation can be retarded in an emulsion by reducing the density difference between the oil and water phases, decreasing the size of the droplets or increasing the viscosity of the continuous phase. Recently, a model was proposed identifying factors that contribute to the creaming and sedimentation of droplets in Pickering emulsions[32].

2.2 Pickering Emulsion

Emulsions stabilized by solid particles are referred to as Pickering emulsions. The first paper that reported the adsorption of solid particles at the air-water interface was published by Ramsden[33]. However, the paper published by Pickering[15] was considered the first report of oil-in-water emulsion stabilized by solid particles adsorbed at the surface of oil droplets, hence the term Pickering emulsion. In a two-phase liquid system, these Pickering emulsions are formed by the self-assembly of colloidal particles at the fluid-fluid interface as shown as the densely packed layer in **Figure 2.2** [34]. Pickering sought a new emulsifier and an understanding of the nature of emulsification for insecticidal purposes. He discovered that a solid particulate emulsifier from sulphates of iron and copper brought about paraffin-in-oil emulsions that are stable to coalescence and creaming[15].

Studies investigating Pickering emulsions continue to receive attention, despite being known about for over a century[25][9][10] due to its wide applicability to industries such as food, agriculture, environmental e.t.c in which emulsions play an important role. Over the years, the work of Ramsden and Pickering on solid stabilization of Pickering emulsions has continued to expand especially in the area of the alteration of wettability of surfaces of solid particles with wide applications [28], [35], [36]. Pickering emulsions research has been relevant in the world of medicine, pharmaceuticals, cosmetics, food, agricultural, environmental remediation, climate change, to mention a few. This is due in part to its ease of application, high levels of stability, simplicity, and bioavailability[37].

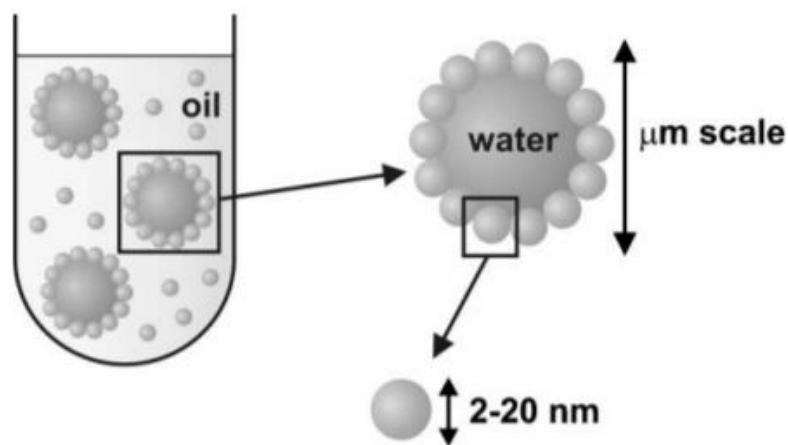


Figure 2-2: Schematic of nanoparticle self-assembly at the water-oil interface[34]. *Reproduced by permission of the Royal Society of Chemistry.*

2.3 Roles of Particles as Pickering Emulsion Stabilizer

Some advantages of emulsion stabilization by solid particles, instead of surfactants, is the high resistance to coalescence and the elimination of adverse side effects contributed by the

surfactants. For example, in the pharmaceutical and cosmetic applications, surfactants have been known to show adverse effects such as irritancy and hemolytic behaviour [38]. Due to these disadvantages, a wide variety of micro- and nanoscale particles with different sizes and shapes have been used as additives to stabilize emulsions[4]-[8].

Until recent years, most research in the area of Pickering emulsions using particles of intermediate hydrophobicity has been performed with chemically synthesized particles or materials. Some monodispersed nano- or microparticles such as silica, latex particle has also been employed in Pickering emulsions. In this study, naturally occurring compounds such as starch and clay were used as the main interfacial additives.

Some important factors that affect the performance of particles as Pickering emulsion stabilizers are presented in the subsequent sub-sections. Some of these factors include inter-particle interaction, particle size, particle type, concentration, surface charge and wettability of the solid particles.

2.3.1 Colloidal Stabilization Basics

Colloidal systems are two-phase systems in which one phase (dispersed phase) is dispersed in a second phase (continuous phase). Emulsions, aerosols, foams, smokes, and sols are kinds of such colloidal systems. Colloidal particles, varying in types, shapes and size of a few nanometres to several micrometre range may assemble between two fluids as emulsifiers[40]. Stokes and Evan described particle sizes that exhibit colloidal behaviour as dispersed particles which are larger than 1nm in at least one dimension; particles in colloidal systems that are smaller than this cannot be differentiated from true solutions [41].

Stabilization of many industrial processes is largely influenced by liquid-solid colloidal systems, e.g clay dispersions in ceramics or latex in paint industries[11], [42]. Colloidal particles

continually move around in dispersions due to Brownian motion. In 1940, Derjaguin and Landau, and Verwey and Overbeek in 1940 developed the DLVO theory, which relates the stability of a colloidal system to the sum of Van der Waals attraction and electrostatic repulsive forces exerted between particles, as they approach each other while undergoing Brownian motion[23][43].

The DLVO theory takes into account the attractive and repulsive forces between charged particles as they approach each other and proposes that an energy barrier exists as a result of the repulsive forces hindering the two particles from adhering to each other [44][45]. It suggests that the stability of the particles in the solution depends on the total interaction energy, V_T , which is the sum of van der Waals attraction potential (V_{VA}) and electrostatic repulsion potential (V_{ER}), between two particles dependent on their separation distance, as shown in Equation 2.2.

$$V_T = V_{VA} + V_{ER} \text{ ----- (2.2)}$$

V_{VA} is the short-range attractive potential between the particles, while V_{ER} , describes the repulsion that exists between charged particles as a result of the electric double layer overlap. If $V_{ER} > V_{VA}$, the net potential is repulsive, a stable colloidal system exists. If $V_{VA} > V_{ER}$, the net potential is attractive, and an unstable colloidal system exists, particles aggregate. **Figure 2-3** shows the plots of the interaction potential between colloidal particles as a function of particle distance[23].

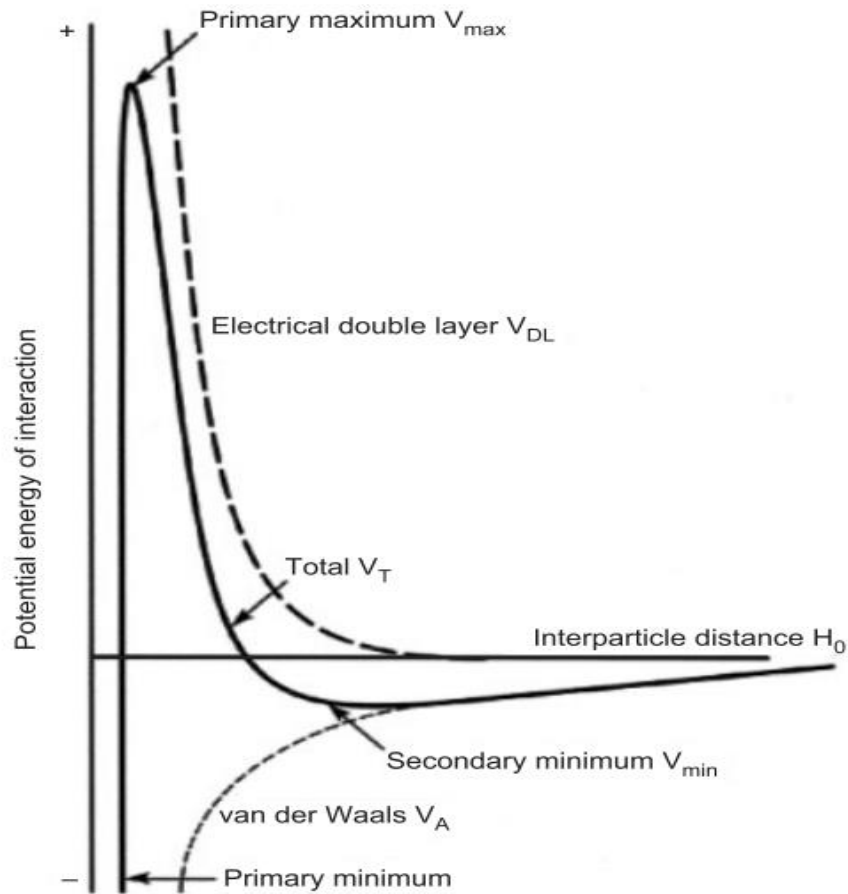


Figure 2-3: Diagram of the DLVO interaction showing the interaction energy versus interparticle separation distance. *Reprinted with permission[23] Copyright John Wiley & Sons.*

The surface charge is pH and ionic strength dependent and is acquired by a particle in the dispersing medium by either dissociation of surface groups or by the adsorption of ions from the surrounding solution[46]. The particle surface hence attracts oppositely charged ions to form an electrical double layer as shown in **Figure 2-4**. The electrical double layer consists of the Stern layer (has ions strongly bound to the surface), characterized by decreased electric potential with increasing distance from the particle surface[47]. Counterions are freely distributed in the diffuse layer surrounding the particles where they are less firmly associated and bound by a slipping plane. The slipping plane is an imaginary boundary inside which the particles and ions exist as a

stable entity that moves as a unit upon the application of an electric field in the solution [47]. The potential at the slipping plane is the Zeta potential and it is a suitable measure of the magnitude of repulsive interaction between colloidal particles. A key stabilizing mechanism for particle dispersions in aqueous solutions is the electrical repulsion arising as a result of the overlap of the electric double layers of the particles.

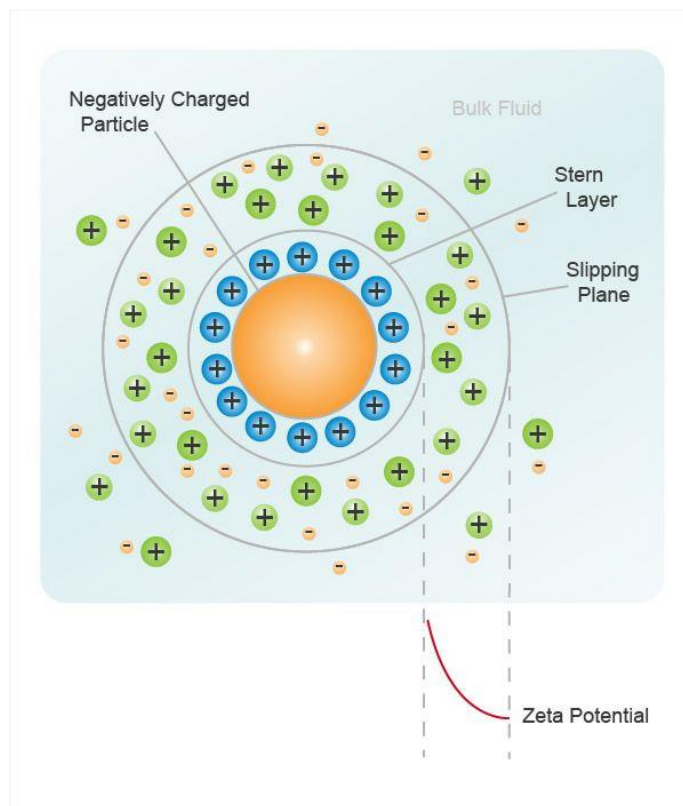


Figure 2-4: Schematic of zeta potential definition. *Reprinted with permission[48] from Particle Technology Labs*

The above DLVO theory often fails when particles are in close proximity to each other, closer than a few nanometers apart. Other interactions such as structural/steric stabilization and hydration forces that may exist between particles (called non-DLVO forces) are excluded from

the classical DLVO theory are explored in-depth elsewhere[49]. Repulsion as a result of steric stabilization is usually achieved by the adsorption of long-chain polymers onto the surface of the particles. If the thickness of the adsorbed coating is sufficient, there will be enough steric repulsion between the polymer layers such that the van der Waals forces become too weak to lead to an adhesion.[23]

2.3.2 Particle type and size

Solid particles of colloidal dimension can adsorb at air-liquid or liquid-liquid interfaces and change their physical property. The properties of Pickering emulsions are impacted by the type, size of the particle and the interaction between the particles at the water-oil interface. These particles are sufficient to stabilize emulsions[24], [50], classifying them as surface-active particles. A wide variety of particle types have been used as emulsion stabilizers to date: silica, polystyrene latex particles, metal oxides and sulphates, disk-like clays and carbon, waxes and microgels[36], [51], [52]. The effectiveness of these particles as emulsion stabilizer depends on their shape, size, wettability, inter-particle interactions, as well as the emulsion medium[25]. Particles that act as Pickering stabilizers are smaller than emulsion droplets. Nanometric sized solid particles of the sub-micron range around ~ 100 nm allow the stabilization of larger droplets with diameters approaching a few microns[38].

2.3.3 Particle concentration

Particle concentration in a system will significantly affect the characteristics and stability of Pickering emulsions [21][29]. Apart from a few recent studies, which showed stable emulsions with a low surface coverage of the droplets by particles, increasing the particle concentration will reduce the drop diameter[55]. Particles in a dispersion interact frequently as a result of the agitation of the system, Brownian motion, and sedimentation. This interaction is influenced by

particle concentration and impacts the stability of the dispersion and hence, properties of the Pickering emulsion.

The oil-water interface has been probed in several studies to investigate the interactions between particles that exist in a monolayer, properties of a monolayer of particles and those particles that reside in the bulk phase. The studies span from the use of Langmuir trough to measure surface pressure as a function of 2D-density of interfacial particles[56] to the measurement of interparticle long-range interactions at an oil-water interface[57].

If particles readily adsorb at the oil-water interface, the coalescence of droplets will be limited, and stability enhanced. If the particles do not aggregate, a monolayer is formed as a film surrounding the droplet. Particle aggregation leads to a dense layer formation around the drops which govern droplet size and stability of the system[58].

2.3.4 Particle wettability

Particle wettability is a key parameter in understanding particle behaviour at liquid interfaces. The contact angle describes the wettability between the solid and the oil/water interface. The contact angle is the angle at which a fluid-fluid interface meets the solid surface. Measured through the most polar of the two fluids, θ_{ow} exists at each point of the three-phase contact line where the solid and the two fluids meet[59]. **Figure 2-5:** shows a schematic diagram of a single solid particle(s) located at the oil (o)-water (w) interface. The three interfacial tensions (γ) are related to the contact angle θ_{ow} by the Young equation, presented in equation 2.3.

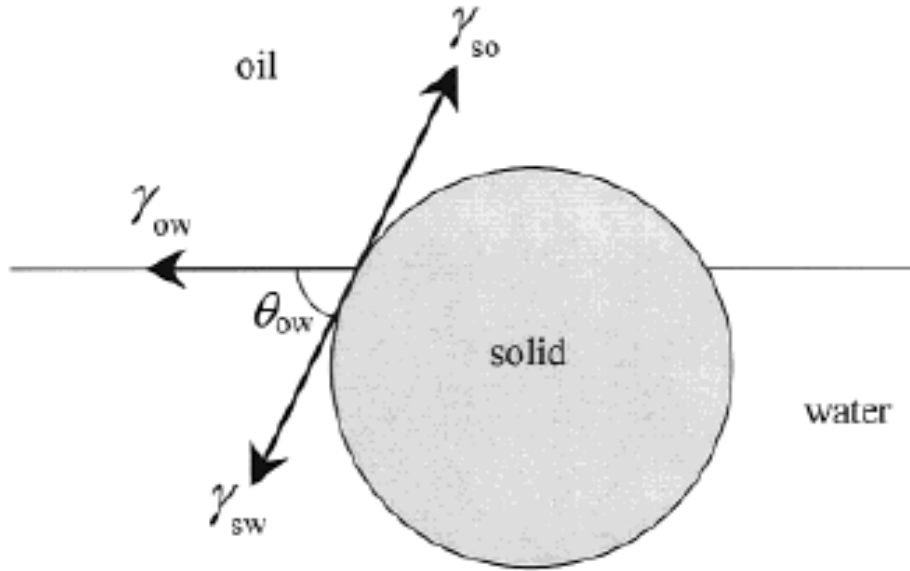


Figure 2-5: Schematic diagram of a spherical solid particle at an oil-water interface showing the various interfacial energies and the three-phase contact angle measured into the water phase. Adapted with permission from [59] Copyright 2002 American Chemical Society.

$$\gamma_{so} - \gamma_{sw} = \gamma_{ow} \cos \theta_{ow} \quad \text{-----(2.3)}$$

The energy of attachment of adsorption of a single spherical nanoparticle to the oil-water interface E is shown in equation 2.4. The energy has been shown to relate to the stability of emulsions containing adsorbed particles.

$$E = \pi r^2 \gamma_{ow} (1 - \cos \theta_{ow})^2 \quad \text{-----(2.4)}$$

For a particle-stabilized emulsion, solid particles that exhibit partial wettability with both fluid phases of the emulsion are required. $\cos \theta_{ow}$ is negative when the particle is removed into water. Previous studies have shown that the use of highly hydrophobic or hydrophilic particles results in less stable emulsions while the most stable emulsions are obtained with the use of particles with intermediate wettability[11], [24], [60], [61]. Surfaces of solid particles can be modified to alter their hydrophobicity in order to satisfy the conditions of partial wettability. The energy of

attachment of the particles at the fluid interface depends on the contact angle (θ_{ow}) the particles make with the fluid-fluid interface[24] and the interfacial tension, γ_{ow} [62]. Thus, Pickering emulsions can be stable to coalescence depending on the hydrophobicity of the particles.

Hydrophilic particles exhibit low contact angle (measured into the aqueous phase) and preferentially stabilize oil-in-water (o/w) emulsions. More hydrophobic particles with substantially higher contact angle can stabilize water-in-oil (w/o) emulsions. The changeover in this behaviour occurs at $\theta_{ow} = 90^\circ$. The energy of attachment of a single particle to an oil-water interface passes through a maximum also at $\theta_{ow} = 90^\circ$, and it has been shown that this consideration links directly to the stability of both types of emulsions[24]. This energy can be of several orders of magnitude higher than thermal energy which gives rise to irreversible interfacial adsorption[51], [63].

Several studies have established that certain particles can stabilize emulsions depending on several parameters such as particle size, particle shape, wetting behaviour, aggregation of particles at the interface, etc.[15], [33], [35], [54], [64], [65]. Of these parameters, the stabilizing effect of particles is accomplished by the contribution of the formation of the interfacial layer which is influenced by their wetting behaviour of the particles between phases. **Figure 2-4** shows the varying wettability of a solid particle at the oil-water interface[34].



Figure 2-6: Variation in wettability of solid particle at the oil-water interface at contact angles $> 90^\circ$ and $< 90^\circ$ respectively[34]. *Reproduced by permission of the Royal Society of Chemistry.*

It depicts the favorability of the stability of water-in-oil and oil-in-water emulsions at contact angles greater or less than 90° respectively[66].

Particles that are equivalently wetted in both the aqueous and oil phases are known to form an interfacial layer between the droplets that stabilize either oil-in-water or water-in-oil emulsions against coalescence[15], [17], [54], [64], [67]. Strongly hydrophilic or hydrophobic particles prefer to remain dispersed in the aqueous or lipophilic phase. Hence, they cannot act as emulsion stabilizers against coalescence. On the contrary, particles of colloidal dimensions that are more wetted in the aqueous phase than in the lipophilic phase can act as a stabilizing agent for oil-in-water emulsions. For particles that have the opposite wetting behaviour, they stabilize water-in-oil emulsions[33], [54], [64].

2.4 Phase Inversion of Emulsions

When one aqueous liquid (water) mixes with another immiscible liquid (oil), and the system is agitated, the water disperses as the water drops form a water-in-oil emulsion (W/O). Continuous addition of the water eventually leads to an unstable system at a certain high concentration of water; this instability results in an oil-in-water (O/W) emulsion. The phenomenon, by which the morphology of the emulsion transforms from W/O to O/W, or vice versa, is called “phase inversion”.

2.4.1 Phase Inversion Phenomenon

Some of the factors that influences phase inversion includes change in the volume fraction of the dispersed phase, viscosities of the dispersed and continuous phases[68], change of pH or temperature[69], induction as a result of destabilization due to the application of external

magnetic fields[70] and variation in the volume fraction of the dispersed phase[53], the hydrophobicity of the emulsifier used and the density difference of the two fluid phases.

The right particle surface chemical nature is essential to obtain emulsions with optimum stability because it determines its wettability. With a change in nature, pH or salt concentration, some particles can invert the type of emulsions which they stabilize from oil-in-water to water-in-oil at fixed water-oil volume ratio; this is known as “transitional” phase inversion[59], [64].

Another type of emulsion inversion experienced when varying the oil-water volume ratio of an emulsion is called "catastrophic" phase inversion [64]. Catastrophic phase inversion has the characteristic of a catastrophe; it implies a sudden change in the behaviour of a system resulting from gradual changes in its conditions. Catastrophic phase inversion is induced by increasing the fraction of the dispersed phase.

For particles of intermediate hydrophobicity, catastrophic inversion of emulsions typically occurs upon increasing the volume fraction of water, and emulsion stability to sedimentation or creaming increases as inversion point is approached. This inversion seems to occur through multiple emulsion formation, where some of the continuous phases are enclosed in the dispersed phase. Ultimately, the continuous phase becomes entirely enveloped within the disperse droplets and hence phase inversion occurs[71].

In a traditional surfactant system, an emulsion inversion at a fixed oil-water ratio is affected by the surfactant hydrophilic-lipophilic balance (HLB) number, by changing the electrolyte concentration or the ratio of surfactants in a mixture[72]. For particulate emulsifiers, the equivalent of the HLB number is θ_{ow} , the contact angle of the particle at the oil-water interface, which corresponds to the particle wettability. The particle's wettability can be varied by

modifying the particle surface chemistry by adding a surfactant, chemically grafting different groups[73]–[75] or changing the pH of the system[69]. These factors will affect the degree of charge on the particles if the particles have ionizable groups on their surface. Increasing or decreasing the particle surface charge will either make the particles more hydrophilic or hydrophobic[71].

2.4.2 Phase Inversion Occurrence

The onset of phase inversion was monitored using a conductivity probe for the first time by Quinn and Sigloh [76]. It has been widely used ever since as a means to monitor dispersions conductivity and indicates the continuous phase during phase inversion experiments. Catastrophic phase inversion (the only type considered in this thesis), is characterized by a significant increase in conductivity fluctuations and the electrical conductivity measurements are used to distinguish between W/O and O/W emulsions. **Figure 2-7** shows a typical W/O to O/W phase inversion process indicating the change in electrical conductivity of the emulsions[77].

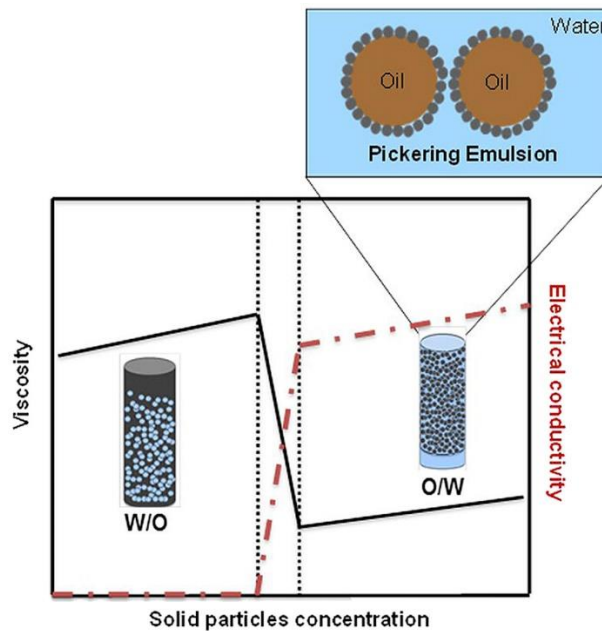


Figure 2-7 Diagrammatic representation of W/O to O/W phase inversion process. *Reprinted with permission of [77] Copyright Elsevier.*

The conductivity of W/O emulsions is extremely low at the beginning of the phase inversion experiment and suddenly increases at the critical volume fraction of the dispersed phase at which phase inversion occurs. A corresponding viscosity change is known to accompany the reported phase change. For water-in-oil type Pickering emulsion, viscosity increases with an increase in contact angle as described by the proposed viscosity model by Pal[54].

Chapter 3: Materials and Experimental Methodology

3.1 Introduction

This chapter presents the materials and the experimental methodologies that were employed in this study. The chapter augments the materials and methodologies presented in the subsequent chapters which were written in manuscript form.

3.2 Materials

3.2.1 Interfacial Additives - Starch

Starch is a natural, renewable, biocompatible, biodegradable, non-toxic polymer, existing in nature as the major storage polysaccharide in plants[78] and it is advantageous for use as interfacial additives. The two types of starch nanoparticles used in this work were experimental grade, supplied by EcoSynthetix. These were hydrophilic starch nanoparticles (HSNP) and hydrophobic starch nanoparticles (HOSNP). A variety of plants can be processed to extract starch granules. Ecosynthetix starch nanoparticle is produced via a patented reactive extrusion process[79] and has been widely used in industrial applications such as a binder in paper coating[80], in production of bio-based latexes for adhesive applications[81] and particulate stabilizers in the food industry[82].

3.2.2 Interfacial Additives - Nanoclay

Inorganic solid particles that exist in nature, such as clay mineral are inherently hydrophilic, adsorbing at the interface due to ionic surface characteristics. Clay is a tactoid of layered silicate platelets in which each layer is of a few nanometers in thickness and about a hundred nanometers in diameter[83]. A silicate layer has cationic surface characteristics of an alkaline metal on the surface, such as Mg, Ca, and Na, which leads to hydrophilic surface characteristics. If the layered

tactoids are fully exfoliated, individual platelets disperse as nano- or micron scale-sized, non-uniform plates with a high aspect ratio and form a temporary network structure due to the charged surface of the platelet[68]. Depending on exfoliation or dispersion of the clay, the size of the clay varies from sub-micrometre to nanometer, and therefore colloidal and interfacial localization can be expected in an emulsion [84]. **Figure 3-1** shows the structure of montmorillonite.

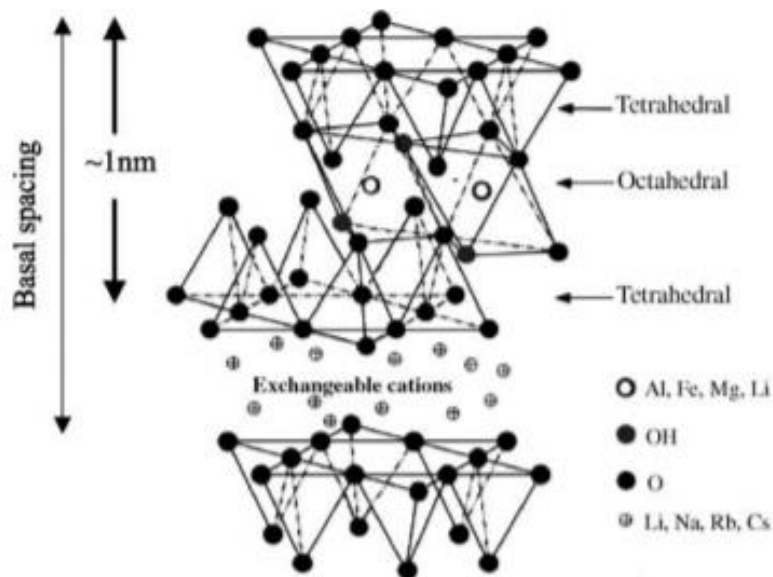


Figure 3-1: Montmorillonite Layered Structure. *Reprinted with permission [83] from Elsevier.*

To obtain the stabilizing behaviour with clay, particles have been applied to emulsions, together with surfactants, electrolytes, organic compounds like oppositely charged layered double hydroxides[73], [85]–[87] and have recently been easily modified to alter their hydrophobicity in order to enhance its role as colloidal stabilizers. Examples of clay modifications for emulsion stabilization are by adsorption of Asphaltenes, resins or other hydrocarbons which renders the

clay minerals hydrophobic, a crucial factor in the stabilization of water-in-crude oil emulsions[60], [88] using commercially available organically modified clay minerals[84].

Clays are very important in the oil sands industry. A typical ore in the Athabasca oil sands contains between 8 to 14 weight percent bitumen and 3 to 5 weight percent water. The balance is solids, mainly coarse sands, and fine silts and clays, which are in an unconsolidated form and impregnated with bitumen[89].

The major clay components of the Ft. McMurray oil sands formations are 40–70 wt. % kaolinite (K); 28–45 wt. % illite (I) and 1–15 wt. % montmorillonite (M). Among these clays, M clay has the highest affinity to water and swells when hydrated, while I have very poor and K does not have an affinity to water and has little swelling characteristics[90].

These clays are the important cause of fine suspension formation in tailings ponds. They appear in fine fraction and have very low settling velocity because of their small size as well as negative repulsive charges on their surface-structure. In industry, particles bigger than 44 μm are known to settle readily while particle sizes less than 2 μm are termed as fines and sizes less than 0.3 μm are termed as ultra-fines. A stable colloidal system is formed by these ultra-fines that strongly enhance the stability of the oil sands tailings and mainly hinder settling[91]. Significant reduction in bitumen recovery has been linked to high fines content and relatively high concentrations of calcium or magnesium[92]. It is therefore imperative that processes that enhance the oil recovery despite the presence of these fines or clay particles can benefit bitumen extraction[80],[92][93]. This work seeks to broaden the understanding of the microscopic properties of the interface between starch nanoparticles, modified nanoclay and O/W emulsions, which could potentially lead to an improvement in enhancing oil recovery from bitumen or oil sand.

3.2.3 Water

Ultra-pure water with $\sim 18 \text{ M}\Omega \cdot \text{cm}$ was employed as the dispersant for the dispersed phase.

3.2.4 Oil

Mineral oil was employed as the continuous phase.

3.2.5 Surfactant

Cetyl Trimethyl Ammonium Bromide (CTAB), a quaternary ammonium surfactant, was used as one of the surfactants in this study. CTAB is a hydrophilic cationic surfactant with a high affinity for negatively charged clay surfaces. The treatment of clay with a CTAB can render clay surfaces very hydrophobic. CTAB is a cationic surfactant consisting of a cationic organoamine with a 19-carbon tail attached to the amine group (**Figure 3-2**). The IUPAC name is hexadecyltrimethyl-ammonium. **Table 3-1** shows the physicochemical properties of CTAB.

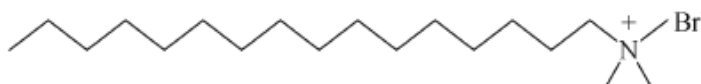


Figure 3-2: Molecular Structure of CTAB

Table 3-1: Properties of CTAB

Properties	CTAB
Molecular formula	$\text{C}_{19}\text{H}_{42}\text{BrN}$
Molar mass	364.45 g/mol
Appearance	White powder
Purity	99.9%
Density	1 g/cm^3

3.2.6 Other Materials

Supplementary materials employed in this study include biocides (Acticide), salts (sodium chloride), hydrochloric acid, sodium hydroxide, cleaning agents (ethanol and acetone),

fluorescent dyes (Auramine O, Nile Blue, Nile Red), and 1,2-propanediol. The supplier and purity of the materials are listed below **Table 3-2**:

Table 3-2: Materials and sources

Material	Source	Purity	Comment
Acticide	Proprietary		For starch preservation
Sodium Chloride (NaCl)	Sigma Aldrich	99.9%	Employed as supporting electrolyte and to prevent clay swelling.
Hydrochloric Acid (HCl)	Fisher Scientific	98.9%	For pH
Sodium Hydroxide	Sigma Aldrich	99.9%	For pH
Ethanol	Commercial Alcohols	Analytical Grade	Cleaning solvent
Toluene	Sigma Aldrich	Analytical Grade	Dilution solvent
Acetone	Sigma Aldrich	Analytical Grade	Cleaning solvent
Octanol	Sigma Aldrich	99%	Used for Oil extraction
1,2 - Propanediol	Sigma Aldrich	>99.5%	For stain preparation
Auramine O	Sigma Aldrich	Dye content >80%	For fluorescent microscopy - Nanoclay
Nile Blue	Sigma Aldrich	>75%	For fluorescent microscopy - Starch
Nile Red	Sigma Aldrich	>98%	For fluorescent microscopy – Mineral Oil

3.3 Experimental Methods

3.3.1 Sample Preparation-Dispersion

3.3.1.1 Starch Nanoparticle (SNP)

For starch nanoparticle dispersion, a known amount of SNP was dispersed into 0.01M NaCl to make a 2 wt.% stock solution. The stock solution was used to generate concentrations of 0.1, 0.2, 0.4 and 1 wt.% SNP by serial dilution.

3.3.1.2 Clay

The types of clay particles were dispersed as follow:

a) Hydrophilic Clay - MMT

The clay dispersion method for the experiment was modelled after the method used by Michot et al[93].

Clay dispersion method

- Disperse approximately 40 g/L MMT clay in water.
- Continuously stir the suspension for approximately 24 hours to make an aqueous dispersion.
- Exchange the suspension three times against 1 M NaCl to eliminate calcium ions (Ca^{2+}).
- Wash the suspension by centrifugation and re-dispersion of the solid in deionized water; repeat this cycle until the supernatant is chloride-free as indicated by a silver nitrate test[93] and/or the conductivity of the suspension is below $5\mu\text{S}/\text{cm}$ [94].
- The final suspension becomes the stock solution. Discard the impurities (such as quartz, silica, feldspar, mica, etc.) at the bottom of the centrifuge tube.

Size Fractionation

Size fractionation will be used to reduce the polydispersity of the clay platelets as needed.

- Centrifuge the purified clay suspension at 5000 g for approx. 90 min.
- Separate the bottom section and categorize it as size class 1.

- Re-centrifuge the supernatant at 12,000 g for 90 min to yield a second size class 2,
- Re-centrifuge the resultant supernatant at 35,000 g for 90 min to yield a final size class 3.
- Re-dilute the three size classes in MilliQ water, adjusting to a solid concentration range of 0.1 to 1 wt %.
- Measure the size distribution and polydispersity of the suspensions using Malvern Zetasizer.

b) Bentonite Nanoclay - Sigma

- Add Milli-Q water into a beaker and lower the homogenizer turbine (fully submerged)
- Gradually add a predetermined quantity of nanoclay into 2L of water to make 5 wt.% stock solution
- Disperse for approximately 30 minutes
- Measure the pH – nanoclay dispersion has a pH of 9.
- Record the conductivity

c) Bentonite Nanoclay - Treated with CTAB

Bentonite nanoclay and CTAB were added to the water phase as follows:

- To a known volume of clay suspension (1 or 2 wt. %) prepared in (b) above, add enough mass of CTAB for the desired surfactant concentration range of 0.01 to 0.04wt.%

- Stir the mixture for 20minutes until fully dispersed
- Leave stirring while covered using a magnetic stirrer for 24hrs

Concentrations of nanoclay and surfactants are in reference to the water phase before homogenizing with oil.

3.3.2 Preparation of Emulsions

The emulsions were prepared as outlined below:

- 1) Add a known volume of white mineral oil into a beaker – continuous phase.
- 2) Stir using Gifford-Wood homogenizer – this will constitute the continuous phase.
- 3) Monitor and record the conductivity of emulsion.
- 4) Gradually add aqueous starch, nanoclay or their hybrid solution (dispersed phase) while continuously shearing the mixture allowing a minute or two between each addition.
- 5) Monitor and record the conductivity readings until phase inversion occurs.

Figure 3-3 and Figure 3-4 shows the homogenizer and the experimental set up used for the preparation of the emulsion.

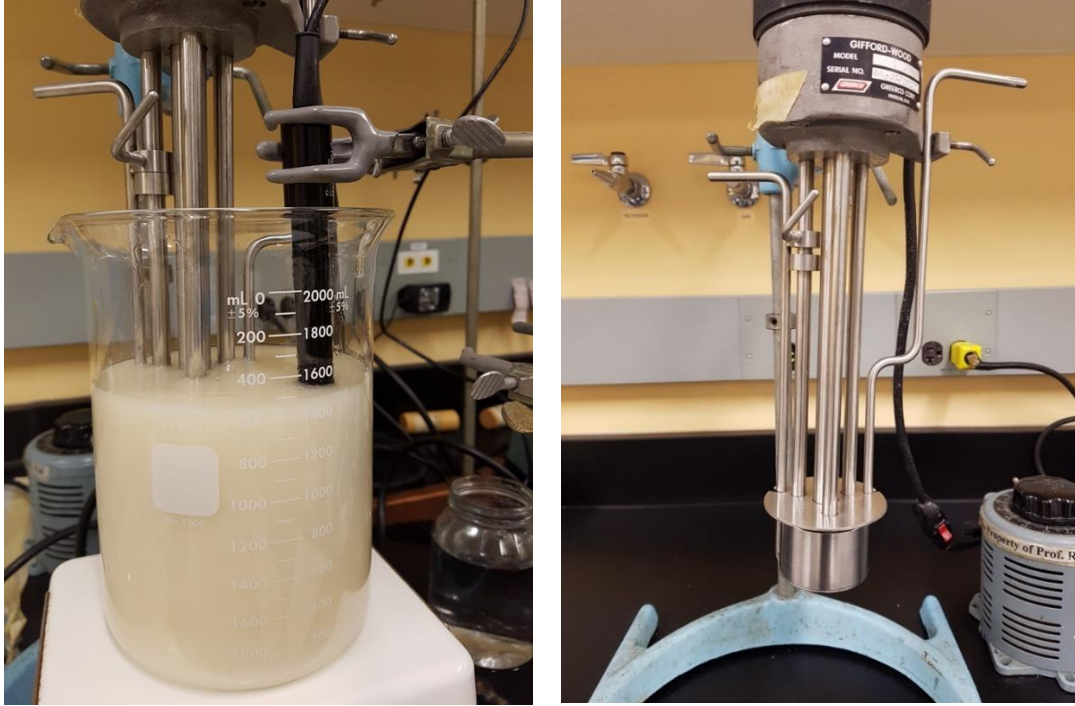


Figure 3-3: Picture showing Gifford-Wood homogenizer used for the experiment

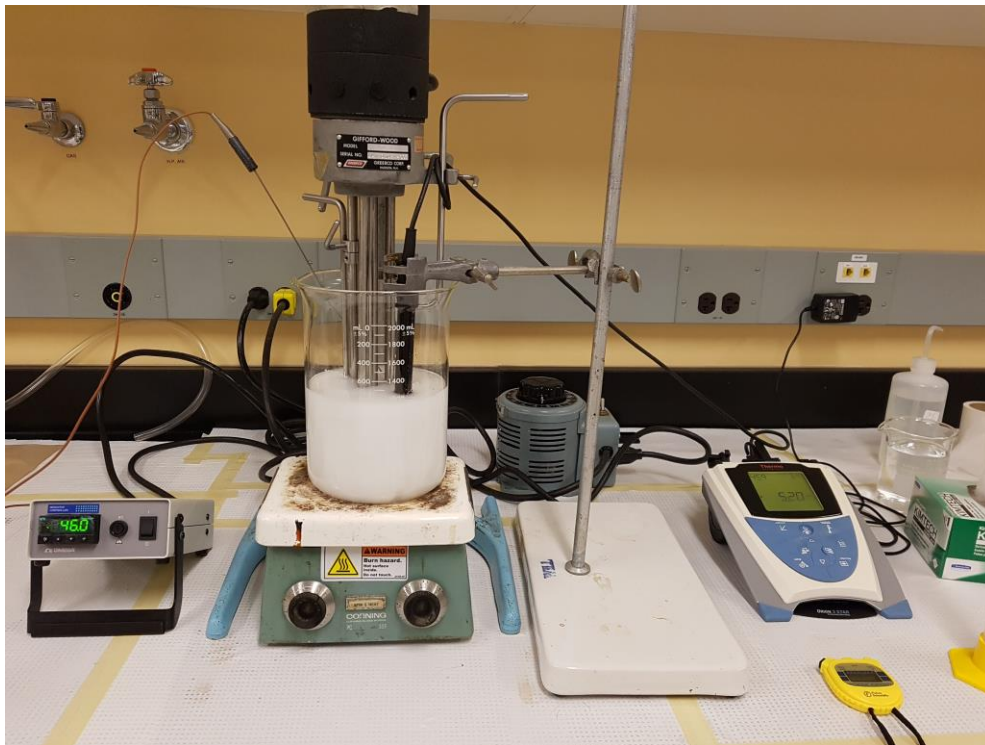


Figure 3-4: Picture showing the set-up employed for the phase inversion experiment

3.3.3 Measurements

3.3.3.1 pH

A Fisher Accumet pH meter to conduct measurements of the pH of dispersed starch and nanoclay solutions.

3.3.3.2 Conductivity

The conductivity of the samples was performed upon dispersion of interfacial additives and on-line during experiments to monitor the phase inversion point. A Thermo Orion 3 Star conductivity meter equipped with a dual-channel conductivity probe: 013005 MD, 0 – 200 mS/cm was used to perform electrical conductivity measurements[95]. The conductivity meter was calibrated by using a calibration standard of 1413 μ S/cm conductivity value purchased from Thermo-Fisher Scientific. The calibration was carried prior to experimentation on a daily basis.

The following procedure was used for the calibration:

- A) Adjusted the Thermo Orion conductivity to the calibration mode and selected the units of measurements in μ S/cm accordingly
- B) “Cond” calibration set-up is selected using the “up” arrow key. Line key is pressed until the CELL constant was displayed
- C) A vial containing measurement standard and stir bar is placed on a stirrer plate to stir
- D) Conductivity probe is rinsed with deionized water and placed in the standard while stirring
- E) The cell constant and conductivity value of the calibration standards were displayed on the screen
- F) Line select key is used to move the icon on the screen. The cell constant is entered manually using the up/down arrows to adjust.
- G) Line select key is used to move the icon to the top line and the measurement key is used to return to the measurement mode.

In literature, electrical conductivity has been used to determine the type of emulsions and predict the stability of W/O and O/W emulsions systems[96].

3.3.3.3 Dynamic Light Scattering and Zeta Potential

Sample for DLS measurements was prepared by first diluting the stock suspension to 0.1 wt. % and allowing larger particles to settle under gravity for 24 h and using the supernatant as the stock suspension. This prevents the time-dependent variations in scattering intensity due to particle sedimentation. The size, size distribution, and the zeta potential were measured using the Malvern Zetasizer.

3.3.3.4 Surface/Interfacial Tension

The spreading and wetting behaviour of the nanoclay and nanoclay-starch solution against oil and water will likely differ. This wetting behaviour influences the location of these particles at the O/W interface. Depending on the hydrophobicity of the particles, the particle location and the extent of coverage of the interface will be examined by the IFT and contact angle measurements. The IFT and contact angle measurements will be conducted using the axisymmetric drop shape analysis profile (ADSA-P) technique. **Figure 3-5** shows the picture of the ADSA-P used for this study.

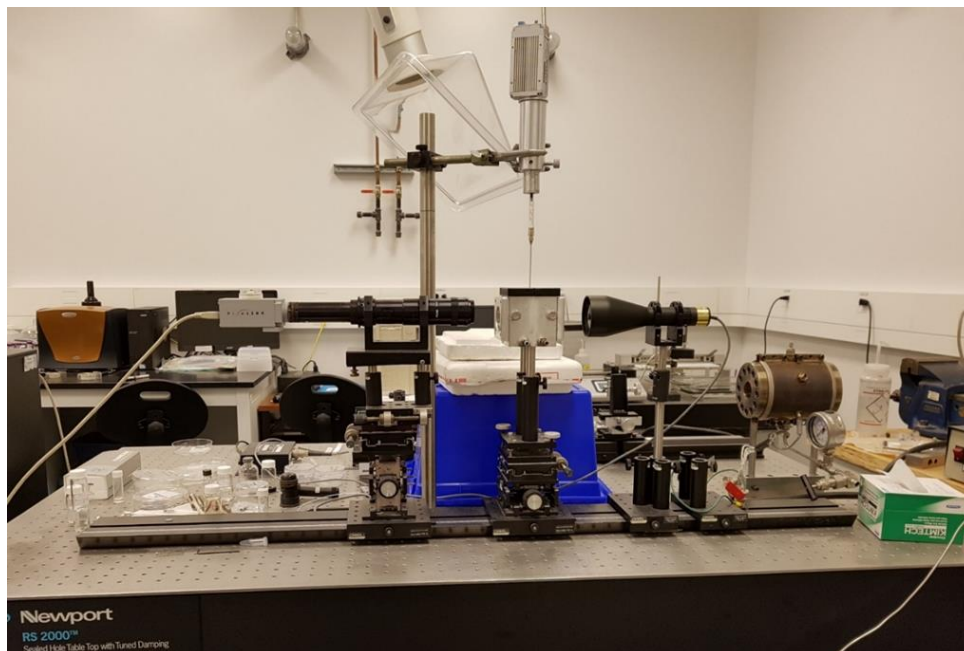


Figure 3-5: Axisymmetric Drop Shape Analysis-Profile experimental set-up

3.3.3.5 Contact Angle

Contact angle measurements provided the information on the degree of hydrophobicity of the clay-starch system. The contact angle of pure water, starch solution, and mineral oil drops were examined on a clay particle substrate to obtain the wetting behaviour of the clay particles. Contact angle measurements were performed using the sessile drop method with the same apparatus.

3.3.3.6 Spin coating

Interfacial additives particulate dispersions were spin-coated on pre-cut and prewashed microscope slides using the SCS G3-8 Spin Coater system. All samples were dried in an oven at 80°C.

3.3.3.7 Microscopy

Two different microscopy experiments were conducted using Scanning Electron Microscopy (SEM) and Confocal Microscopy.

3.3.3.7.1 Scanning Electron Microscopy (SEM)

The morphology of nanoclay powder was probed by scanning electron microscopy (SEM) equipped with energy dispersive spectroscopy (EDX) using an FEI Quanta Feg 250 ESEM with an acceleration voltage of 20 kV and a magnification of 1000× in SE mode (WATLab, University of Waterloo). The nano-powders were dried at room temperature and uniformly spread over a 1mm X 1mm area. These were attached over a carbon tape and supported by aluminum studs.

3.3.3.7.2 Confocal Microscopy

Confocal microscopy was used to visualize and confirm the presence and/or organization of both HSNP and nanoclay platelets at the oil-water interface. For confocal microscopy, a Leica TCS SP5 confocal laser scanning microscope (CLSM) with a Radius 405 nm laser coupled to an upright Leica DM 6000B microscope was used in fluorescent mode. Fluorescent dyes were used to stain the interfacial additives in the emulsion samples. A 0.01 wt.% Nile Blue solution was prepared and used to stain the starch nanoparticles. 0.01wt% of Nile Red solutions were also prepared in 1,2-propanediol and was used to stain the mineral oil. Auramine O was used to stain the negative nanoclay particles at room temperature. The solutions were stored in a dark place. Approximately 5 ml of sample were thoroughly mixed with a 20 µL aliquots of stain. 80µL of stained samples were placed on a concave glass slide and covered with a coverslip ensuring that all air gap is eliminated before imaging.

The fluorescence from the samples was excited by a helium-neon (HeNe) laser for Nile Blue A at 633nm, an Argon laser for Nile Red at 488nm and 460nm for Auramine O respectively. Images were processed using the image analysis software Image J.

Chapter 4: Effects of Starch Nanoparticles on Phase Inversion of Pickering Emulsions

An abridged version of this chapter was published in the Canadian Journal of Chemical Engineering and under the authorship of Sileola B Ogunlaja, Rajinder Pal and Kaveh Sarikhani

4.1 Introduction

Emulsions are dispersions of oil and water. There could be three different types of emulsions: water-in-oil (W/O), oil-in-water (O/W) or multiple emulsion. Emulsions are stabilized against coalescence using interfacial additives such as molecular surfactants and amphiphilic solid particles. Emulsions stabilized by solid particles are referred to as Pickering emulsions. The first paper that reported the adsorption of solid particles at the air-water interface was published by Ramsden[97]. However, the paper published by Pickering[98] was considered the first report of oil-in-water emulsion stabilized by solid particles adsorbed at the surface of oil droplets, hence the term Pickering emulsion. Some advantages of emulsion stabilization by solid particles, instead of surfactants, is the high resistance to coalescence and the elimination of adverse side effects contributed by the surfactants. For example, in the pharmaceutical and cosmetic applications, surfactants have been known to show adverse effects such as irritancy and hemolytic behaviour [38]. Due to these advantages, a wide variety of micro- and nanoscale particles with different sizes and shapes have been used as additives to stabilize emulsions[39], [99]–[102].

The process of altering the morphology of an emulsion from W/O to O/W emulsion or vice versa is called “phase inversion”. There are two types of phase inversion depending on the type of triggering mechanisms: transitional phase inversion triggered by varying the HLB (hydrophilic-lipophilic balance) of surfactant or wettability of the particles[64] and catastrophic phase

inversion triggered by altering the formulation or the mixing conditions, including the W/O ratio, phase viscosities, and stirring protocols[103]. Previous studies have shown that factors such as inclusion kinetics and duration of stirring before phase inversion could be responsible for the relationship between phase inversion and the system parameters such as W/O ratio, surfactant concentration and viscosity ratio[103], [104]. Binks and Lumsdon[64] investigated the relationship between particle wettability and phase inversion and concluded that the addition of particles that prefer the continuous phase or varying the particle ratio by employing particles with different wettabilities affect the phase inversion point. In addition to varying particle ratio, it has also been reported that the wettability of particles can be modified in response to changes in pH and temperature[105], triggering phase inversion.

The main objective of this study is to investigate the effects of the different concentrations of selected nanoparticulate additives on the catastrophic phase inversion point and to identify the triggering factors for the phase inversion using different oils. The published studies mostly tend to focus on one area at a time to explain the influence of additives whereas our goal is to investigate the interplay between phase inversion phenomenon, separation behaviour and interfacial properties (interfacial tension and contact angle) to elucidate the role played by the interfacial additives in stabilizing Pickering emulsions. The interfacial additives selected for investigation are starch-based. Starch is a biocompatible, biodegradable, non-toxic polymer, existing in nature as the major storage polysaccharide in higher plants[78]. Two types of experimental grade interfacial additives are used: hydrophilic starch nanoparticles (HSNP) and hydrophobic starch nanoparticles (HOSNP). The phase inversion experiments in this work are conducted using a continuous injection of aqueous phase (dispersed phase before inversion) to

oil, in contrast, to simply preparing a series of emulsions with different compositions and determining their phase continuity.

Our results indicate that increasing the volume fraction of the dispersed phase induces catastrophic phase inversion of W/O emulsion to O/W emulsion. The HSNPs are effective in delaying the phase inversion of emulsions from W/O to O/W type. A direct correlation exists between the delay in phase inversion and an increase in the concentration of the HSNPs. For HOSNP, phase inversion from W/O to O/W emulsion is delayed further due to an increase in the hydrophobicity of the nanoparticles. The interfacial tension decreases as the drop ages at a given starch concentration. The contact angles for both HSNP and HOSNP are within the intermediate wettability range that confirms the irreversible adsorption of nanoparticles at the oil/water interface leading to increased stability of emulsions.

This study broadens our fundamental understanding of the stability and phase inversion behaviour of Pickering emulsions in the presence of starch nanoparticles using continuous injection experiments. Such studies are necessary for the improvement of the processing conditions required for the production of industrial Pickering emulsions.

4.2 Materials and Methodology

4.2.1 Materials

4.2.1.1 Ultra-pure Water

Ultra-pure water was obtained by passing deionized water through a GE Osmonics E4 water purification system that uses a combination of UV irradiation, ultrafiltration, and ion exchange to remove bacteria, organic impurities, and residual particles. The resultant ultra-pure water

employed for the experiment had a consistent resistivity of approximately $18 \text{ M}\Omega\cdot\text{cm}$ and a surface tension of $\sim 72.9 \text{ mN/m}$ at 25°C .

4.2.1.2 Oil

The characteristics of the oils which were used in the experiments are presented in **Table 4-1**.

Table 4-1: Source and Purity of Mineral Oil Used.

White Mineral Oil Purity FG		Density (kg/L @ 15°C)	Viscosity (mPa.s @ 25°C)	Purity	Supplier
Oil A	WO 15	0.847	22.9	99%	Petro-Canada
Oil B	WO 35	0.855	64.5	99%	

4.2.1.3 Interfacial Additives

The additives of primary interest in this work were two different types of experimental grade starch nanoparticles: Hydrophilic starch nanoparticles (HSNPs) and hydrophobic starch nanoparticles (HOSNPs). These experimental grade biobased samples are unique insoluble discrete particles which form colloidal dispersions in water. Further characteristics of HSNP and HOSNPs are presented in **Table 4-2**.

Table 4-2: Characteristics of Hydrophilic and Hydrophobic Starch Nanoparticles

Particle type	Mean Size (nm)	PDI	Zeta potential/mV (0.1 wt.% at 25°C)	Contact angle, Θ_{ow} ($^\circ$)
HSNP	20.9 ± 1.8	0.53 ± 0.08	-12.5 ± 1.0	46 ± 2.2
HOSNP	52.9 ± 5.8	0.46 ± 0.05	-8.0 ± 0.8	120 ± 3.1

The DLS (dynamic light scattering) measurements were used to determine the size, polydispersity index (PDI) and zeta potential. The three-phase contact angle, θ_{ow} was obtained from the sessile drop method

4.2.1.4 Other Chemicals Used

High purity NaCl (> 99.8%, Sigma) was used as an electrolyte and a biocide (Thor Chemicals) was used as a preservative for the starch solution. HPLC grade acetone (Aldrich) and distilled absolute ethanol were used as cleaning solvents. Nitrogen (Praxair ultrapure 5.0) was used as a drying agent throughout the experiments.

4.3 Experimental Methodology

4.3.1 Preparation of nanoparticle dispersion

The HSNP was dispersed using a variable speed Gifford-Wood homogenizer (Model 1-L; rotor-stator Type) by adding a known amount of starch into a 0.01 M NaCl solution, with 0.15% biocide. The NaCl was added to increase the conductivity of the starch solution, while the addition of the biocide was necessary to prevent bacterial growth in the starch solution. For the HOSNP, the aqueous phase was initially heated to 52°C, while continuously stirring to enhance a complete dispersion. Various concentrations of the additive were mechanically agitated using the homogenizer at high speed for approximately 30 minutes of shearing until the starch was fully dispersed and completely lump-free[106]. Conductivity measurements were recorded pre-dispersion (aqueous phase only) and post-dispersion (starch solution). Both HSNP and HOSNP concentrations were varied from 0 to 2% by weight based on the aqueous phase. The dispersed solutions were cooled to room temperature before they were employed for the emulsification experiments as the dispersed phase.

4.3.2 Emulsion preparation and characterization

Emulsification of the oil-water-particle mixture was achieved using the homogenizer described above. Two different methods were used to prepare the emulsion depending on whether it was used for phase inversion experiment or emulsion stability experiment.

4.3.3 Phase inversion experiments

The emulsions were prepared by sequentially adding the aqueous phase to a known amount of the agitated oil (continuous) phase. A time interval of between 1 - 2 minutes was allowed between each addition while mixing continued until phase inversion occurred as shown schematically in **Figure 4-1**. The conductivity and temperature readings were recorded on-line per addition. The conductivity measurement was determined by using a Thermo Orion 3 Star conductivity meter equipped with a dual-channel conductivity probe: 013005 MD, 0 – 200 mS/cm. The volume fraction of water was varied at constant interfacial additive (nanoparticles) concentration. The phase inversion point was signified by a sudden spike in the observed conductivity. A drop test was also used to determine the emulsion type by introducing a sample of the emulsion into a beaker of pure water and pure oil[64]. According to the drop test, the continuous phase is indicated by the bulk fluid in which the emulsion sample is readily dispersed.

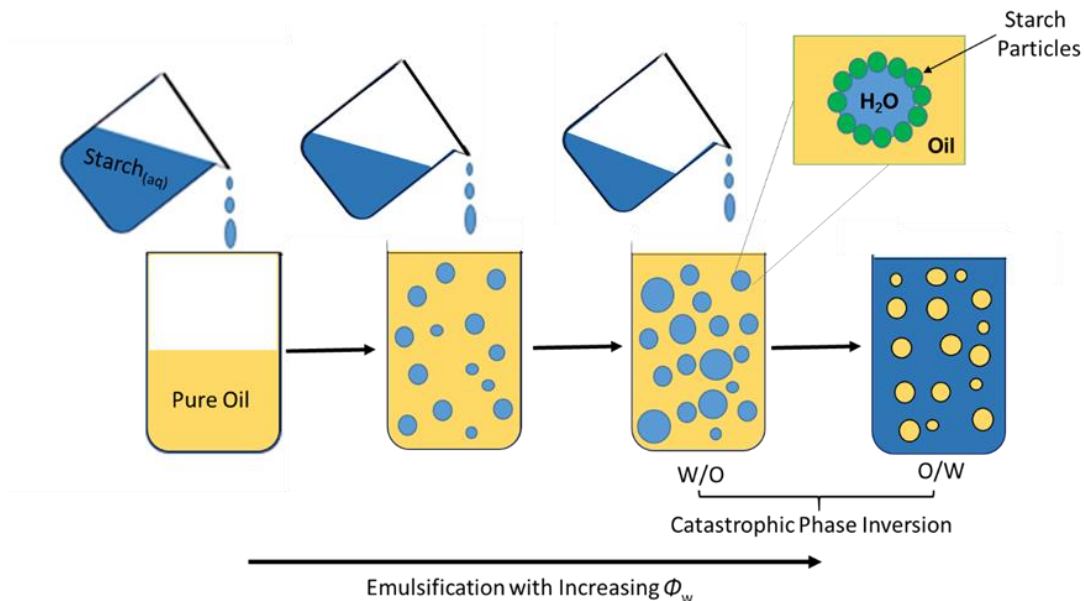


Figure 4-1: Schematic representation of the catastrophic phase inversion by emulsification. The starch solution is sequentially added to the W/O emulsion until a phase inversion occurs with the formation of an O/W emulsion

4.3.4 Stability experiments

The W/O emulsions were prepared using a direct route by shearing the known amounts of the aqueous phase (25%) and the oil phase (75%) in the homogenizer at high speed for about 5 minutes, to provide sufficient emulsification time. After the 5 minutes mixing, the emulsion was quickly transferred into a 500 mL graduated cylinder. Then, a camera was employed to record the coalescence of the aqueous-phase droplets for all the varying concentrations of interfacial additive. The stability of the W/O emulsion was assessed by observing the destabilization rate of the emulsion as depicted by the increase in the volume of the aqueous phase, separated from the emulsion.

4.3.4.1 Dynamic Light Scattering (DLS) and Zeta Potential Measurements

The size and size distribution of 1mg/mL aqueous dispersions of HSNP and HOSNP were determined by dynamic light scattering (DLS) using a Zetasizer Nano-ZS (Malvern Instruments Ltd. Worcestershire, U.K.) with a He–Ne laser operating at 633nm frequency. At that low concentration, HSNP size distribution can be seen in **Figure 4-2** to exhibit a narrow size distribution with a number based nanoparticle diameter of approximately 20.9 nm. The HOSNP size distribution is shown in **Figure 4-3**, the number based nanoparticle diameter of HOSNP is approximately 52.9 nm. Electrophoretic mobility was also measured using the Zetasizer Nano-ZS at 25°C with an equilibration time of 120 seconds. The starch dispersions were analyzed using three measurement cycles of 20 runs each. The zeta potentials were obtained to be -12.5 ± 1.0 mV for HSNPs and -8.0 ± 0.8 mV for HOSNP.

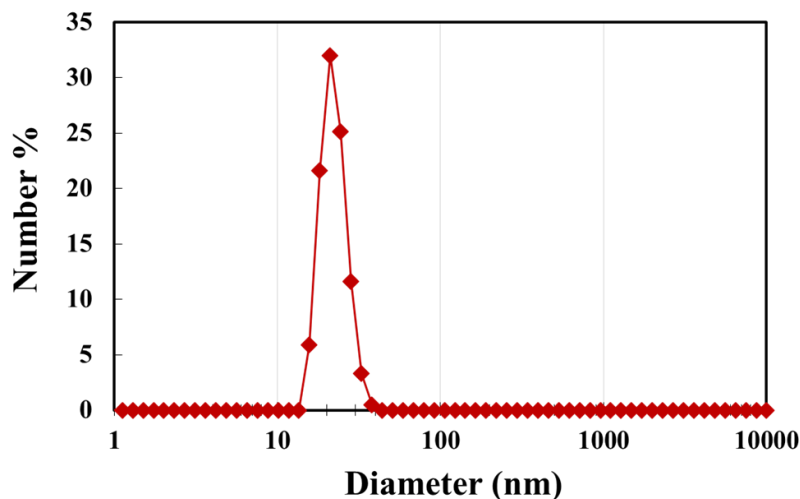


Figure 4-2: Size and distribution of Hydrophilic Starch Nanoparticles determined using DLS

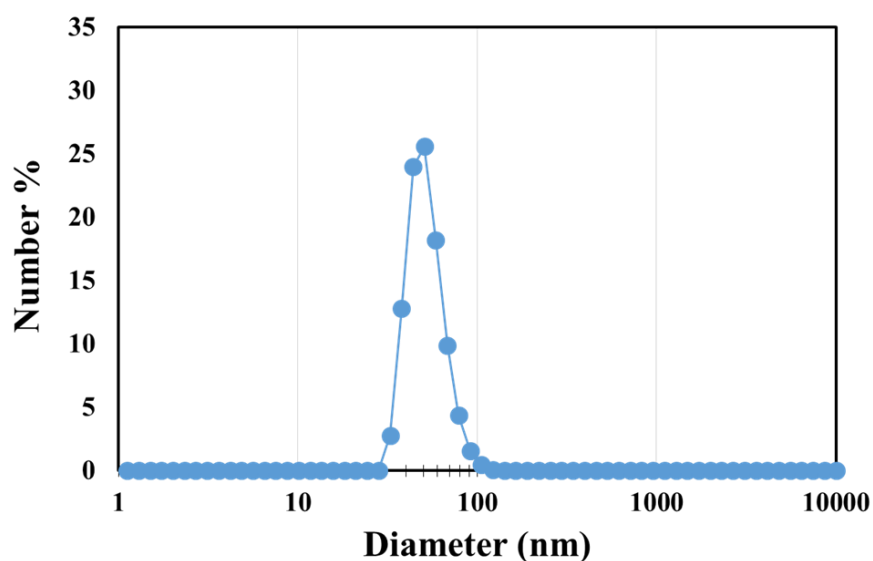


Figure 4-3: Size and distribution of Hydrophobic Starch Nanoparticles determined using DLS

4.3.5 Interfacial tension measurements

The drop shape method (pendant drop) is the most commonly used method to determine the interfacial tension as it offers many advantages over other methods. Some of the advantages of using the drop shape method for measuring the interfacial tension include the ability to use a small volume of liquid; its applicability to liquid-vapour and liquid-liquid interfaces; and broad

ranges of temperature and pressure. A detailed procedure of this method can be found elsewhere[107]–[110]. In the interfacial tension experiments, a pendant drop of suitable size was formed at the end of a stainless-steel holder that was connected to a 500 μL syringe (Gastight, Hamilton Co Model 1750 TLLX) with a blunt needle of diameter 1.8 mm. The drop was formed inside a sealed quartz cuvette (Hellma 330984) containing the mineral oil as shown in **Figure 4-4**. The starch solution was loaded onto a syringe and lowered into a cuvette filled with the lower density oil phase. Measurements were taken upon the insertion of the aqueous droplet into the oil. The dynamic oil-water interfacial tension was measured for varying starch nanoparticle concentrations in the aqueous phase.

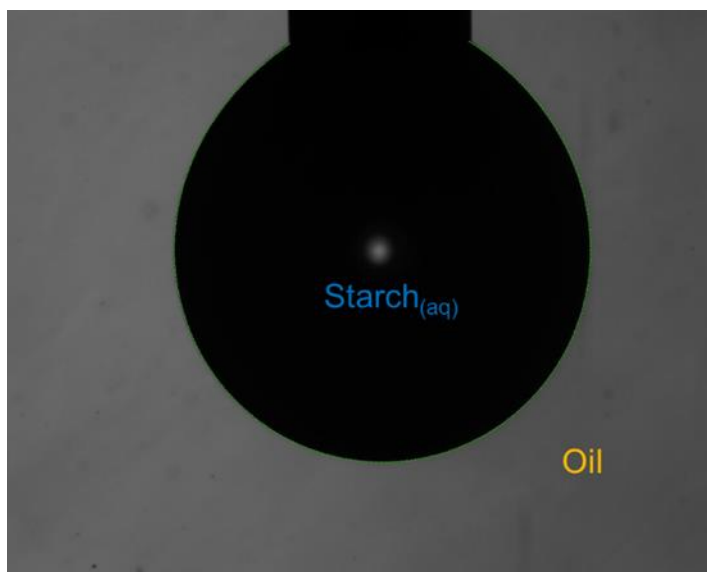


Figure 4-4: A typical pendant drop image of the aqueous phase in mineral oil

The cuvette containing the drop was housed in an optical viewing cell[111] through which the pendant drop was monitored during the experiment. A magnified image of the pendant drop was acquired by a charged coupled device (CCD) monochrome camera and a microscope. The digital image was transferred to a computer and the resulting interfacial properties of the drop were

obtained. A simplified schematic of the experimental set-up using digital image processing from a pendant drop is shown in.

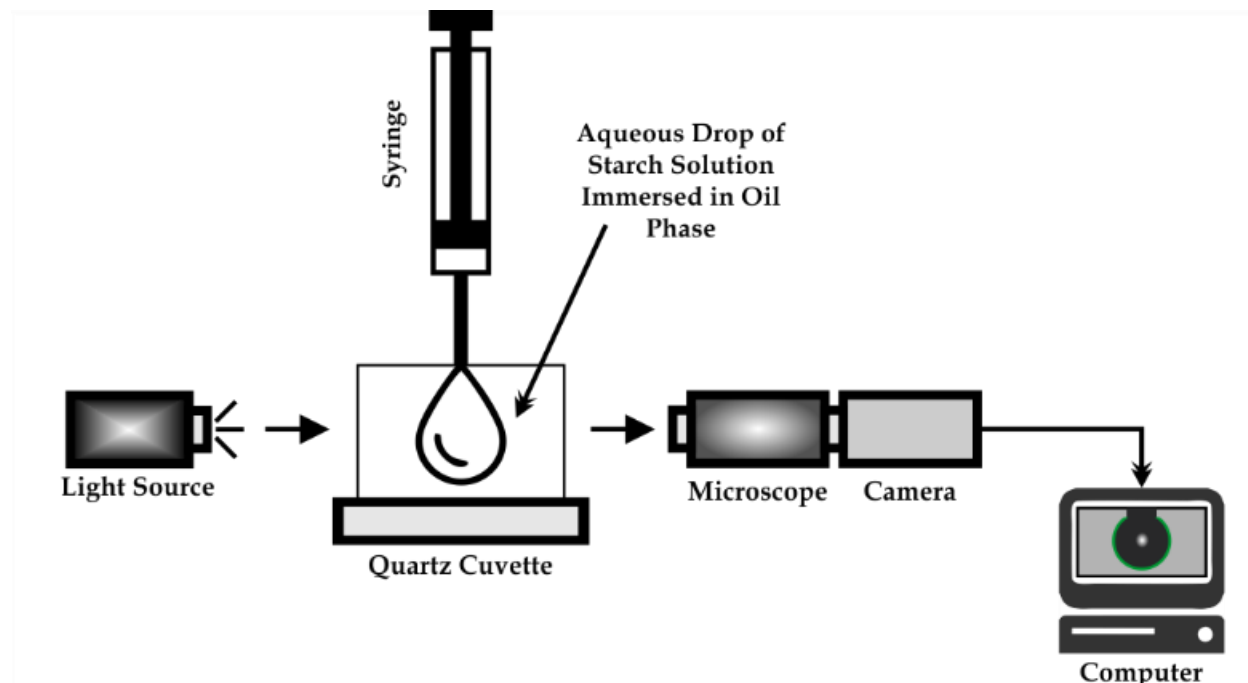


Figure 4-5: Schematic of the Pendant Drop Method for Measuring Interfacial Tension

4.3.6 Contact Angle measurements

The contact angles of HSNP and HOSNP were measured using the sessile drop method of the ADSA-P. The particles were pelletized using a hydraulic press to obtain a suitable surface of the substrate on which the contact angles of water, oil and starch nanoparticles were determined. The pellets were placed in an oven at 55°C overnight to get rid of any moisture. The pelletized particles were placed in a rectangular optical glass cell, into which the oil phase was already added, and the advancing contact angles of water drops of volume, approximately 50 μL under oil were measured. A simplified schematic of the experimental set-up for contact angle measurement from a sessile drop is shown in **Figure 4-6**.

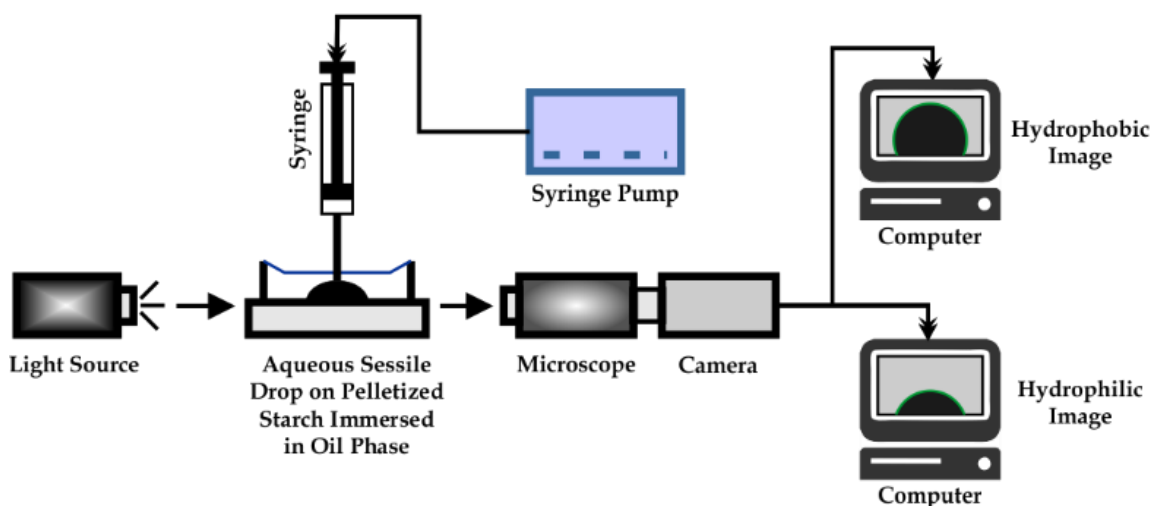


Figure 4-6: Schematic of the Sessile Drop Method for Measuring Contact Angle

4.4 Statistical Analysis

The experimental data was conditioned by using Grubb's test to determine any outliers which were removed before conducting other statistical analysis. All the experiments were conducted in triplicates.

4.5 Results and Discussions

4.5.1 Phase Inversion

4.5.1.1 Effect of Interfacial Additive Concentration on Phase Inversion

Hydrophilic Starch Nanoparticles: The type of emulsion (W/O or O/W) can be determined by its electrical conductivity. The W/O emulsion has a very low conductivity as the continuous phase (oil) of the emulsion is nearly non-conductive. The O/W emulsion, on the other hand, is highly conductive due to the high electrical conductivity of the continuous phase (water). **Figure 4-7** shows the variation in conductivity with the addition of the aqueous phase (HSNP dispersion in

water) to the oil. The emulsions formed at water volume fractions with very low conductivity are W/O type emulsions. The phase inversion of W/O type emulsion to O/W type emulsion is depicted by a sharp increase in the conductivity. The drop test was also employed to further verify the occurrence of phase inversion from W/O to O/W emulsion. **Figure 4-7** shows that the phase inversion point is delayed with increasing HSNP concentration. Without the addition of HSNP, the phase inversion of W/O to O/W occurred at a lower volume fraction of water of 0.31. This result is consistent with values obtained by Varun et al[96] who obtained a water volume fraction of 0.329 with the use of similar low viscosity oil. These values obtained in the absence of additives are, however, inconsistent with those predicted by Ostwald[112] in which he reported 0.74 value of water volume fraction.

At 0.1 wt% of HSNP dispersed in the aqueous phase, catastrophic phase inversion of emulsion from W/O to O/W occurs at a water volume fraction of approximately 0.44 whereas at 2 wt% of HSNP dispersed in the aqueous phase, the catastrophic phase inversion of emulsion from W/O to O/W type occurs at a water volume fraction of approximately 0.7. This implies that at high HSNP concentrations, the W/O emulsion is more stable in comparison with the W/O emulsion at low HSNP concentration.

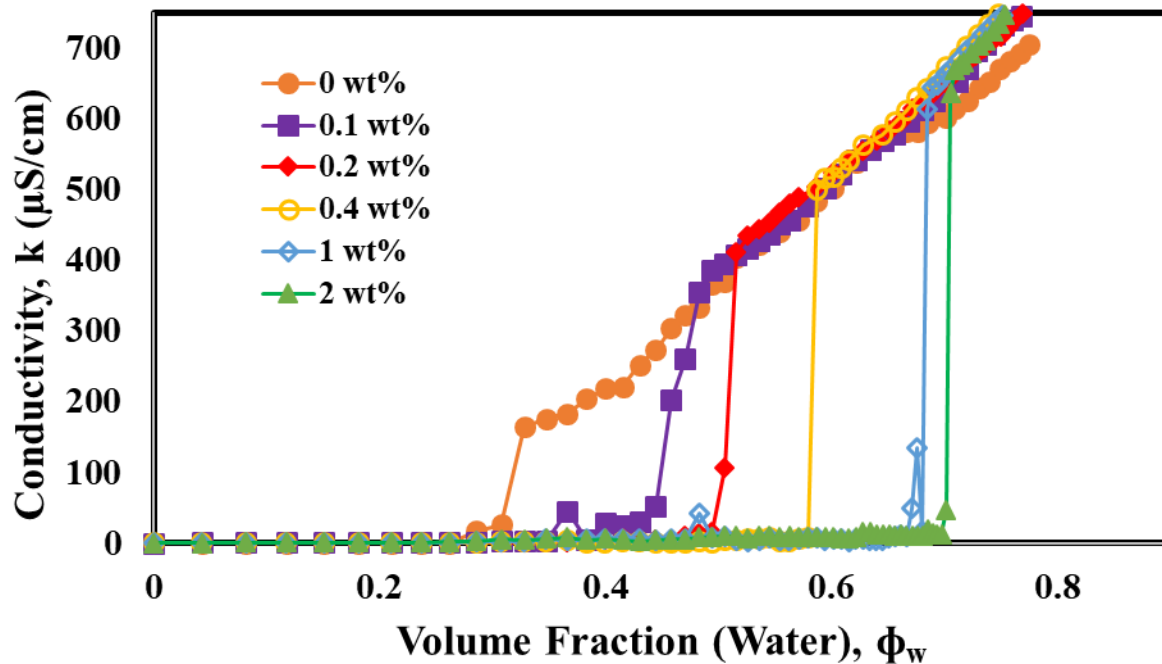


Figure 4-7: Conductivity of water-mineral oil emulsions stabilized by hydrophilic starch nanoparticles as a function of the volume fraction of water; The [HOSNP] are 0 (filled circle), 0.1 (filled square), 0.2 (filled diamond), 0.4 (open circle), 1 (open diamond) and 2 (filled triangle) % by weight based on the aqueous phase.

Figure 4-8 shows the plots of conductivity against volume fraction for varying concentrations of HOSNP. Phase inversion from low electrical conductivity W/O emulsion to highly conductive O/W occurs at a higher water volume fraction upon increasing the HOSNP concentration in the aqueous phase. For example, phase inversion took place at volume fractions of about 0.48 and 0.73 for 0.1 and 2 wt.% HOSNP respectively. These delay observed is also consistent with the findings by Varun et al[96] increase in hydrophobicity of nanoparticles lead to prolonged catastrophic phase inversion from W/O to O/W emulsions. These results further indicate that HOSNP is more effective in producing stable W/O emulsions as compared with HSNP at the same starch concentration.

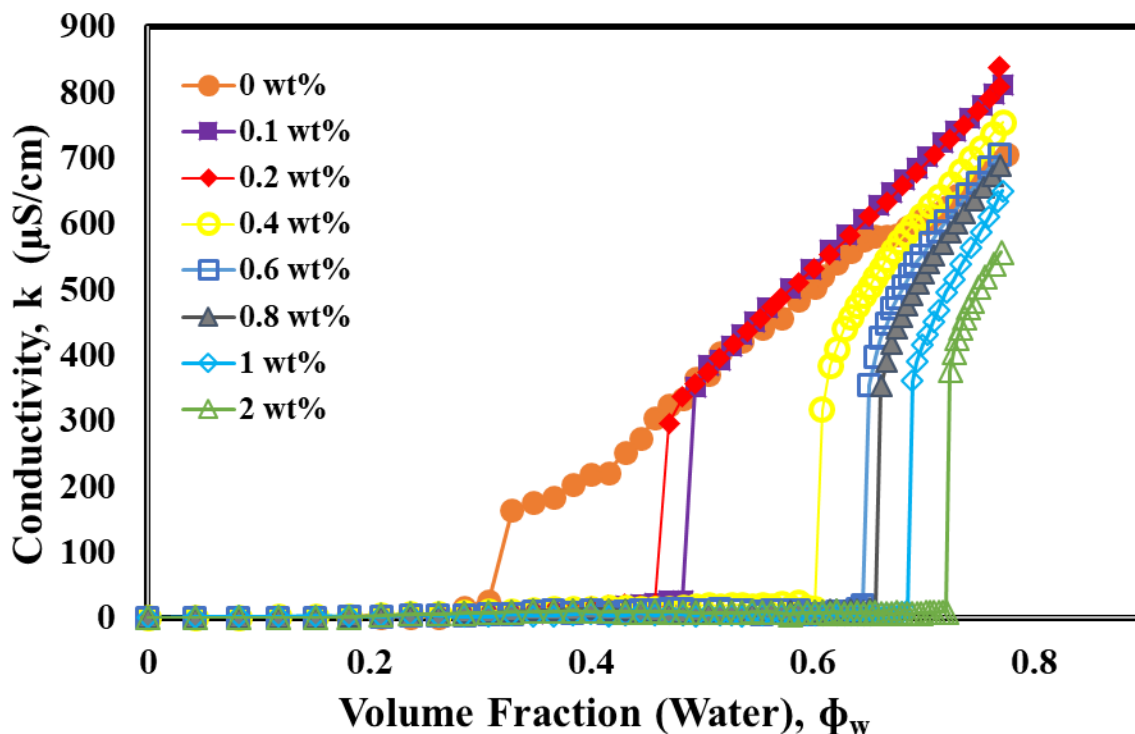


Figure 4-8: Conductivity of water-mineral oil emulsions stabilized by hydrophobic starch nanoparticle as a function of the volume fraction of water; The [HOSNP] are 0 (filled circle), 0.1 (filled square), 0.2 (filled diamond), 0.4 (open circle), 0.6 (open square), 0.8 (filled triangle), 1 (open diamond) and 2 (open triangle) % by weight based on the aqueous phase.

4.5.1.2 Effect of Oil Viscosity on phase inversion

The effect of oil viscosity on phase inversion was investigated using hydrophilic starch nanoparticles. **Figure 4-9** shows the plots of electrical conductivity against volume fraction for varying concentrations of HSNP. For the high viscosity oil (oil B), phase inversion occurs at low water volume fractions of 0.26 and 0.57 at 0 and 2 wt% HSNP respectively whereas for low viscosity oil (oil A), phase inversion occurs at higher volume fractions of water of 0.31 and 0.70 at 0 and 2 wt% HSNP respectively. These results further show that the effect of viscosity is more pronounced at higher concentrations of HSNP. Similar trends have been reported in surfactant-based systems[96] in that the inversion of W/O to O/W emulsion occurs early upon increasing the viscosity of the oil phase.

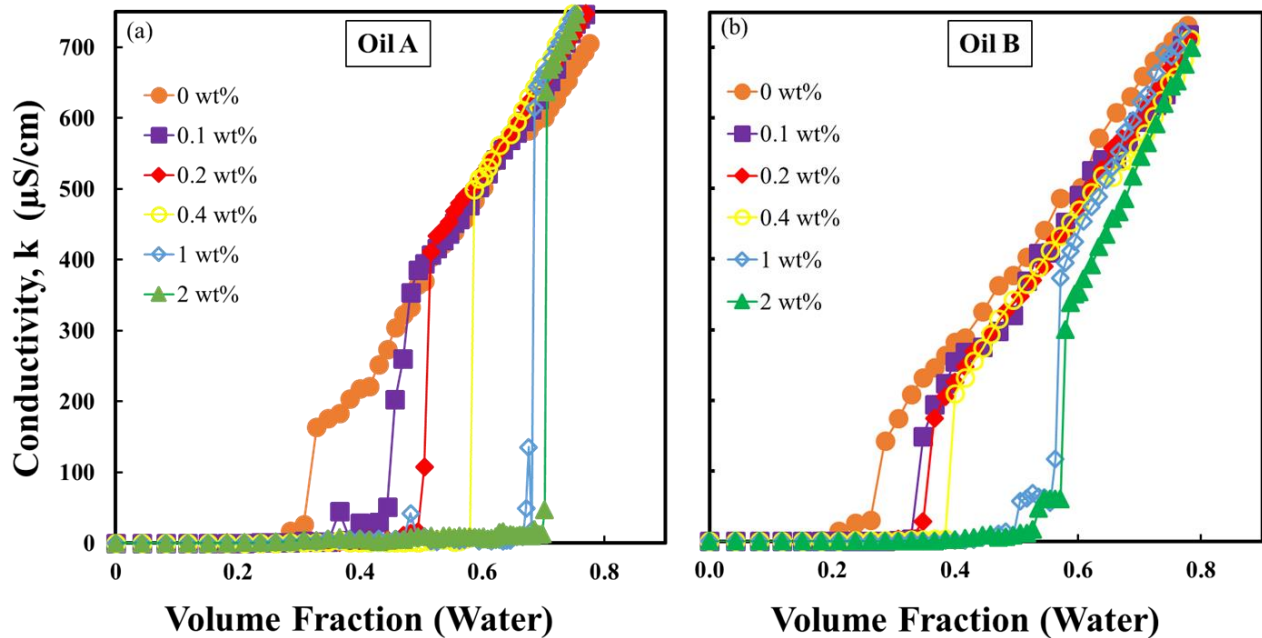


Figure 4-9: Comparison between conductivity data for catastrophic phase inversion from W/O to O/W emulsion as a function of the volume fraction of water by the addition of water to the oil phase. Emulsions are stabilized by hydrophilic starch nanoparticles (HSNP) in (a) Oil A – 15 cSt @ 40°C/104°F and (b) Oil B – 36.1 cSt @ 40°C/104°F. Particle concentrations are 0 (filled circle), 0.1 (filled square), 0.2 (filled diamond), 0.4 (open circle), 1 (open diamond) and 2 (filled triangle) % by weight based on the aqueous phase.

In summary, the phase inversion of W/O emulsion to O/W emulsion was delayed to higher water volume fractions as the concentrations of HSNP and HOSNP dispersed in the aqueous phase were increased. The critical volume fraction of water increased from 31% to 70 % due to an increase in HSNP concentration from 0 to 2 wt.%. Similarly, the critical volume fraction of water increased from approximately 33% to 73% due to an increase in the HOSNP concentration from 0 to 2 wt. %. As an example, **Figure 4-10** depicts the relationship between the critical volume fraction and the HSNP concentration in weight percent. The volume fraction of water that is required for phase inversion increases with increasing HSNP concentrations and nearly plateaus at about 0.7. Regarding the effect of oil viscosity on phase inversion, it is observed to be more pronounced at high concentrations of nanoparticles.

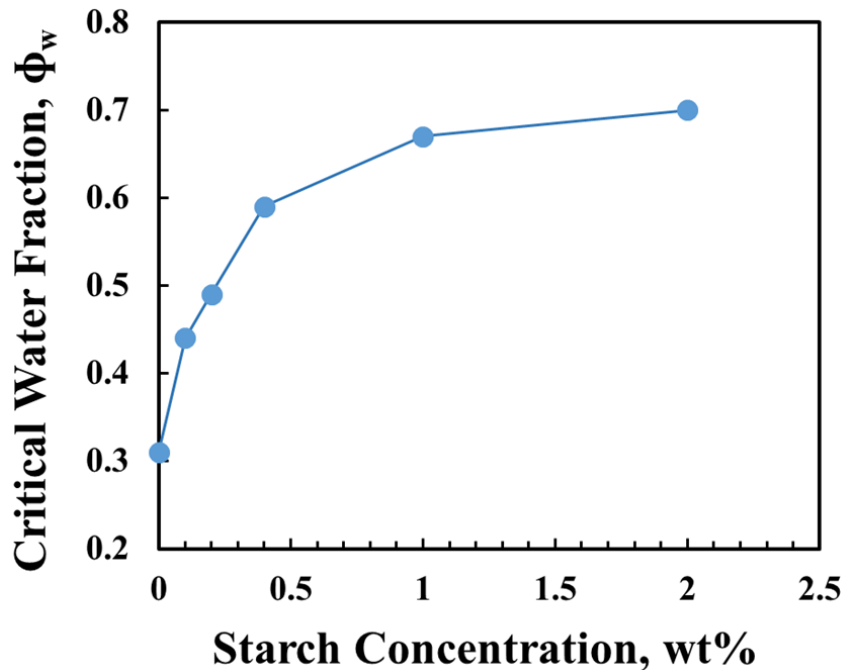


Figure 4-10: Critical Volume Fraction of Water vs HSNP concentration.

4.5.2 Separation Behaviour

The stability of W/O emulsions against coalescence was investigated as a function of starch concentration (varying concentrations of HSNP and HOSNP in the aqueous phase) at a fixed water volume fraction of 0.25. The coalescence of water droplets was monitored by measuring the volume of the aqueous phase separated from the emulsion as a function of time. **Figure 4-11** and **Figure 4-12** show the volume of aqueous phase separated from the emulsion as a function of time for HSNP and HOSNP respectively. In the case of HSNP, the relative instability of the W/O emulsion is evident from **Figure 4-11** as almost all of the aqueous phase is recovered within 400 s, regardless of the starch concentrations used.

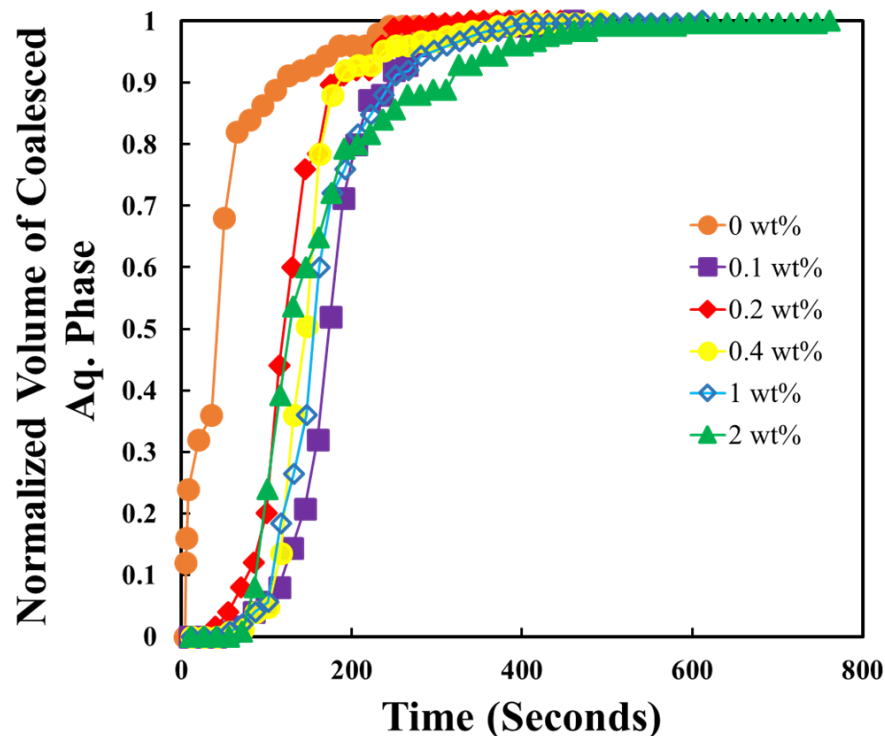


Figure 4-11: Normalized volume of coalesced aqueous phase against time for W/O Emulsion using HSNP. The [HSNP] are 0 (filled circle), 0.1 (filled square), 0.2 (filled diamond), 0.4 (open circle), 1 (open diamond) and 2 (filled triangle) % by weight based on the aqueous phase.

In the case of HOSNP, the W/O emulsion is relatively more stable as the coalescence rate of the aqueous phase droplets decreases with increasing starch concentration (see **Figure 4-12**). The time required for 50% of the aqueous phase to coalesce and separate from emulsion (t_{50}) is shown in **Figure 4-13** for both interfacial additives (HOSNP and HSNP). The rate at which the aqueous phase coalesces and separates from the W/O emulsion is indicative of emulsion stability. The higher the stability of water droplets against coalescence, the slower is the rate of coalescence of the aqueous phase and hence prolonged phase separation. The W/O emulsions stabilized by HSNP were observed to coalesce faster. The time needed to separate 50% of the aqueous phase from the emulsion (t_{50}) was relatively small (162s at 0.1 wt%). The W/O emulsions stabilized by HOSNP exhibited higher stability ($t_{50} = 230$ s at 0.1 wt%) due to higher hydrophobic content. Interestingly both HSNP and HOSNP stabilized emulsions exhibit peaks in

t_{50} at 0.1 and 1 wt% (see **Figure 4-13**) starch nanoparticle concentrations. At about 0.2 wt% starch, t_{50} plots exhibit a minimum. The exact reasons for maxima and minima observed in t_{50} plots are not clear.

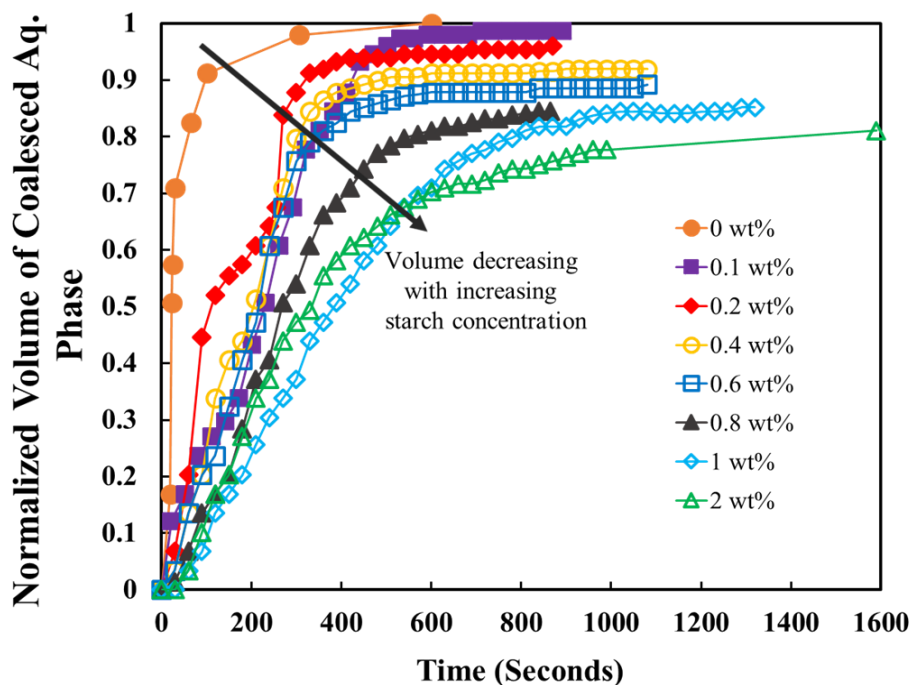


Figure 4-12: Normalized volume of coalesced aqueous phase against time for W/O Emulsion using HOSNP. The [HOSNP] are 0 (filled circle), 0.1 (filled square), 0.2 (filled diamond), 0.4 (open circle), 0.6 (open square), 0.8 (filled triangle), 1 (open diamond) and 2 (open triangle) % by weight based on the aqueous phase.

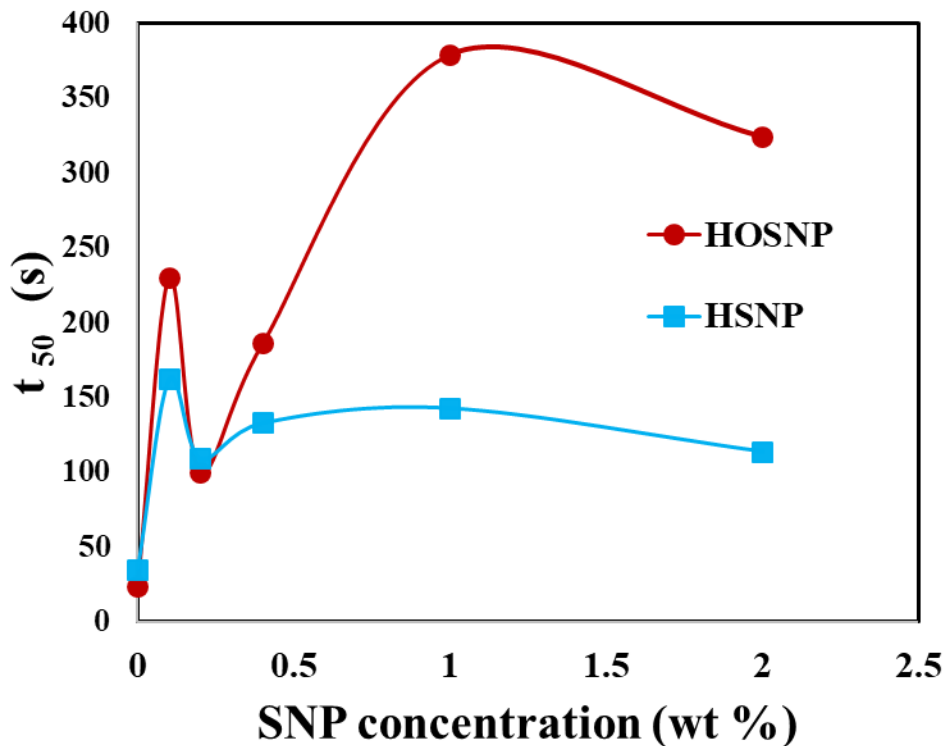


Figure 4-13: Time at 50% phase separation as a function of starch concentration for 0, 0.1, 0.2, 0.4, 1 and 2% by weight based on the aqueous phase (pre-inversion) respectively. [HOSNP] - Filled circle and [HSNP] - filled square.

4.5.3 Interfacial Tension (IFT)

The effects of HSNP and HOSNP on interfacial tension at the oil-water interface were investigated to confirm the stability behaviour of starch-stabilized W/O emulsions. The surface tensions of pure mineral oil and water, measured at room temperature, were 30 ± 0.2 mN/m and 72.89 ± 0.11 mN/m, respectively in agreement with the literature[113].

Figure 4-14 shows the dynamic interfacial tension measurements at the mineral oil-water interface during the adsorption of HSNP on a pendant drop of water in oil. The results presented elucidate the dependence of the oil-water interfacial tension on the starch concentration of the aqueous phase with and without 0.01M sodium chloride and 0.15% biocide present in the

aqueous phase. As can be seen in the plots, the interfacial tension decreases with the ageing of the droplet due to gradual adsorption of HSNP at the droplet-oil interface. The interfacial tension also decreases with an increase in the concentration of HSNP (0.1 and 1% by weight in the aqueous phase). This observation is consistent with the reduction in interfacial tension of oil-water systems reported in the literature[114] upon the adsorption of nanoparticles at the droplet surface. To ascertain the influence of salt and biocide on the interfacial tension, the experiments were repeated with HSNP dispersed in ultra-pure water. The results are shown in **Figure 4-14b**. The observed dynamic interfacial tensions were much higher when salt and biocides were present in the aqueous phase. It has been shown in the literature[115] that the presence of salts in solution impacts interfacial activity by lessening the solution's ability to reduce interfacial tension.

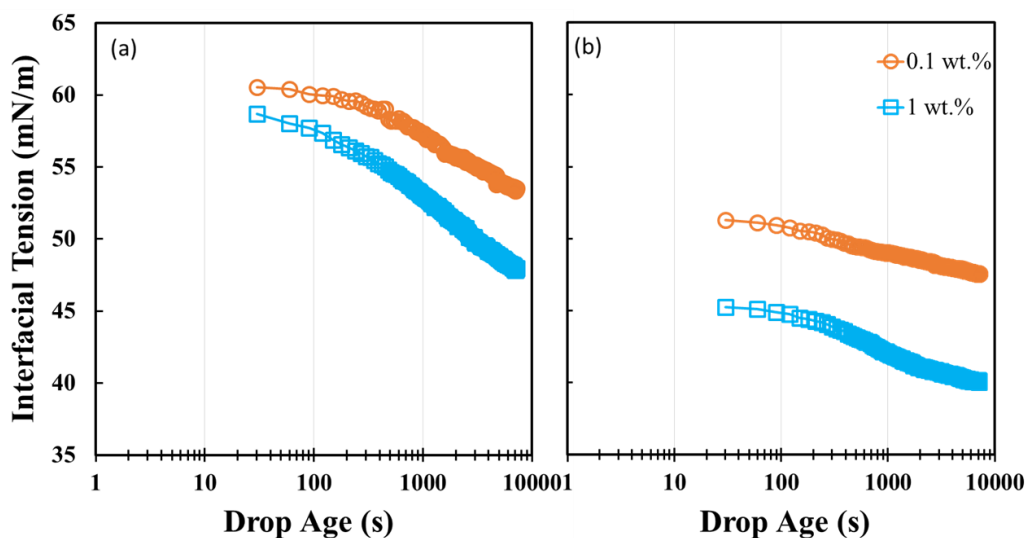


Figure 4-14: Dynamic interfacial tension measurements at mineral oil-water interface containing HSNP solutions in concentrations 0.1 (open circle) and 1 (open square) % by weight dispersed in (a) 0.01M NaCl and 0.15% biocide (b) Pure water.

Figure 4-15 shows the variation of the mineral oil-water interfacial tension with the HOSNP concentration in water. As observed in the case of HSNP, the interfacial tension decreases with

the ageing of the droplet. Interestingly, the interfacial tension now increases with the increase in the additive (HOSNP) concentration from 0.1 to 1 wt%. However, with the ageing of the droplet, the difference in interfacial tension due to different additive concentrations decreases. It appears from the plots shown in **Figure 4-15** that the interfacial tension at higher concentrations of additive eventually becomes less than that observed at lower additive concentration. This behaviour of lower interfacial tension supports the higher stability results obtained at high HOSNP concentrations during the phase inversion experiments. Based on the interfacial tension measurements, it is likely that aggregates of HOSNP nanoparticles are formed initially, which then slowly migrate to the interface as the drop ages. The subsequent much-reduced interfacial tension could be due to the rearrangement of the aggregates at the interface. Chevalier and Bolzinger [3] explained the possibility of this occurrence when nanoparticles exhibit a tendency to aggregate in water.

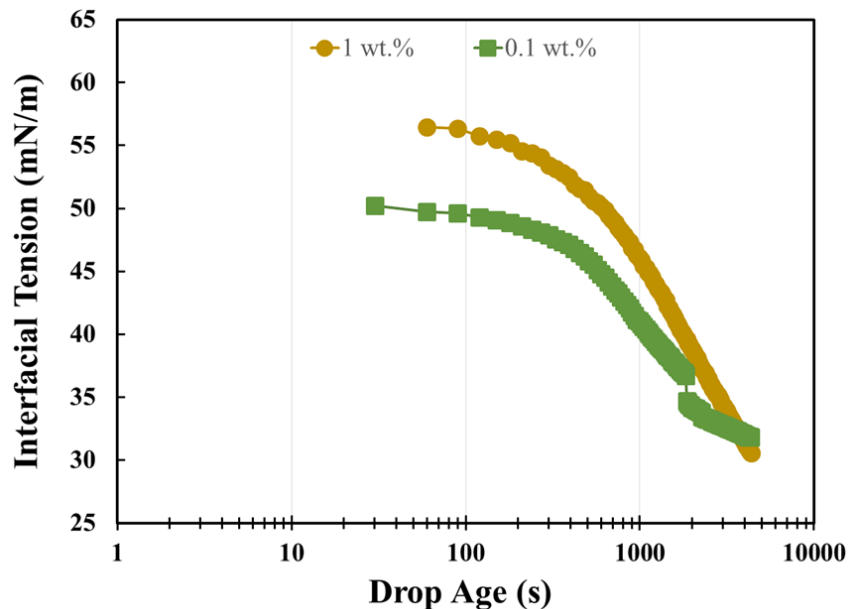


Figure 4-15: Dynamic Interfacial Tension measurements at mineral oil-water interface containing HOSNP solutions in concentrations 0.1 (filled square) and 1 (filled circle) % by weight.

4.5.4 Contact Angle

The contact angle (θ) made by the particles with the oil/water interface dictates the stability of solid-stabilized emulsions[69]. Hydrophobicity has been shown to depict the preferred emulsion type by particles. Hence, the stability of emulsion was evaluated based on the wettability of the adsorbed particles as depicted by the θ . The 3-phase contact angle for the HSNP and HOSNP was measured using the sessile drop method. **Figure 4-16** shows the images of the 3-phase contact angle formed by 50 μ L water dispensed onto the surface of pelletized HSNP and HOSNP immersed in the oil phase respectively. The advancing contact angles for HSNP and HOSNP were estimated to be $46 \pm 2.2^\circ$ and $120 \pm 3.1^\circ$ respectively, measured through the water phase. The results indicate that HSNP and HOSNP are suitable for Pickering emulsion stabilization. The contact angles are within the intermediate wettability range confirming that the particles are adsorbed irreversibly at the oil/water interface leading to the formation of stable emulsions. This observation is consistent with the literature[63].

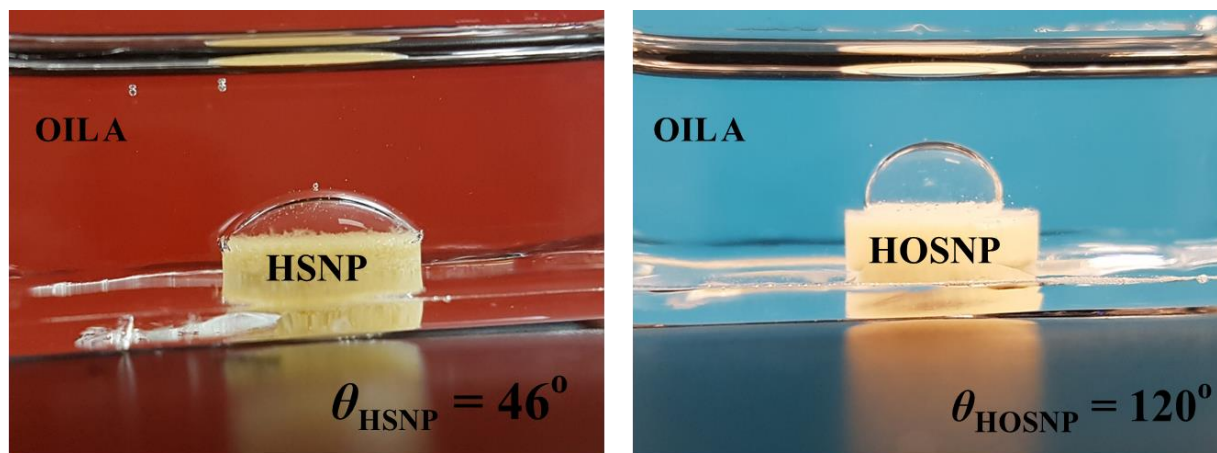


Figure 4-16: Images of Sessile Drop on Pelletized Starch Immersed in the Oil Phase

4.5.5 Synergistic effect of HSNP-CTAB system on the phase inversion

Initial investigation of the phase inversion of W/O to O/W emulsion was explored with varying concentrations of CTAB ranging from 0 to 0.5 wt.% in the aqueous phase. This was essential to identify the effects of only CTAB on W/O emulsion before investigating the synergistic effects of both HSNP and CTAB. CTAB addition impacted the phase inversion of W/O to O/W emulsions as shown in **Figure 4-17** and **Figure 4-18**. With the addition of CTAB, an initial increase in the critical volume fraction was observed, which peaked at 0.05wt.%, implying a delayed inversion. Beyond the CMC region, the critical volume fraction decreased which favours the formation of oil-water emulsions.

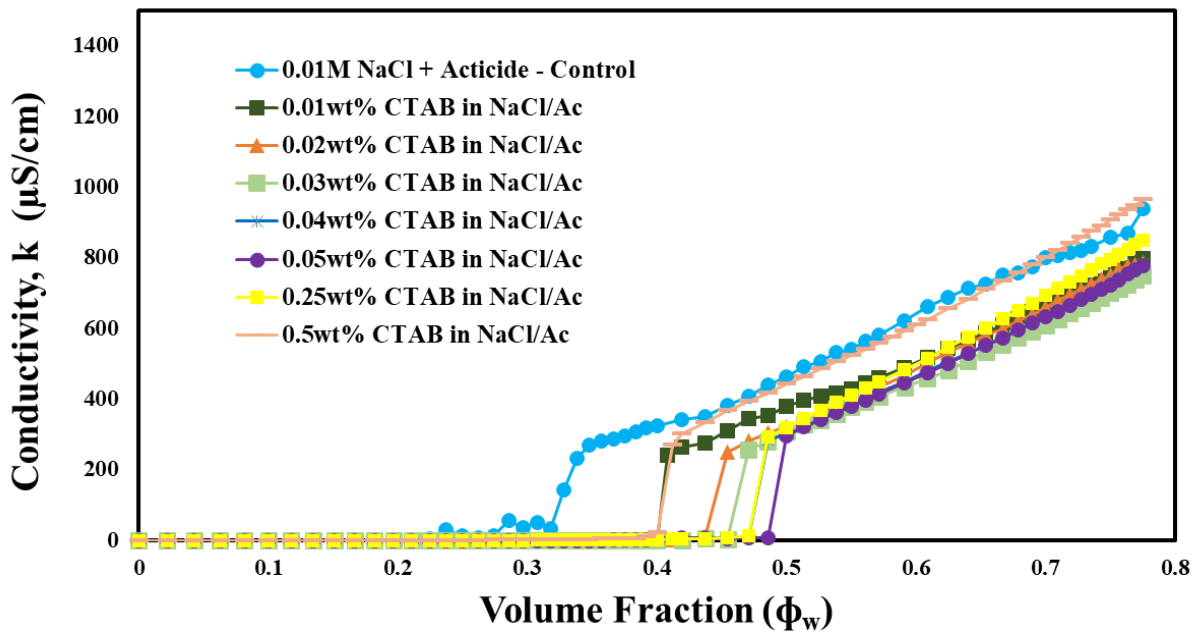


Figure 4-17: Conductivity data for W/O to O/W phase inversions of CTAB in an electrolyte medium (0.01M NaCl/Ac) at varying concentrations.

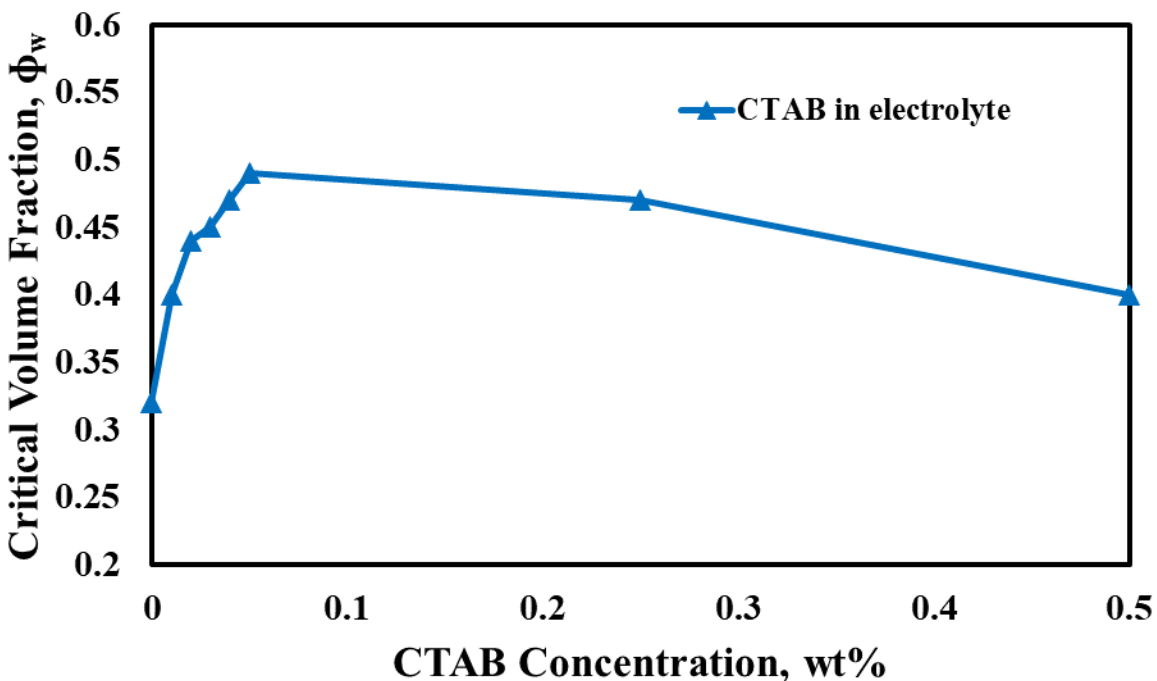


Figure 4-18: Critical Volume Fraction of water versus CTAB concentration (0, 0.01, 0.02, 0.03, 0.04, 0.05, 0.25 and 0.5 wt%)

Subsequently, the effects of different concentrations of CTAB on HSNP stabilized W/O emulsion at constant HSNP concentration were investigated. **Figure 4-19** shows the inversion point as a function of varying CTAB concentrations (0, 0.01, 0.02, 0.03, 0.04, 0.05, 0.25 and 0.5 wt.%) at constant HSNP concentration of 1wt%. As shown in **Figure 4-20**, an increase in the concentration of CTAB resulted in an initial drop in the phase inversion point. Around the CMC concentration (0.01 and 0.05wt%), no significant change was noticed. This observation could be due to the formation of micelles in the bulk phase. After that, the phase inversion point eventually decreased beyond the CMC point. Hence, CTAB addition favours early inversion of W/O to O/W emulsions.

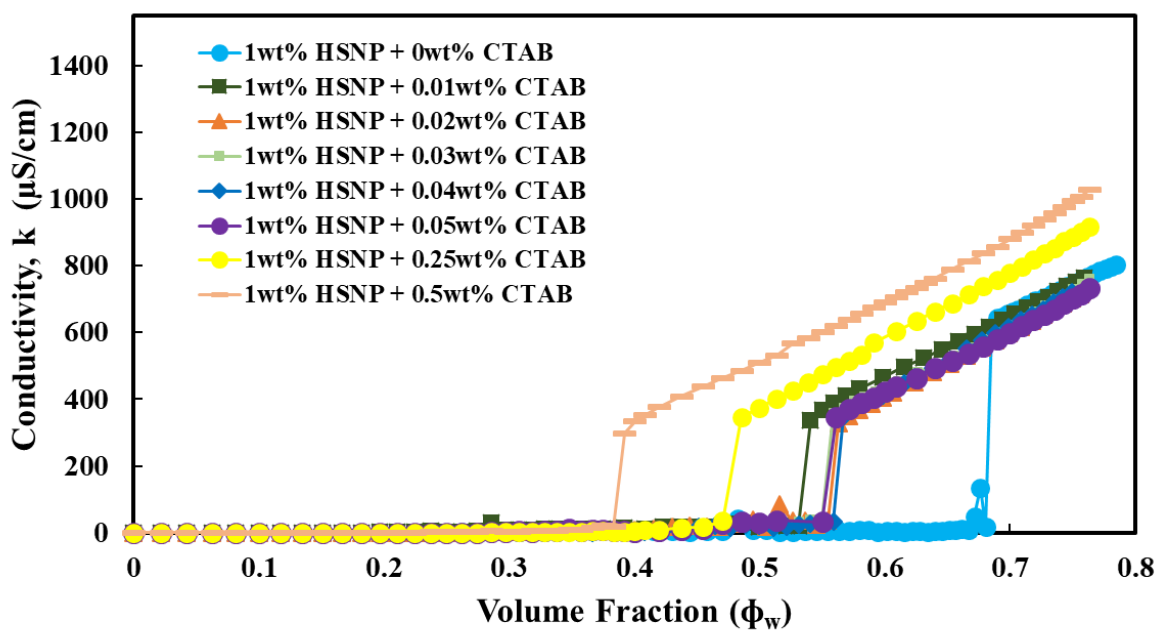


Figure 4-19: Conductivity data for W/O to O/W phase inversions of HSNP-CTAB mixture at fixed 1wt.% HSNP concentration and varying CTAB concentrations.

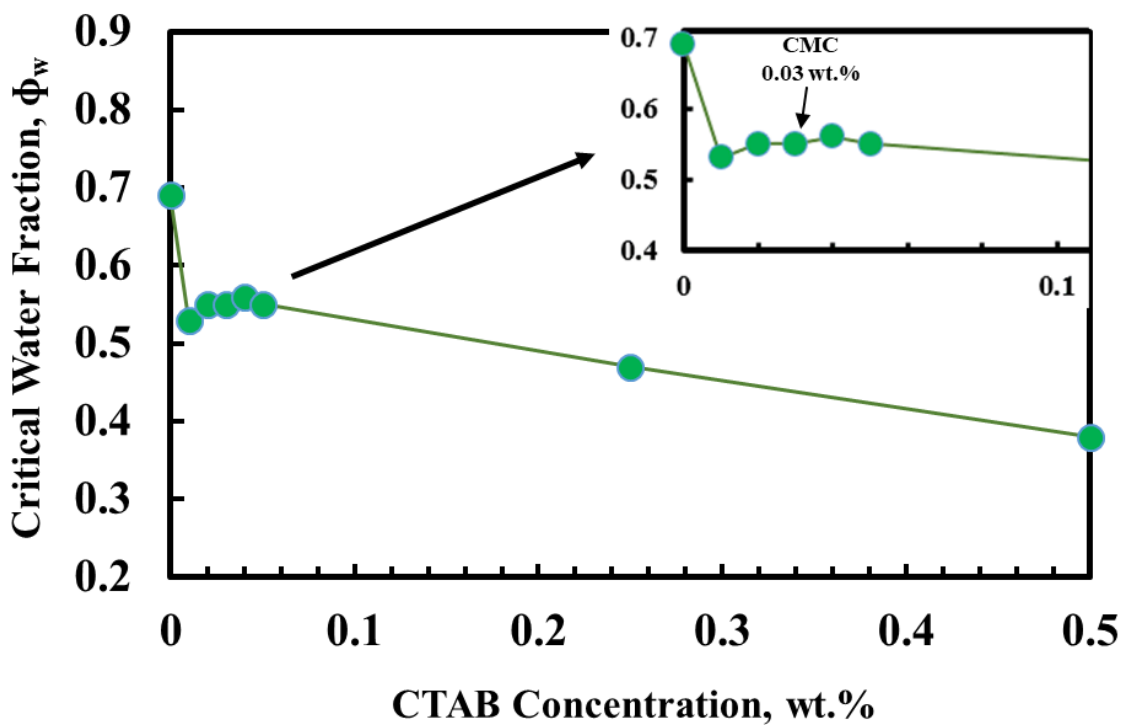


Figure 4-20: Critical Volume Fraction of water at fixed 1wt.% HSNP against CTAB concentration (0, 0.01, 0.02, 0.03, 0.04, 0.05, 0.25, 0.5 and 1wt%).

4.5.5.1 Separation Behaviour

The separation behaviour of the W/O emulsion at a fixed concentration of HSNP in the aqueous phase and fixed water volume fraction of 0.25 was investigated as a function of CTAB concentration as described by Ogunlaja et al[116]. The volume of the aqueous phase separated from the emulsion as a function of time is shown in **Figure 4-21** for HSNP. The time required for 50% of the aqueous phase to coalesce and separate from emulsion (t_{50}) is shown in **Figure 4-22**. **Figure 4-22** shows a faster rate of coalescence of the aqueous phase at low concentrations of CTAB; hence O/W emulsions are favoured as a result of CTAB addition. This favorability is slowed down around the CMC region. Further data beyond the 0.05wt.% was not possible because HSNP-CTAB solutions with CTAB concentrations beyond 0.05wt% foamed excessively.

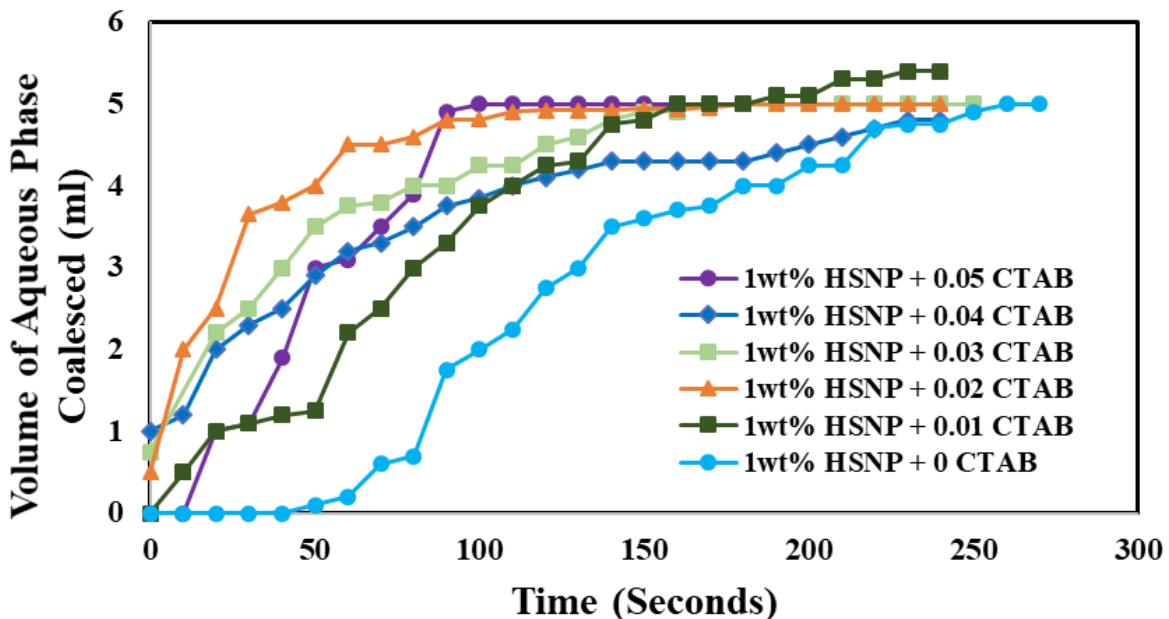


Figure 4-21: Volume of coalesced aqueous phase against time for W/O emulsion for HSNP - CTAB mixture at fixed 1wt% HSNP and varying CTAB concentration at a fixed ϕ_w of 0.25

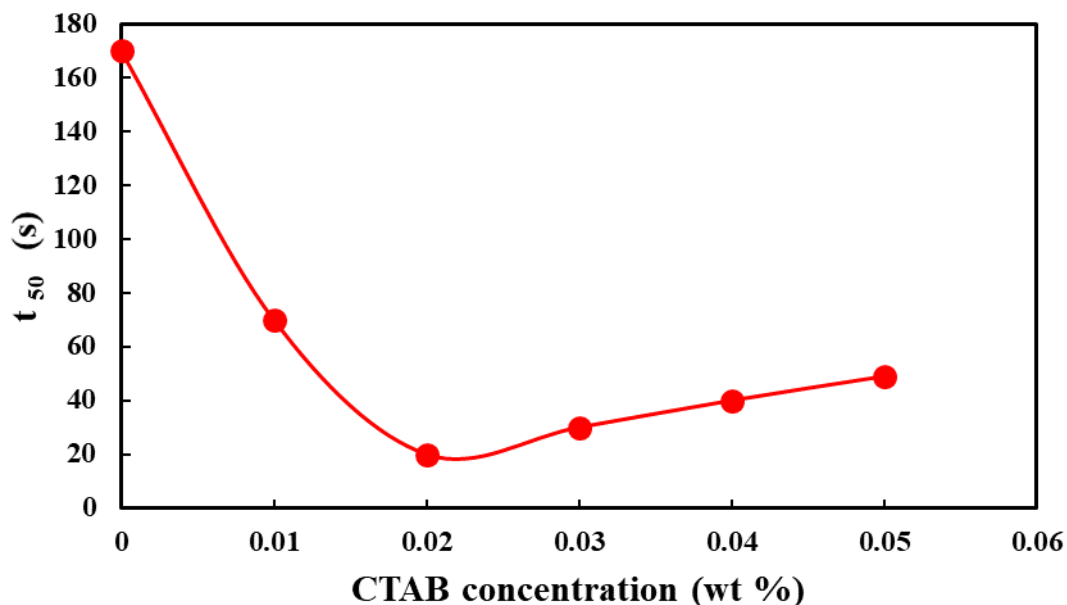


Figure 4-22: Time for 50% phase separation with constant 1wt.% HSNP as a function of CTAB concentrations of 0, 0.01, 0.02, 0.03, 0.04 and 0.05wt.% by weight based on the aqueous phase (pre-inversion) and a fixed volume fraction of water, ϕ_w of 0.25 respectively.

Figure 4-23 shows a comparison between the critical volume fraction of HSNP/CTAB hybrid (HSNP concentration is fixed at 1wt%) and CTAB only as a function of CTAB concentration in weight%. It is observed that the CTAB promotion of O/W emulsion is always enhanced in the presence of HSNP. As seen in the orange plot, the presence of CTAB instantly sped up the phase inversion phenomenon thereby decreasing the critical volume fraction of water from 69% to 63% due to the addition of 0.01 wt.% CTAB. Around the CMC region, the inversion seemed to hover around the volume fraction of 55%, beyond this region, O/W is again favoured. Whereas for CTAB alone in the electrolyte medium, W/O emulsion was initially favoured with an increase in the volume fraction of water from 31% to 49% until the CMC region where the behaviour is reversed and O/W is favoured once again.

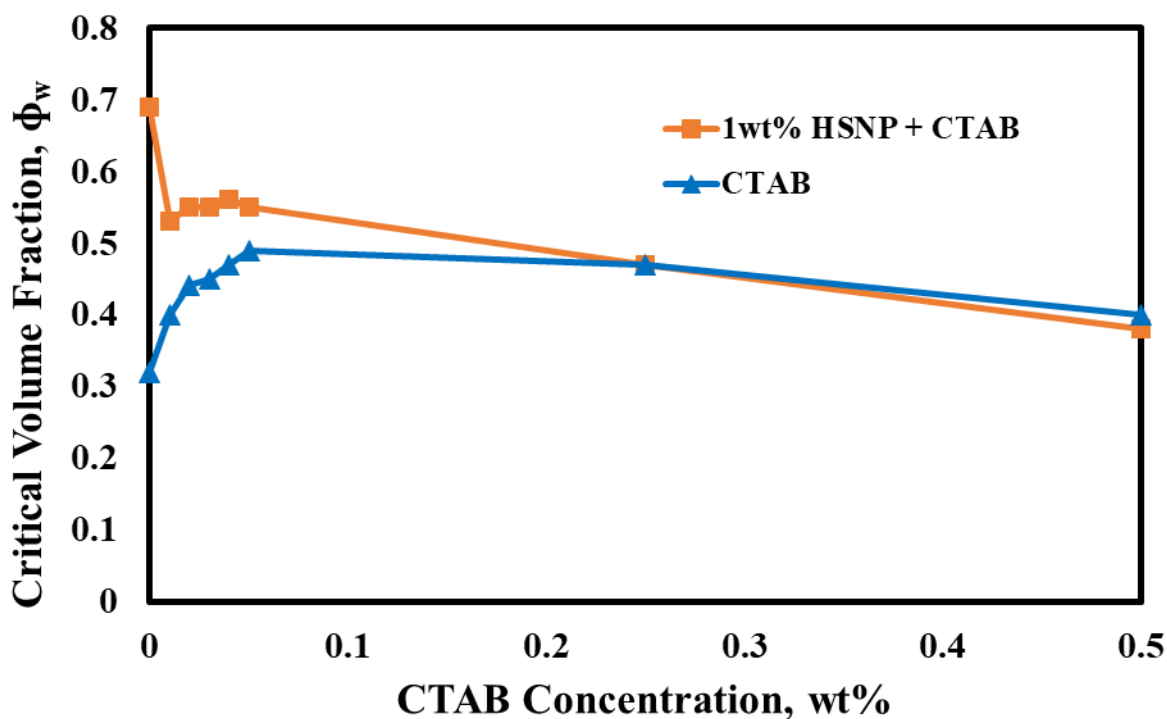


Figure 4-23: Comparison of Critical Volume Fraction of water against CTAB concentration in wt.% for HSNP/CTAB (Orange) and CTAB only (Blue) W/O emulsions.

4.5.5.2 Surface tension of HSNP/CTAB solutions

Surface tension experiments were performed to probe the interfacial properties of CTAB mainly at lower concentrations around the CMC range observed in phase inversion experiments as shown in **Figure 4-24**. The following observations were realized during the surface tension experiments. Using CTAB alone in the lower concentration range of 0.01 to 0.05 wt%, there was no significant difference in the observed surface tension with respect to the drop age. For 1wt% HSNP, the surface tension was observed to decrease as the drop ages. Thermal degradation of drop hindered longer run times as previously presented. Upon the addition of 1wt% HSNP to the same CTAB concentration range of CTAB, the surface tension further decreased with increasing CTAB concentration, showing the possible effect of HSNP.

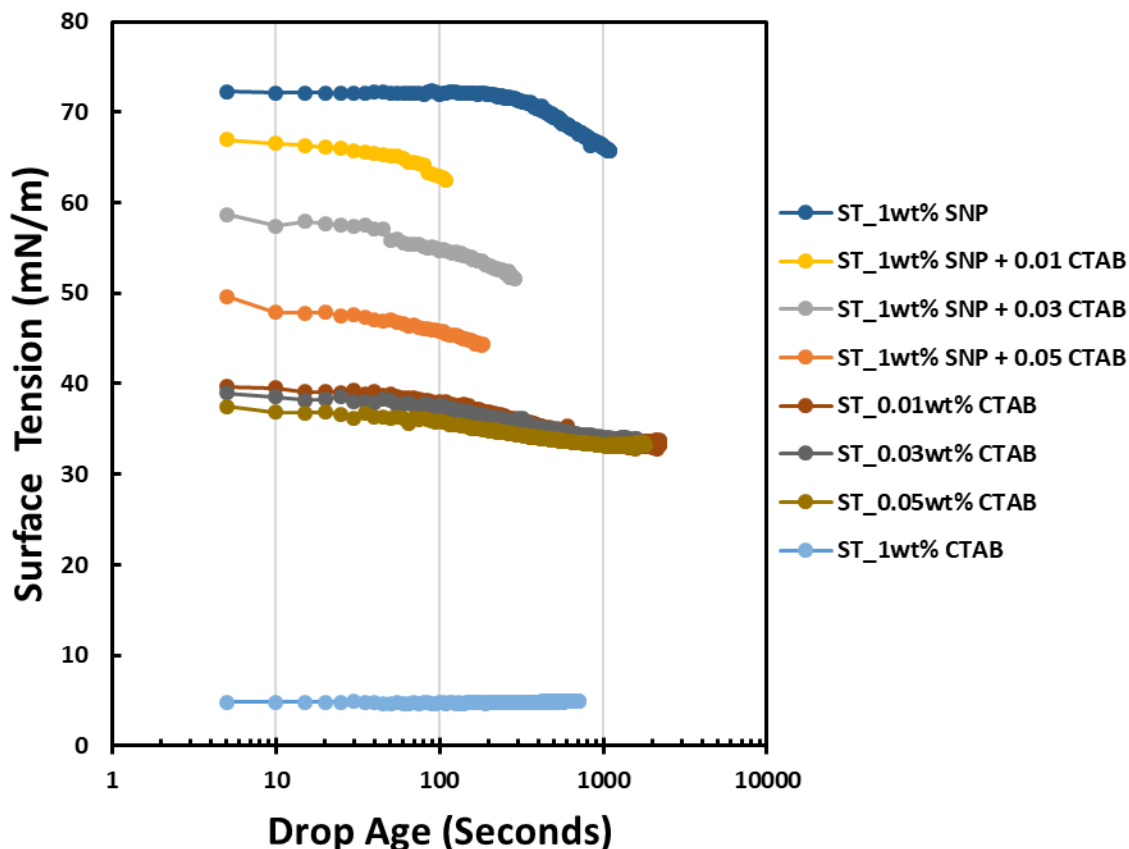


Figure 4-24: Surface tension measurements of water droplets containing 1wt% HSNP with and without CTAB (concentrations of 0.01, 0.03 and 0.05wt%) versus the drop age.

4.5.6 Synergistic effects of HSNP and Nanoclay in Non-electrolyte medium

The stabilization effect of HSNP/nanoclay hybrids was conducted in a pure non-electrolyte aqueous phase without the addition of preservatives. Bentonite nanoclay was chosen as the co-stabilizer with no addition of acticide and salt.

4.5.6.1 Effects of Stabilizing water-in-oil emulsion at different concentrations of Hydrophilic Starch Nanoparticle (HSNP) in MilliQ

HSNP concentrations were varied from 0 to 1% by weight based on the aqueous phase. The dispersions were allowed to cool down and used as-is for the phase inversion experiment. **Figure**

4-25 shows that the phase inversion point was delayed with increasing HSNP concentration up to the critical volume fraction point as observed previously. Catastrophic phase inversion of the emulsion from W/O to O/W occurs at a water volume fraction of approximately 0.48, 0.34, 0.26, 0.33 and 0.52 for 0.1, 0.2, 0.4, 1 and 2 wt.% HSNP respectively.

However, an interesting inversion behaviour was noticed at all concentrations except for 0.1 and 2wt%. For 0.2, 0.4 and 1wt.%, the W/O initially inverted to a mid-O/W. At this level, despite the continuous addition of the aqueous phase to the emulsion, the conductivity remains relatively the same and later drops to a lower conductivity and then proceeded to increase and eventually to a final O/W phase. In addition, it was also observed that the higher the concentration of the HSNP, the longer the emulsion stays at the mid-O/W phase. This signifies that the different concentrations of the HSNP affect the characteristics of the W/O phase inversion.

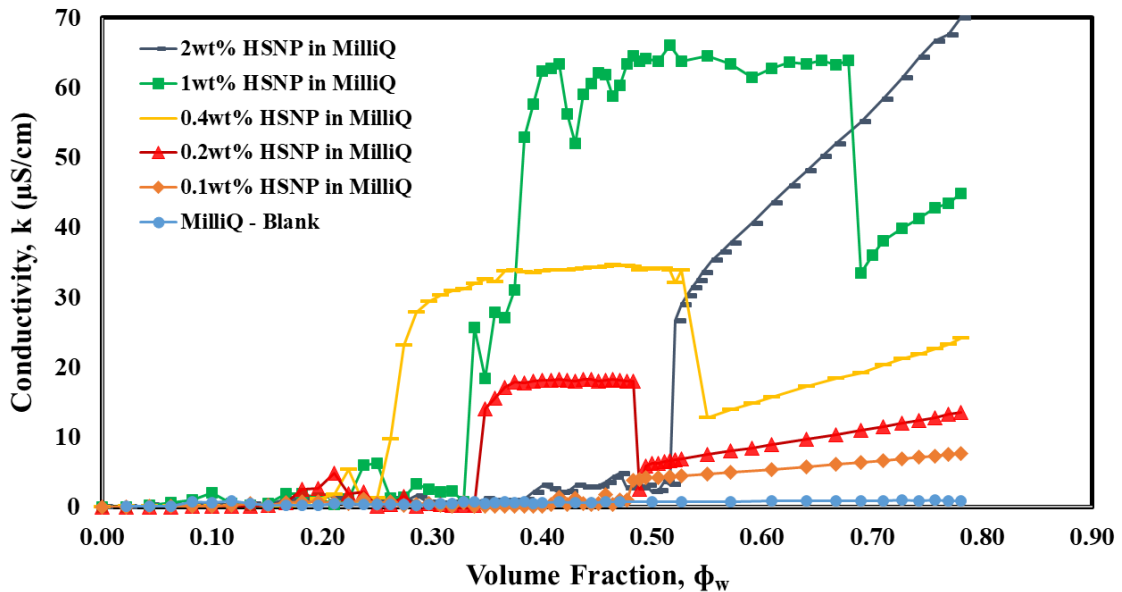


Figure 4-25: Conductivity of water-mineral oil emulsions stabilized by HSNP as a function of the volume fraction of water.

4.5.6.2 Confocal Laser Scanning Microscopic Analysis of Emulsions

To further explain the observed trend in **Figure 4-25**, it was hypothesized that the starch nanoparticles are forming a shell-like nanoparticulate layer on the oil-water interface. Confocal laser scanning microscopy (CLSM) was used to explain the stability effect of HSNPs. HSNPs and mineral oil are non-fluorescent; Nile blue and Nile red were used as fluorescence dyes to visualize them under the microscope respectively. **Figure 4-26** shows the bright field and confocal laser scanning microscopy images of mineral oil-in-water emulsion stabilized by 1wt% HSNP. HSNPs are visualized to coat the surface of the droplets and hindering coalescence.

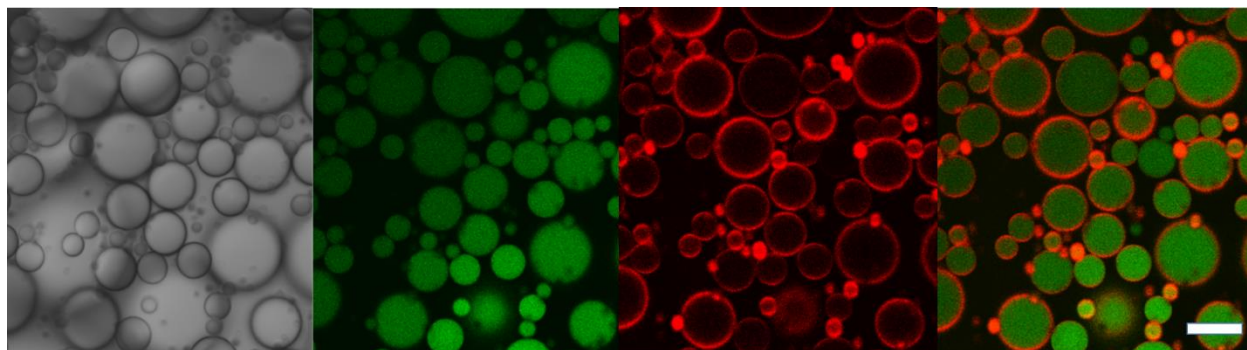


Figure 4-26: Bright-field (BF) and confocal laser scanning microscopy (CLSM) images of mineral oil-in-water (1:1 by volume) emulsions stabilized by 1wt.% HSNP. A water-soluble fluorescent dye, Nile blue, which binds to HSNP was used to stain the starch and is coded red; the oil phase was stained Nile Red and is coded green. The scale bar corresponds to 50 μ m.

4.5.6.3 Effects of HSNP/Nanoclay Hybrid on phase inversion in MilliQ

The synergistic effect of HSNP/Nanoclay hybrid on phase inversion of mineral oil-water emulsions was investigated. Dispersed solutions of 1wt% HSNP and 1wt% nanoclay, mixed in the ratio 20:80, 50:50 and 80:20 respectively were employed as the aqueous phase. The variation in the conductivity against the water volume fraction is shown in **Figure 4-27**. The observed behaviour is similar to what was observed for 1wt% HSNP in MilliQ in **Figure 4-25** above. The W/O inverts to mid-O/W, thereafter, despite the continuous addition of the aqueous phase to the

emulsion, the conductivity remains relatively the same and later drops to a lower conductivity and then proceeded to increase and eventually to a final O/W phase. It was seen that as the clay fraction of the HSNP/clay mixture increases, the higher the conductivity range at which the mid-O/W emulsion peaked before reverting to the final O/W emulsion and the length of time spent and the volume fraction in this transitioning mid-O/W stage reduced with increasing clay content. This signifies that the presence of the nanoclay in the HSNP/nanoclay mixture seems to have an effect on the overall behaviour of the W/O emulsion.

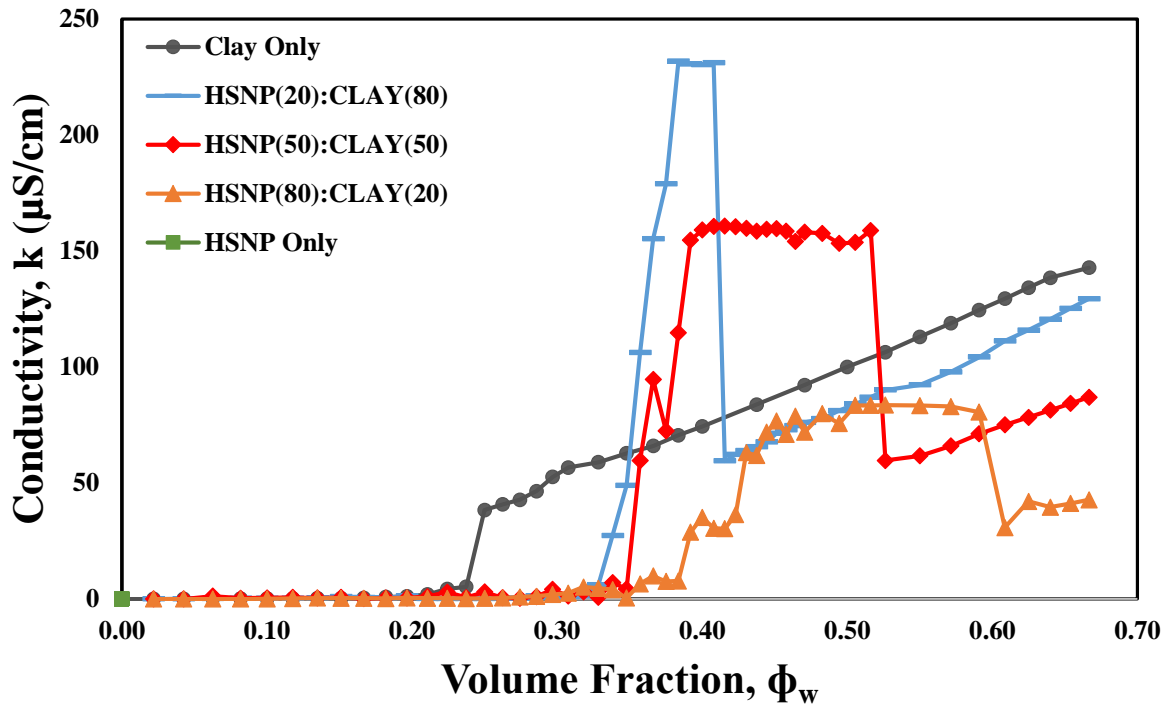


Figure 4-27: Conductivity of water-mineral oil emulsions stabilized by 1wt% HSNP: 1wt% Clay hybrid as a function of the volume function of water

4.6 Conclusions

The following conclusions can be drawn concerning the effects of HSNP and HOSNP nanoparticles on phase inversion and stability of Pickering emulsions:

- Both HSNPs and HOSNP are effective in delaying the phase inversion of emulsion from W/O type to O/W type. There is a direct correlation between the delay in phase inversion and the increasing concentration of the nanoparticles. In the absence of nanoparticles, the catastrophic phase inversion of W/O to O/W type emulsion occurs at approximately 0.3 volume fraction of water. However, this critical volume fraction increases with the increase in the nanoparticle concentration in the aqueous phase.
- The stability of W/O emulsions with respect to the coalescence of droplets increases with the increase in nanoparticle concentration and nanoparticle hydrophobicity.
- With the higher viscosity oil, the phase inversion of W/O to O/W type emulsion occurs earlier, depicting relatively less stable emulsions.
- The interfacial tension between water and mineral oil decreases with time at different concentrations of nanoparticles.
- For HSNPs, the interfacial tension-time plot shifts towards lower values with the increase in the nanoparticle concentration.
- For HOSNP, the interfacial tension decreases as the drop ages like in the case of HSNPs. However, the opposite effect is observed with respect to nanoparticle concentration. At a high nanoparticle concentration, the interfacial tension values are observed to be higher initially due to the aggregation of nanoparticles. The migration of nanoparticles to the interface is expected to occur slowly due to the aggregation of nanoparticles. However, the steady-state interfacial tension values tend to decrease with the increase in the nanoparticle concentration, as expected.

- The measured contact angles are within the intermediate wettability range that confirms the effectively irreversible adsorption of nanoparticles at the oil/water interface resulting in stable emulsions.
- Different concentrations of the HSNP and nanoclay, either separately or combined as a mixture can affect the characteristics of W/O emulsion phase inversion, following similar trends.

Chapter 5: Effects of Bentonite Nanoclay and Cetyltrimethyl Ammonium Bromide Modified Bentonite on Phase Inversion of Water-In-Oil Emulsions

An abridged version of this chapter was published in the Colloids and Interfaces journal and under the authorship of Sileola B Ogunlaja and Rajinder Pal

5.1 Introduction

Various types of solid materials that have been used as particulate stabilizers for water-in-oil (W/O) or oil-in-water (O/W) emulsions include clays, silica, iron oxides, barium sulphate, alumina and calcium carbonate [64]. One of the crucial characteristics of these particles that impacts their effectiveness in stabilizing emulsions is their wettability[51], [63]. Particles with contact angle greater than 90° tend to form stable W/O emulsions whereas particles with contact angle smaller than 90° tend to form stable O/W emulsions[117]. The wettability of the solid particles has been known to be altered by surface modification using surfactants[64]. The trapping of particles at the oil-water interface is controlled by the particle wettability. At the interface, the particle experiences a potential energy minimum, which is directly related to the contact angle. Equation (5.1) gives the Gibbs free energy (ΔG) required to remove a particle (of radius r) from the interface to the potential energy reduction for attachment of the particle at the interface [63].

$$\Delta G = \pi r^2 \gamma_{ow} (1 \pm \cos \theta_{ow})^2 \quad (5.1)$$

where γ_{ow} is the interfacial tension of the oil-water interface and θ_{ow} is the three-phase contact angle the particle makes with the o/w interface measured through the water phase. The fluid into

which the particle is removed dictates the sign on the $\cos \theta_{ow}$. It is negative when the particle is removed into water.

Clays are a broad class of inorganic layered structures. Bentonite is a smectite clay mineral type, an absorbent aluminum phyllosilicate clay, also referred to as Montmorillonite (MMT) [118], [119]. MMT is commonly used in research studies for the synthesis of organoclays due to its abundance, adsorption properties, high cation exchange capacity, nanometric dimensions, high aspect ratio and extreme water-swelling characteristics [120]–[122]. The stabilization effect of nanoclays in multicomponent systems has attracted interest in a wide range of applications in the industry due to its economic and environmental benefits [5], [73], [117], [123], [124].

The homogenization of a mixture of aqueous and non-aqueous phases by means of high-shear mechanical agitation, yielding either a W/O emulsion or an O/W emulsion, is mostly enhanced by the addition of particulate modifiers like nanoclays. The particulate modifiers are able to migrate to the interface, forming a Pickering interface with a high interfacial shear modulus [84]. With the help of a surfactant, poorly hydrophobic nanoclays can be modified such that they can be preferentially located at the oil-water interface. The adsorption of cationic surfactants at low aqueous concentrations has been shown to alter the wettability of mineral surfaces by making them more hydrophobic [125]–[127]. A cationic surfactant such as cetyl trimethyl ammonium bromide (CTAB), is hereby expected to readily attach itself to negatively charged clay surfaces via columbic attraction [125]. **Figure 5-1** shows a schematic diagram illustrating the multiscale representation of W/O emulsion stabilized by surfactant-modified nanoclay before the occurrence of phase inversion.

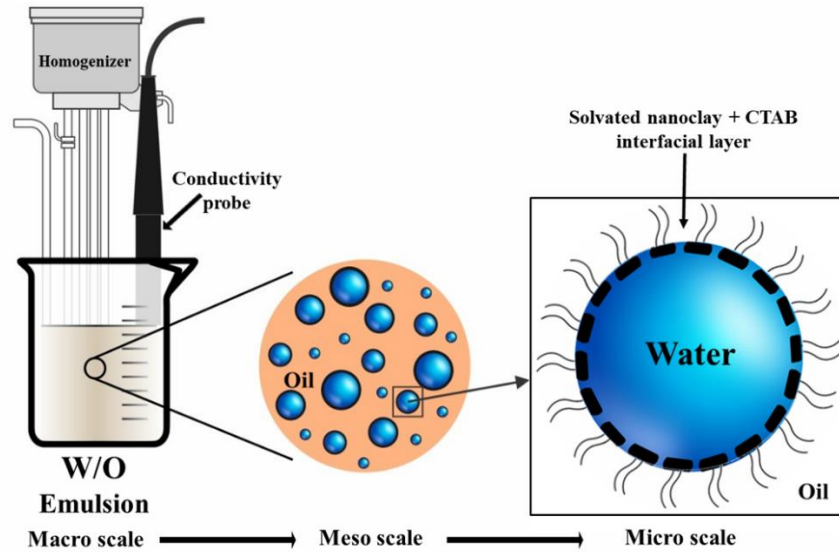


Figure 5-1: Schematic of a multiscale W/O emulsion system with an emphasis on water droplet stabilized by surfactant modified nanoclay.

The aim of this study is to evaluate the stability of nanoclay stabilized W/O emulsions formulated with various degrees of surfactant modification of nanoclay. The effects of unmodified and surfactant-modified nanoclay on catastrophic phase inversion of W/O emulsion to O/W emulsion are determined experimentally. The adsorption of CTAB on to the nanoclay has a strong influence on the three-phase contact angle as well as the critical volume fraction of water where phase inversion takes place from W/O to O/W emulsion.

5.2 Materials and Methodology

5.2.1 Materials

The hydrophilic bentonite nanoclay powder purchased from Sigma Aldrich consists of 98% sodium montmorillonite. The particles of untreated nanoclay powder are approximately 6-micron in size. The powder particles are agglomerates of the clay layer stacks, which disperse fully into a nano-sized dimension in water due to the strong hydrophilicity of clay. The exfoliated clay has a thickness of 1 nm and a lateral dimension of 100-150 nm. The agglomerates of the clay layer

stacks disperse fully into a nano-sized dimension in water due to the strong hydrophilicity of clay. Cationic surfactant, CTAB was purchased from Sigma Aldrich chemicals. Both nanoclay and surfactant were used as received. White mineral oil (PetroCanada) was used to prepare the emulsions. Ultrapure water with a resistivity of 18.2 M Ω , surface tension of 71.5 mN/m and pH of 6-7 at 25 °C was used for the preparation of emulsions.

5.2.2 Methodology

5.2.2.1 Aqueous Dispersions of Nanoclay

The dispersions of various concentrations of the hydrophilic bentonite nanoclay powder were prepared using the Gifford-Wood homogenizer as previously described elsewhere [116]. In brief, a known amount of the nanoclay was dispersed into the ultra-pure water at 5wt% without any chemical addition. Lower nanoclay concentrations were obtained by serial dilution. The emulsions were homogenized using Gifford-Wood homogenizer at 5500 rpm for 45 minutes. Conductivity, temperature and pH parameters were recorded immediately after homogenization. Care was taken to ensure that the same condition was maintained for all experiments to allow a true comparison of data.

5.2.2.2 Preparation of CTAB-Modified Bentonite Nanoclay

The aqueous nanoclay-CTAB samples were prepared with a fixed nanoclay concentration of 1wt% obtained from serial dilution of the stock 5wt.% solution. While stirring with the homogenizer, a measured amount of the cationic surfactant, CTAB is added gradually at room temperature in different concentrations ranging from 0.01 to 0.5wt% to impact the hydrophobicity of the nanoclay. This mixture which constituted the NC-Bt-CTAB hybrid was stirred at 600 rpm for 20 hours using a magnetic stirrer and kept at a temperature of 25 \pm 0.9°C. To ensure equilibration, an equilibrium time of 20 hours was selected for all experiments. The

NC-Bt-CTAB dispersions showed excessive coagulation beyond CTAB concentrations of 0.1wt%. Conductivity, pH, and temperature of the solutions were recorded before further analysis.

5.2.2.3 Preparation of Emulsions

The W/O emulsions were prepared using the Gifford-Wood homogenizer by sequentially adding the aqueous phase (solutions of nanoclay, with and without surfactant) to a fixed volume of the agitated continuous oil phase. Conductivity, pH, and temperature data of emulsion were taken after each addition.

5.2.2.4 Confocal Microscopy

The adsorption of the CTAB modified nanoclay particles on the oil droplet surface results in increased emulsion stabilization. **Figure 5-2** shows the use of a laser-induced confocal scanning microscope to confirm the adsorption of particles on the emulsion droplet surfaces. This shows the organization of nanoclay platelets at the oil-water interface.

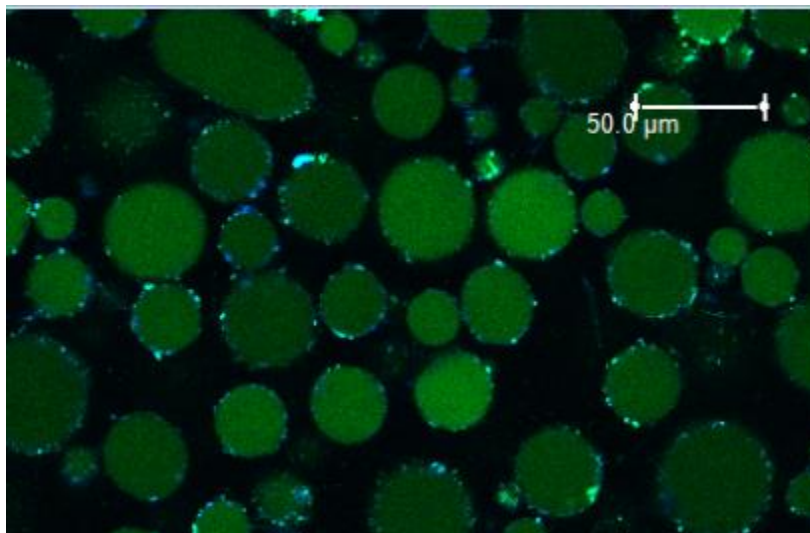


Figure 5-2: Confocal fluorescence microscopy images of mineral oil-water emulsions stabilized by 1wt% nanoclay modified with 0.05 wt.% CTAB Scale Bar = 50μm

5.2.2.5 Contact angle measurement

The contact angle of nanoclay dispersions with varying degrees of surfactant modifications was measured at 20 °C using the sessile drop method of the Axisymmetric Drop Shape Analysis-Profile (ADSA-P). The dispersions containing nanoclay-CTAB were spin-coated onto clean glass slides and were left to dry under vacuum at 80 °C. The three-phase contact angle was measured through the water phase. The dispersion coated glass slides were placed into a Hellma glass cuvette containing mineral oil. A small drop was initially dispensed on the surface of the slide, then a continuous injection of water at a rate of 0.5 μ L/s water was dispensed onto the slides using a syringe pump. A simplified schematic of the experimental set-up for contact angle measurement from a sessile drop is shown in **Figure 5-3**.

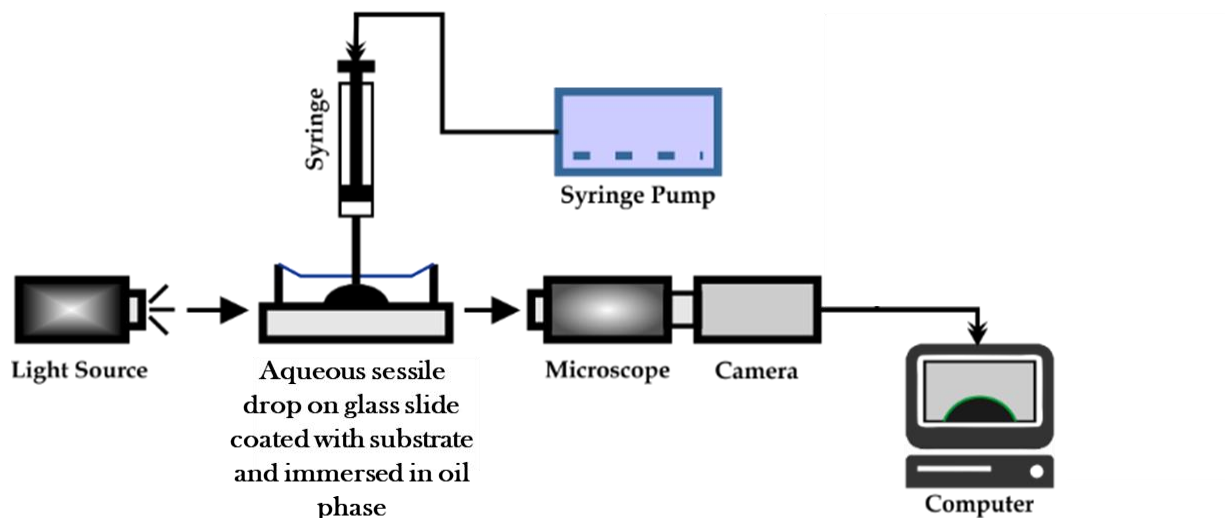


Figure 5-3: Schematic of the Sessile Drop Method for Measuring Contact Angle

5.2.2.6 Dynamic Light Scattering and Zeta Potential Measurements

The particle size and Zeta potential were measured using the Zetasizer Nano-ZS (Malvern Instruments Ltd., Worcestershire, UK) with a He-Ne laser operating at 633 nm frequency. A dip

cell was used to measure the zeta potentials of nanoclay dispersion in the absence and presence of increasing amounts of CTAB, using the Smoluchowski equation for converting measured electrophoretic mobilities.

The lateral dimension of dry exfoliated nanoclay is 100-150 nm. The Dynamic Light Scattering (DLS) measurement gave a much larger size of 740 nm. The most likely reason for this discrepancy is the solvation of nanoclay particles. The strong attraction between the negatively charged nanoparticle surface, stabilized by CTAB, and the matrix fluid in the NC-Bt-CTAB system leads to the formation of a film of matrix fluid on the clay surface, as shown schematically in **Figure 5-4**. The solvation of nanoparticles is a common occurrence [32], [128]. However, some aggregation of nanoclay particles cannot be ruled out.

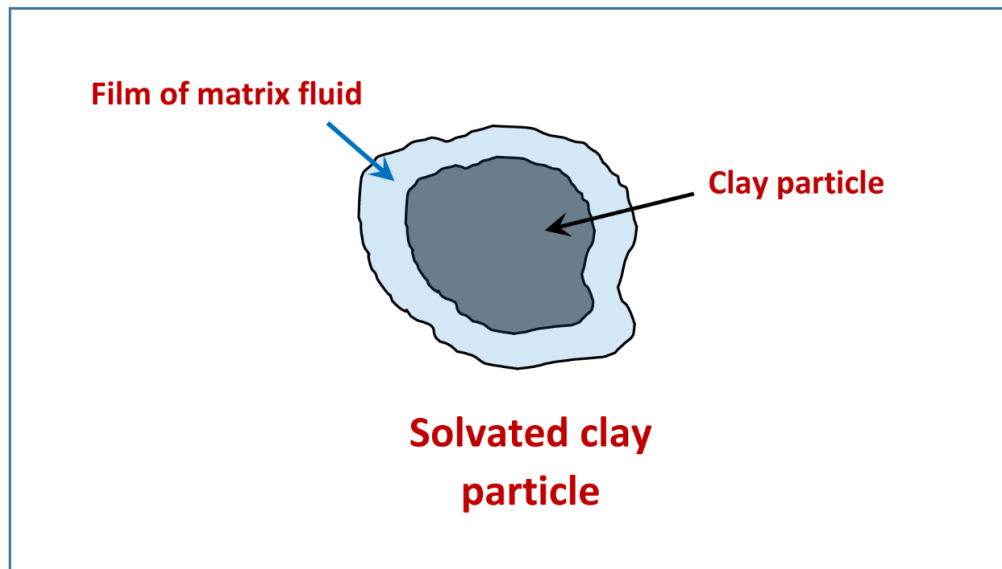


Figure 5-4: Nanoclay coated with immobilized dispersing aqueous film

The effect of CTAB concentration on the electrokinetic property of bentonite nanoclay particles was measured at 25°C, with an equilibration time of 120s and 20 runs of three measurement cycles per sample.

5.3 Statistical Analysis

The experimental data was conditioned by using Grubb's test to determine any outliers which were removed before conducting other statistical analysis. All the experiments were conducted in triplicates.

5.4 Results and Discussions

5.4.1 Material Characterization

5.4.1.1 Electron Microscopy

A FEI QUANTA FEG 250 scanning electron microscope (SEM) was used to study the morphology of the samples. For analyses, dried aqueous dispersions of NC-Bt and NC-Bt-CTAB were mounted onto the equipment platform using carbon tape. Images of the surface morphology of the dispersions are shown in **Figure 5-5**.

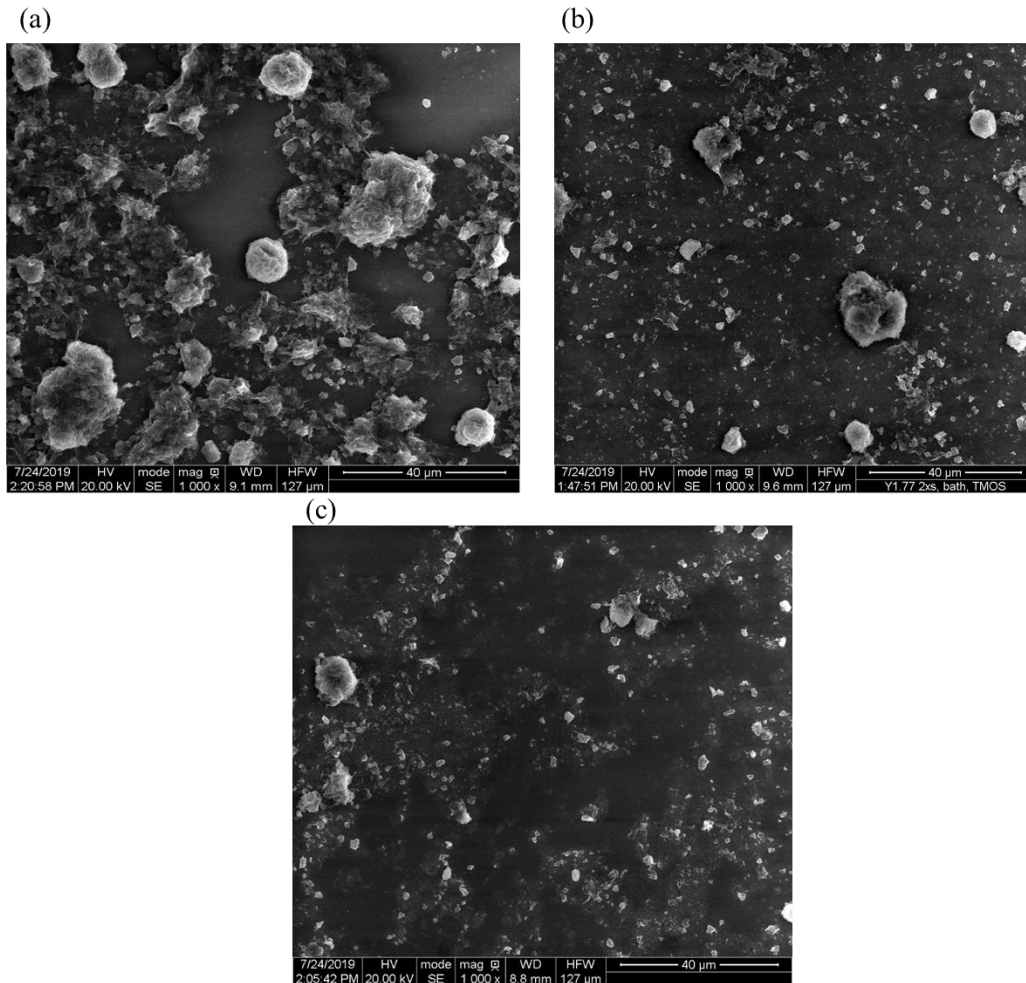


Figure 5-5: SEM Images of dried 1wt% aqueous dispersions of NC-Bt in the presence of (a) 0wt%, (b) 0.05wt% and (c) 0.1wt% CTAB. Scale Bar = 40μm.

The SEM images show the variation in the degree of aggregation in the clay morphology with or without surfactant. **Figure 5-5(a)** shows the clay morphology without surfactant, while **Figure 5-5(b)** and (c) show the clay morphology in the presence of 0.05wt% CTAB and 0.1wt% CTAB, respectively. In the absence of the surfactant, the nanoclay shows a relatively more aggregated morphology with a greater surface area. However, in the presence of surfactant, the SEM images show a reduction in the aggregation and clay particle size. The variation in concentration of CTAB seems to have an effect on the aggregation of clay particles and hence their particle size.

5.4.1.2 Dynamic Light Scattering and Zeta Potential Results

The particle size distribution was measured with at least three separate measurements per dispersion. The size distributions are shown in **Figure 5-6** for two different nanoclay concentrations of 0.1 and 1 wt%. The particle size changes with nanoclay concentration are negligible. The average particle diameter is $740\text{nm} \pm 30\text{nm}$.

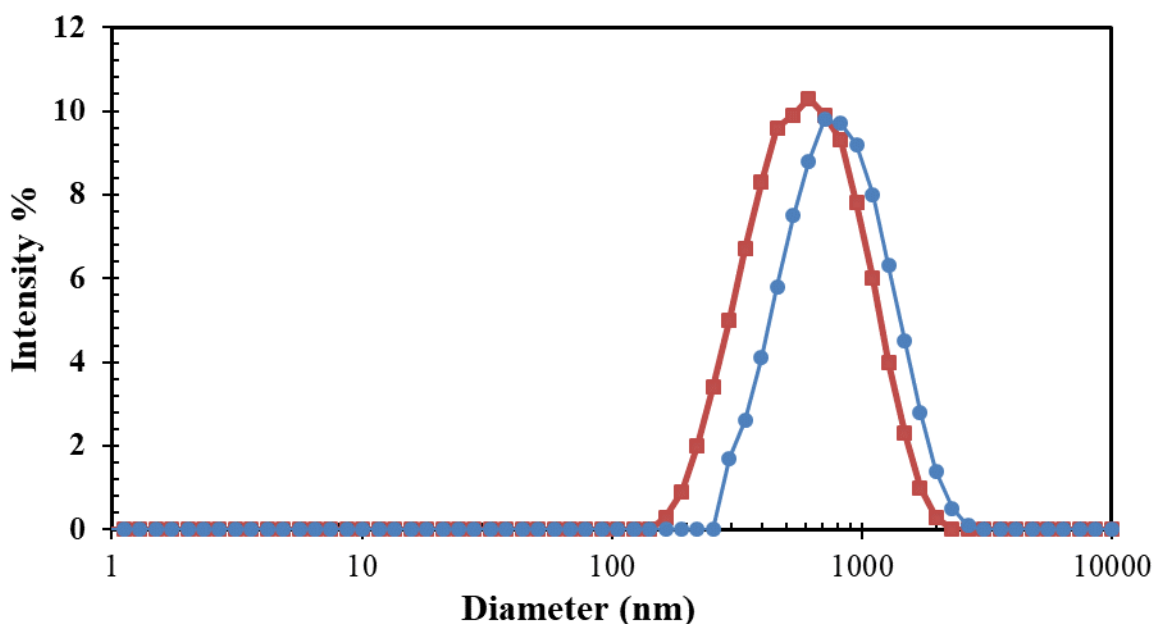


Figure 5-6: Particle size distribution of 0.1wt% and 1wt.% nanoclay dispersion using DLS. 0.1 (blue circle), 1 (red square)

Figure 5-7 presents the change of zeta potential values of nanoclay–CTAB dispersions as a function of CTAB. The zeta potential obtained for NC-Bt dispersion in the absence of CTAB is $-11.4\text{ mV} \pm 0.9$. A slight increase in this value was observed with the addition of a cationic surfactant. This can be explained by the adsorption of cationic CTAB onto negatively charged nanoclay. An eventual sign change noticed beyond the critical micelle concentration of CTAB is likely due to the formation of micelles.

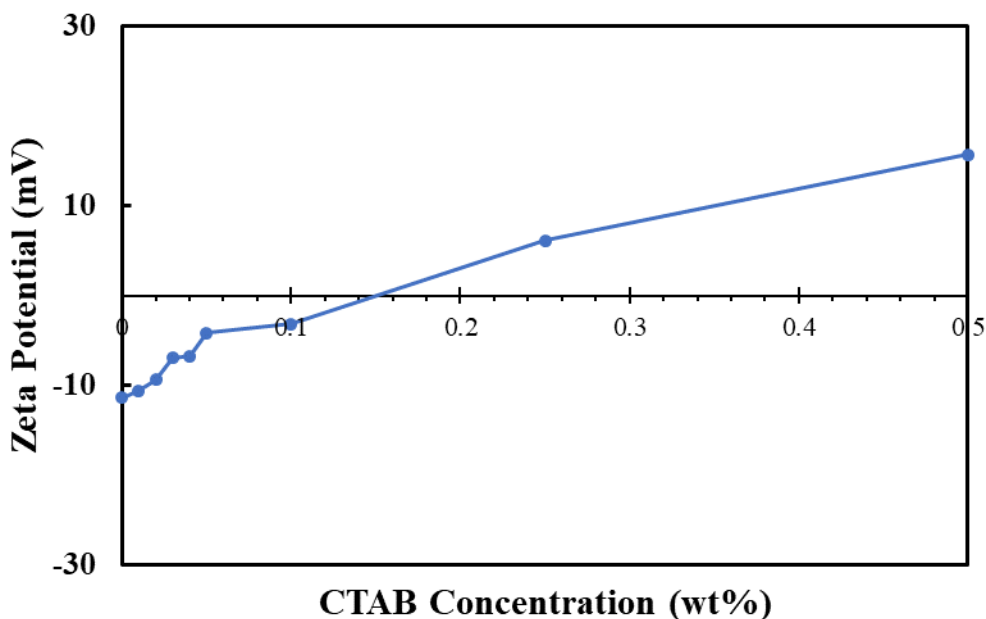


Figure 5-7: Variation of zeta potential and 1wt.% nanoclay dispersion as a function of CTAB concentration

5.4.1.3 Contact Angle

The wettability of particles is widely known to be a predictor of the stability of emulsions. To further elucidate the stability of surfactant stabilized nanoclay emulsions, the contact angles of water drops on the substrates both in air and in oil were measured. The mean of the advancing contact angle of approximately 20 drops was taken for each sample. **Figure 5-8** shows the advancing contact angles of water in air (squares) or in oil (circles) on the substrate coated onto the slides. The contact angle data are plotted as a function of the varying concentration of CTAB in 1wt% nanoclay concentration. **Figure 5-9** shows the selected images of the 3-phase contact angle formed by 40 μ L of water dispensed onto the surface of the glass slides coated with 1wt% nanoclay with various degree of CTAB modification (a) 0 (b) 0.01, (c) 0.03 and (d) 0.05wt%.

The advancing contact angle for the dispersion of 1wt% nanoclay in air was estimated to be $15 \pm 1.2^\circ$ without surfactant and increased to $50 \pm 2.6^\circ$ at the highest concentration of surfactant of 0.05wt%. Upon immersion in the oil phase, the contact angle further increased from $20 \pm 2.9^\circ$ to $68 \pm 3.2^\circ$ of pure clay and surfactant modified nanoclay respectively. The increase in the contact angle with an increase in the degree of modification of nanoclay with CTAB can be attributed to the enhanced hydrophobicity of nanoclay resulting from adsorption of a cationic surfactant CTAB.

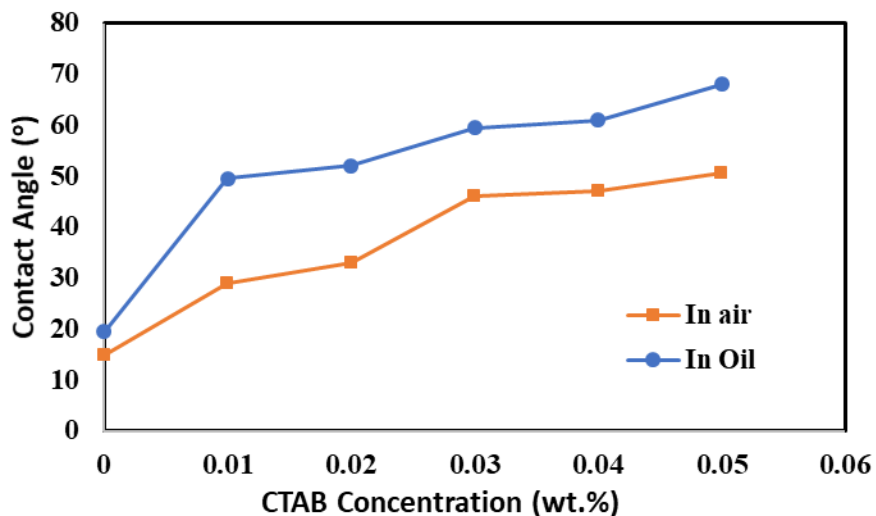


Figure 5-8: Variation of contact angle measured of a water drop in air (squares) and under oil (circles) as a function of the concentrations CTAB concentration in 1wt% nanoclay dispersions

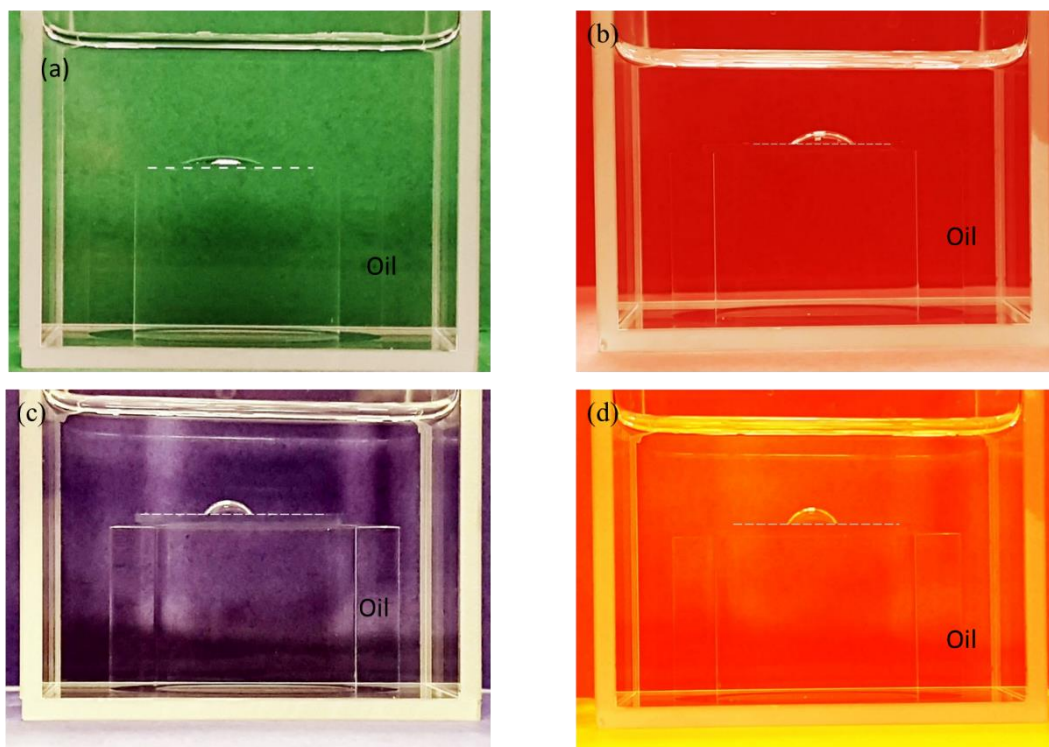


Figure 5-9: Images of sessile drop on glass slides coated with 1wt% nanoclay with CTAB concentration of (a) 0, (b) 0.01, (c) 0.03 and (d) 0.05 respectively immersed in the oil phase

5.4.1.4 Emulsions Stabilized by Unmodified Bentonite Nanoclay

The influence of unmodified bentonite nanoclay dispersed in ultrapure water on the catastrophic phase inversion of a W/O emulsion was investigated. **Figure 5-10** shows the variation in electrical conductivity of the nanoclay-stabilized water-mineral oil emulsions with respect to the volume fraction of water. The emulsions formed at the volume fractions with low conductivity are W/O type emulsions. As shown in **Figure 5-10**, the phase inversion of W/O to O/W emulsion is depicted by the sharp increase in the electrical conductivity which occurred at water volume fractions between 0.22 and 0.31. Further sequential addition of the aqueous phase to the resulting O/W emulsion (after the phase inversion has occurred) led to higher conductivity values, which becomes more prominent with an increase in the weight % of the added clay. As can be seen in **Figure 5-10**, the slope of the electrical conductivity versus water volume fraction relationship,

after phase inversion of W/O to O/W emulsion, increases with the increase in the concentration of nanoclay.

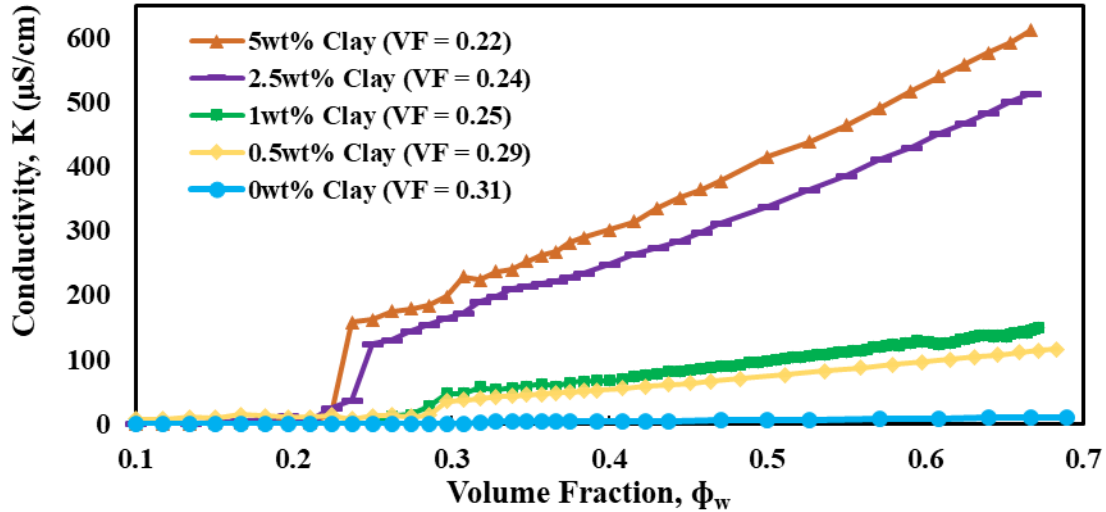


Figure 5-10: Conductivity of water-mineral oil emulsions stabilized by Nanoclay Solutions (0, 0.25, 0.5, 1, 1.75, 2.5 and 5 wt.%) as a function of the volume fraction of water (VF in the legend refers to the volume fraction of water where phase inversion is observed)

To expound the relationship between the critical phase inversion volume fraction of water and the nanoclay concentration, the volume fraction of water where phase inversion took place was plotted against the nanoclay concentration as shown in **Figure 5-11**. **Figure 5-11** shows that the critical phase inversion volume fraction is reduced to lower water volume fractions as the concentration of the dispersed nanoclay is increased. The critical volume fraction decreases from 31% to 22% with an increase in the nanoclay concentration from 0 to 5 wt.%. This is not unexpected as the incorporation of hydrophilic clay into the emulsion system shifts the hydrophilic-lipophilic balance (HLB) of the system towards higher value and hence favouring the formation of an O/W emulsion.

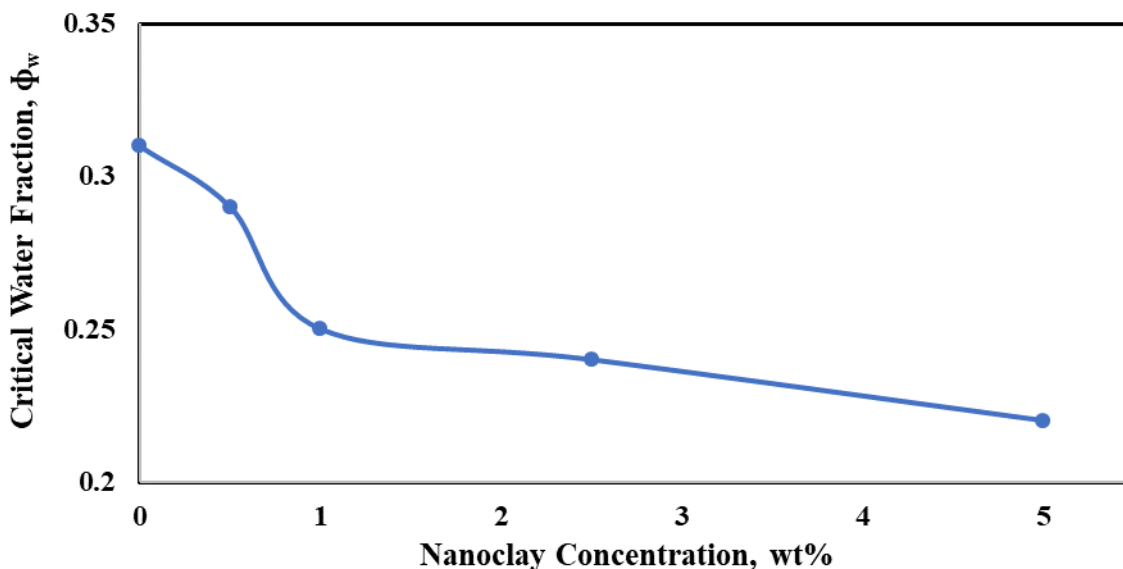


Figure 5-11: Critical volume fraction of water versus nanoclay concentration

5.4.1.5 Emulsions Stabilized Solely by CTAB

The behaviour of cationic surfactant CTAB dispersed in ultrapure water was investigated to determine its effect on the catastrophic phase inversion of W/O emulsion to O/W emulsion.

Figure 5-12 shows the variation in conductivity of the CTAB stabilized water-mineral oil emulsions with respect to the volume fraction of water. As shown in **Figure 5-12**, the phase inversion of W/O to O/W emulsion is depicted by the sharp increase in the conductivity which occurred at water volume fractions between 0.31 and 0.52. Further sequential addition of the aqueous phase to the resulting O/W emulsion after the phase inversion led to higher conductivity values, which become more prominent with the increase in the weight % of the added CTAB. As shown in **Figure 5-12**, the slope of the relationship increases with an increase in the concentration of CTAB. This behaviour is similar to that observed when nanoclay was used as the emulsion stabilizer.

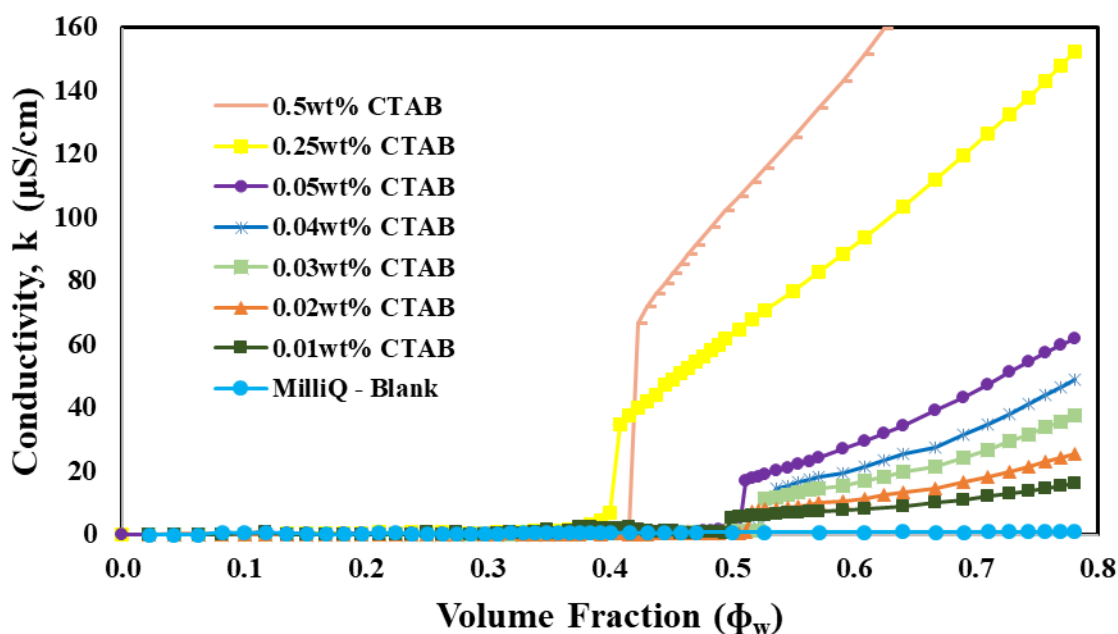


Figure 5-12: Conductivity of water-mineral oil emulsions stabilized by pure CTAB solutions (0, 0.01, 0.02, 0.03, 0.04, 0.05, 0.25, and 0.5 wt.%) as a function of the volume fraction of water.

To illustrate the relationship between the phase inversion water volume fraction and the CTAB concentration, the critical water volume fraction is plotted against CTAB concentration in **Figure 5-13**. The figure shows that the phase inversion of W/O to O/W emulsion is delayed initially to higher water volume fractions of 0.52 as the concentrations of the surfactant CTAB is increased. The trend of the critical volume fraction against CTAB concentration peaked at a CTAB concentration of 0.03 wt.% (the critical micelle concentration of CTAB) and then decreased continuously to a critical volume fraction of 0.4 up to a CTAB concentration of 0.25 wt.%. Higher CTAB concentrations beyond this point (0.25 wt%) had little effect on the critical volume fraction of phase inversion. This behaviour is different from what was observed when nanoclay was used as the emulsion stabilizer, but it is important to note that the selected CTAB concentration range is lower than the nanoclay concentration range by an order of magnitude.

When a higher concentration of CTAB was used, significant foaming of the emulsion was observed.

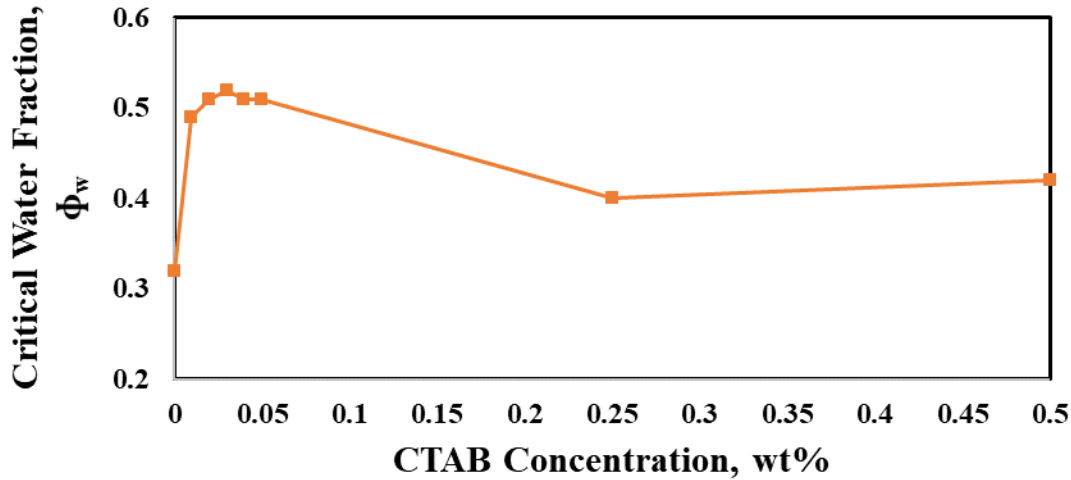


Figure 5-13: Critical volume fraction of water versus CTAB concentration

5.4.1.6 Comparing the effects of CTAB alone and unmodified nanoclay alone on catastrophic phase inversion of W/O emulsions

Figure 5-10 and **Figure 5-12** show a similar trend in the behaviour of the stabilized emulsion regardless of whether nanoclay or CTAB was used as an emulsion stabilizer. Not only do they show a directly proportional relationship between the conductivity of the emulsion and the aqueous phase volume fraction for different weight percent of the stabilizer, the slope of the relationship increases with an increase in the weight percent of the stabilizer. To further investigate the relationship between the critical volume fraction and the concentration of the stabilizer, the stabilizer concentrations were normalized and plotted against the critical volume fraction of water as depicted in **Figure 5-14**. C/C_0 is the normalized stabilizer concentration where C , is the actual sample concentration at the nominal concentration of C_0 . **Figure 5-14** shows that the critical volume fraction of the aqueous phase when CTAB was used as the stabilizer was higher when compared to unmodified nanoclay. Although they both follow similar

trends, it can be concluded that using nanoclay as the stabilizer speeds up the phase inversion process of W/O to O/W emulsion in comparison with CTAB as the emulsion stabilizer.

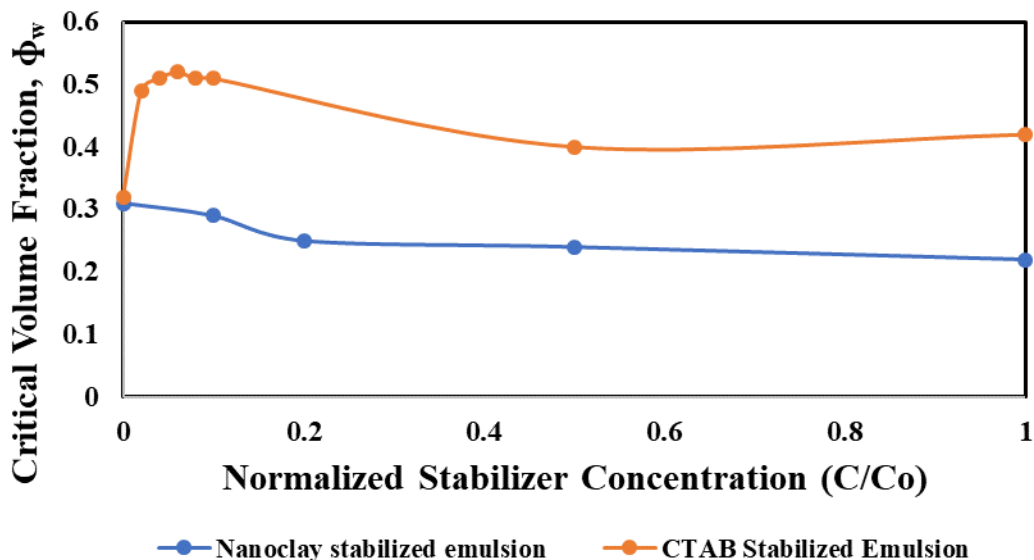


Figure 5-14: Aqueous phase critical volume fraction as a function of normalized concentration for CTAB and nanoclay.

5.4.1.7 Emulsions Stabilized by Surfactant-Modified Bentonite Nanoclay (NC-Bt-CTAB)

The interaction of a clay surface with a polymeric matrix has been commonly enhanced by surface modification [129]. Therefore, we investigated the effects of 1 wt.% nanoclay solution combined with various concentrations of CTAB on the catastrophic phase inversion of W/O emulsion. **Figure 5-15** shows the variations in the electrical conductivity of the nanoclay/CTAB emulsion mix with respect to the aqueous phase volume fraction. The CTAB concentration was increased up to 0.1 wt%. During the experiments, it was observed that the CTAB coagulates the nanoclay at CTAB concentrations beyond 0.1wt% in the presence of oil. Hence the phase inversion experiments were restricted to using nanoclay solutions containing CTAB in the concentration range of 0.01 to 0.1wt.%.

As shown in **Figure 5-15**, the phase inversion of W/O to O/W emulsion is depicted by a sharp increase in the electrical conductivity which occurred at water volume fractions in the range of 0.25 to 0.42. Further sequential addition of the aqueous phase to the resulting O/W emulsion after the phase inversion has occurred, led to higher conductivity values, which become more prominent with an increase in the weight % of CTAB at a constant concentration of nanoclay. This behaviour is similar to what was observed when nanoclay or CTAB alone was used as the emulsion stabilizer as shown previously in **Figure 5-10** and **Figure 5-12**. However, it is evident that the adsorption of CTAB onto the surface of the nanoclay particles leads to the localization of nanoclay particles at the oil-water interface resulting in the delayed inversion process.

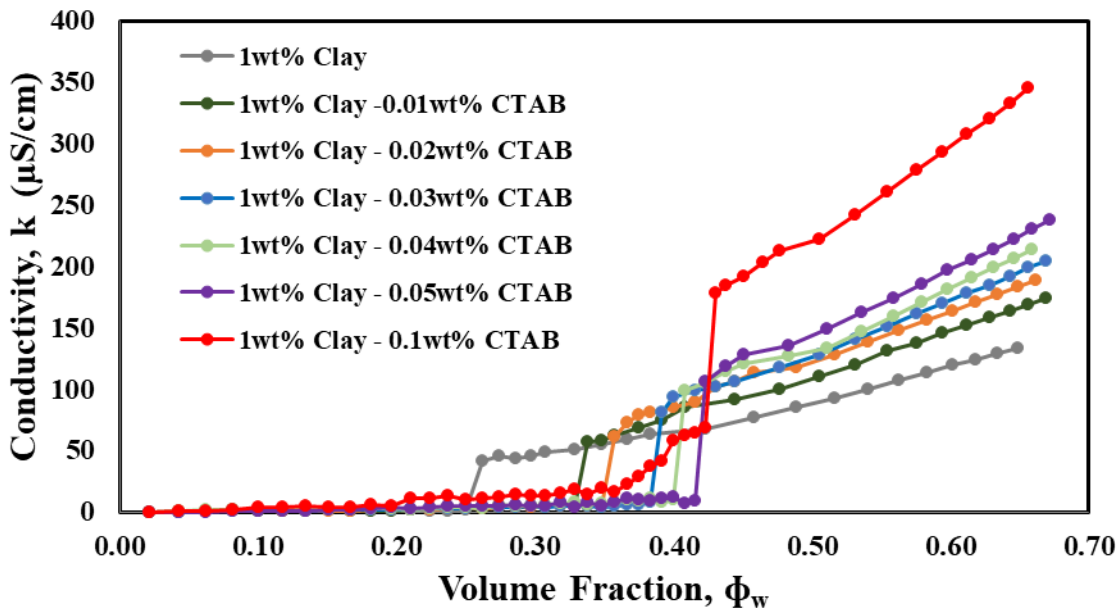


Figure 5-15: Conductivity of water-mineral oil emulsions stabilized by 1wt% Nanoclay at varying CTAB concentration as a function of the volume fraction of water

Figure 5-16 shows the relationship between the critical volume fraction of water and CTAB concentration for emulsions stabilized by CTAB modified nanoclay. The critical water fraction increases from 0.24 to 0.41 with increasing CTAB concentration from 0 to 0.05 wt %. Although

not shown in the figure, the critical volume fraction plateaued from CTAB concentration of 0.05 wt % until 0.1 wt %. The linear relationship between the critical water fraction and the CTAB concentration shown up to 0.05wt% concentration is seen to follow equation 6.2:

$$Y=3.14(C) +0.27 \quad (5.2)$$

where Y = critical water volume fraction and C is CTAB concentration in wt %. Thus the surfactant-modified nanoclay delays the phase inversion of W/O to O/W emulsion up to a CTAB concentration of 0.05 wt%.

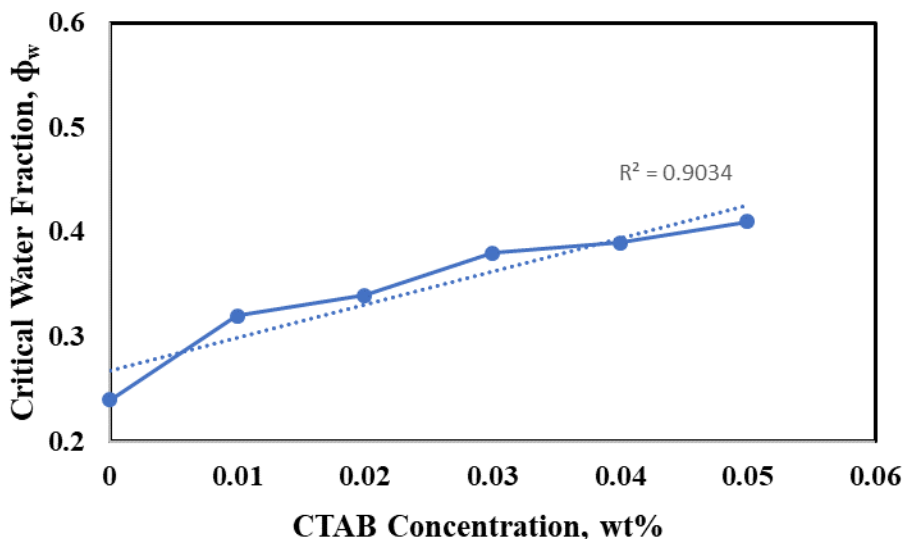


Figure 5-16: Critical volume fraction of water versus CTAB concentration in 1wt% Nanoclay-CTAB mixture

To further investigate the effects of nanoclay on the critical volume fraction of phase inversion of W/O to O/W emulsion, the critical volume fraction of water at varying CTAB concentrations was compared for emulsion stabilized by pure CTAB and emulsion stabilized by 1 wt.% nanoclay + CTAB. The comparison plots shown in **Figure 5-17** are limited to the dilute CTAB concentrations within the Critical Micelle Concentration (CMC) region up to 0.05wt% CTAB.

Figure 5-17 shows that the critical volume fraction of the aqueous phase when pure CTAB was employed as the stabilizer was higher in comparison with CTAB modified nano clay as the stabilizer. Although they both exhibit the same trends, it can be concluded that using the CTAB-modified nanoclay as the emulsion stabilizer speeds up the inversion process when compared to using CTAB alone as the emulsion stabilizer.

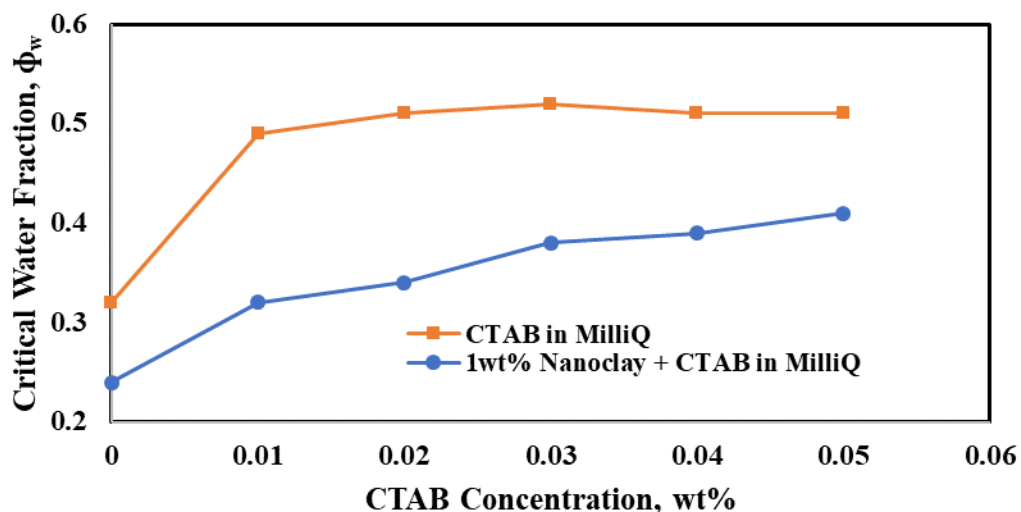


Figure 5-17: Comparison between plots of Critical volume fraction of water versus varying CTAB concentration for pure CTAB and 1wt% Nanoclay + CTAB mixture respectively

5.5 Conclusions

The emulsifying nature of hydrophilic bentonite nanoclay can be enhanced by modification with a surfactant such as cationic CTAB. The zeta potential measurements confirm the alteration of the surface charge of nanoclay as a result of CTAB adsorption. The contact angle measurement confirms increased hydrophobicity of nanoclay particle surfaces due to the formation of a monolayer of cationic CTAB molecules. The critical volume fraction of the aqueous phase, where phase inversion of W/O to O/W emulsion takes place, was higher when CTAB alone was used as the stabilizer as compared with bentonite nanoclay alone. It was evident that the

adsorption of CTAB on to the surface of the nanoclay particles led to the localization of clay particles at the oil-water interface which resulted in the delayed inversion process of W/O to O/W emulsion.

Chapter 6: Preliminary Investigation of the Extraction of Oil from Oil Sands using Starch Nanoparticles

6.1 Introduction

This chapter looks at one area of the potential application of starch nanoparticles in the industry is the area of bitumen extraction from mined oil sands. Oil sands commonly referred to as tar sand or bituminous sand consists of layers of sand deposits mixed with highly viscous petroleum (bitumen). Alberta's oil sands consist of approximately 55-80 wt% sands (mainly quartz), 4- 18 wt% bitumen, 5-34 wt% fine solids (particles smaller than 45 μm), and 2-15 wt% water[130], [131]. Alberta's oil sands reserve accounts for more than 95% of Canada's oil reserves. Approximately 84% of all oil production from Alberta in September 2019 was from oil sand, a 2.1% increase when compared to September 2018[132].

Due to the increasing growth in world energy demand, Alberta oil sands have now become an important source of alternative energy resources[89]. The extraction of oil from oil sand is quite challenging when compared to conventional crude oil extraction because of its high viscosity, low hydrogen to carbon ratio and natural gas[133]. The two main separation methods employed to extract bitumen from oil sands include in-situ and surface mining. The method selected depends on the depth of the crude's deposit. For deposits situated near the surface (< 50 m below surface), the oil sands can be mined and directly processed at an extraction plant, while deeper bitumen reserves are extracted using in-situ mining methods such as steam-assisted gravity drainage (SAGD) and cyclic steam simulation (CSS).

Nanoparticles are particles with a diameter size between 1 and 100 nm. When the size of a particle reduces to nanoscale (i.e., 1–100 nm) the properties changes dramatically as the percentage of atoms at the surface of a material becomes significant, a phenomenon which is

attributed to the large surface area to volume ratio[134]. Quantum confinement, surface plasmon resonance, high adsorption affinity, enhanced catalytic activity, good dispersion ability, and intrinsic reactivity are some of the unique properties associated with nanoparticles[135]. The ability to manipulate the surface functionalities of nanoparticles by understanding and tuning its physicochemical characteristics makes nanotechnology an attractive option for oil sand extraction.

Nanotechnology is a rapidly growing technology with considerable potential applications and benefits[136]. Nanoparticles are used in diverse areas of engineering applications, such as heavy oil upgrading[137]–[139], fuel cell technology[140], [141], polymer nanocomposites[142]–[144], catalysis[145]–[147], and wastewater treatment[37], [148], [149]. The recent interest in the application of nanotechnology in oil sand processing stems from the unique physical and chemical properties of the nano-scale particles[150], the challenges involved in extracting oil from oil sand, the reduction in costs associated with the production and transportation of oil sands and the improvement of the crude quality to meet stricter market specifications with less environmental footprints. The use of nanoparticles in oil sand recovery provides unique opportunities to develop economically and environmentally friendly oil sand extraction processes. Further studies are required to illuminate the intricate interfacial uncertainties associated with nanoparticles' applications in oil sand extractions.

The objective of this phase of this study involves the preliminary investigation of the effects of experimental grade hydrophilic starch nanoparticles (HSNPs) in oil recovery from oil sands. The key goal of this study is to understand how different concentrations of starch solutions affect the recovery of oil from oil sands.

6.2 Materials and Methodology

6.2.1 Materials

The materials used for this phase of the study is presented below:

- 1) Temperature Controlled Shaker
- 2) Vacuum pump
- 3) Mass balance
- 4) Chemicals
 - a. Oil Sand
 - b. Tetrahydrofuran (THF)
 - c. 1-Octanol
 - d. Toluene
 - e. Starch – Ecosynthetix
 - f. Nitrogen gas
 - g. Acetone
- 5) Scintillation Vials
- 6) Pasteur Pipette

6.2.2 Methodology

The protocol used for oil extraction was modelled after the methodology of Yang and Duhamel[151]. In summary, the extraction protocol was carried out as follows:

1. 1g of oil sand was placed in a 30 mL vial
2. 15 mL of aqueous starch dispersions of concentrations 0, 0.01, 0.1, 0.5 and 1wt.% was added respectively.

- 60mg of toluene was measured into a 30 mL vial. All measurements were made in triplicates. **Figure 6-1** shows the triplicate samples prepared for the experiment.



Figure 6-1: Vials containing Oil Sand + Starch Solution + Organic thinner before transfer into an Incubated Shaker

- The vials were placed in an incubated shaker at 45°C and 250RPM for 24hrs. **Figure 6-2** shows the vials in the incubated shaker.



Figure 6-2: Vials in the incubated shaker

5. After shaking, the vials were left to cool down to room temperature. **Figure 6-3** shows the picture of the vials after shaking for 24 hours.

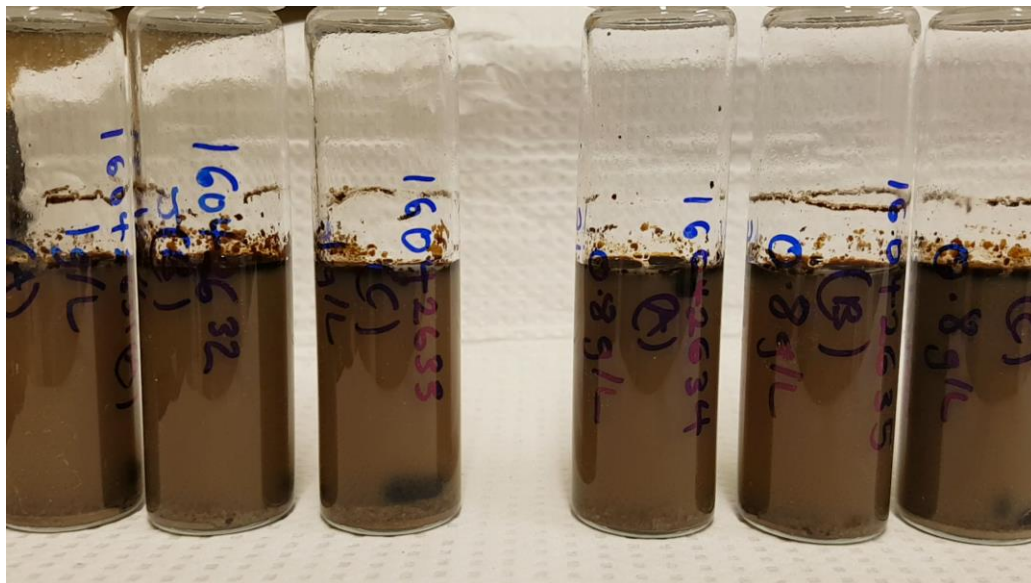
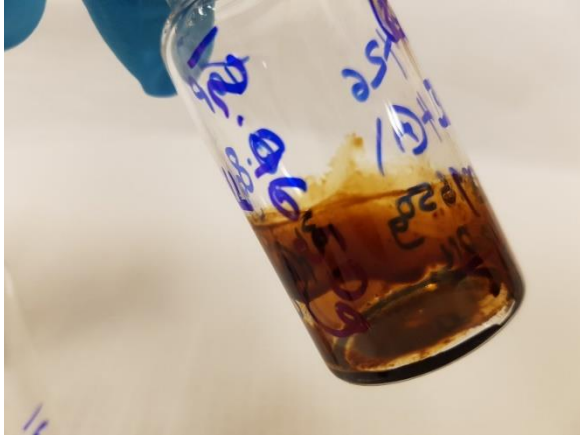


Figure 6-3: Vials after incubated shaking for 24hrs

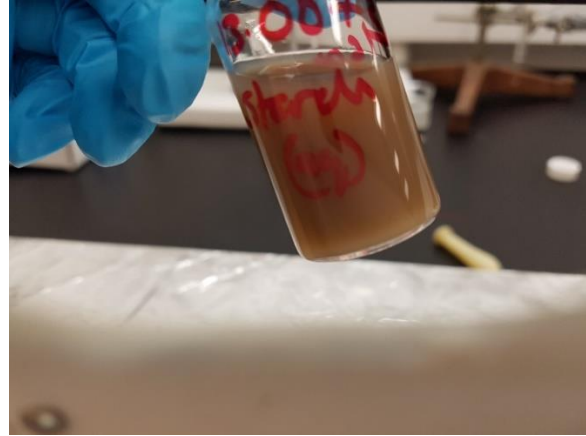
Post incubation bitumen recovery protocol:

1. Toluene was added to the top oil in the vial as an organic diluent to help solubilize the recovered floating oil and around the vial upper wall. The resulting bitumen-in-toluene emulsion was retrieved by a Pasteur pipette into a separate vial. A gentle flow of nitrogen was used to evaporate the residual toluene. The resulting extract is as shown in **Figure 6-4a**.
2. The mid-layer emulsified solution was transferred into a separate vial as shown in **Figure 6-4b**.
3. The bottom layer consisting of sand grain and entrained oil (**Figure 6-4c**) was washed with THF to liberate the entrained oil from the sand matrix.
4. The vials were placed overnight in the vacuum oven to remove remaining co-solvents

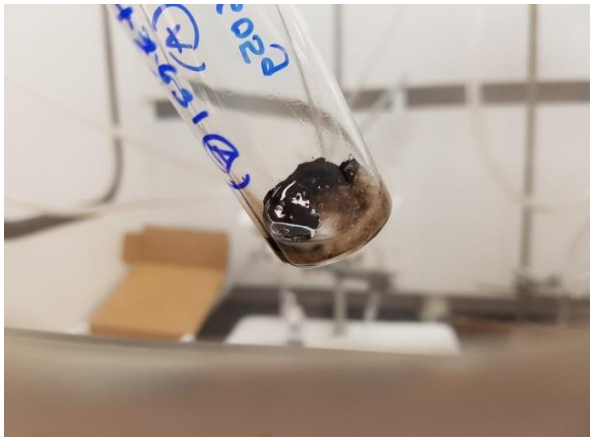
a)



b)



c)



d)

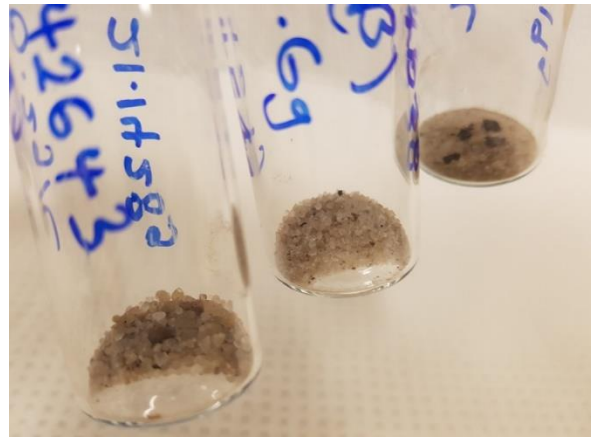


Figure 6-4: Post extraction – (a) Top layer of oil extracted (b) Mid-layer emulsion (c) Loose bottom oil layer on sand grain (d) Residual sand after extraction

6.3 Statistical Analysis

The experimental data was conditioned using Grubb's test to determine any outliers which were removed before conducting other statistical analysis. All the experiments were conducted in triplicates and the error bars are the standard deviations. A t-test was employed to compare the mean of the percent recovery of the blank to the mean of the percent recovery for without octanol. This was done to establish the significance of the data obtained. The P-value (0.04) shows that there is a significant difference in the percent recovery between the blank and the

blank with octanol signifying that the presence of octanol contributed to the increase in percent recovery.

6.4 Results and Discussions

The mass of recovered oil and sand were compared to the original mass of oil sand processed. Results of experiments with differences greater than 10% were discarded. The percentage of oil recovered was calculated as the ratio of the mass of oil extracted (top oil) to the total oil as shown in **Equation 6.1**. Where total oil equals the sum of the top and bottom oil recovered.

$$\text{Recovery (\%)} = \frac{\text{Mass of Oil Extracted}}{\text{Total Oil}} * 100 \quad (6.1)$$

This percentage oil recovery is plotted in **Figure 6-5** which shows that the blank experiment using distilled water yielded a mean percent recovery of approximately 16%. This oil percent recovery further increased with the addition of Octanol, a hydrophobic organic solvent, that is known to interact well with starch[152]. The oil recovery percentage is then observed to be further enhanced with the addition of starch. Hence, it was concluded that the percent oil recovery seems to have a direct proportionality with the starch concentration.

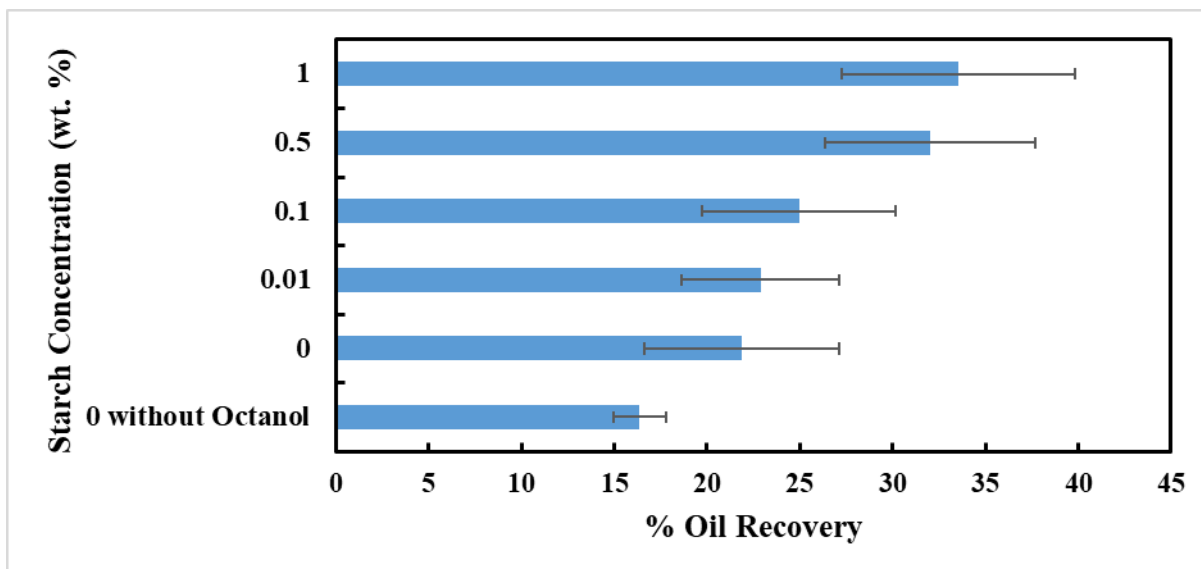


Figure 6-5: Starch concentration with respect to percent oil recovery

The observed trend in the percent oil recovery as a function of low starch concentration is similar to a previous study that used aqueous solutions of thermoresponsive block copolymer (PEG₁₁₃-b-PMEO₂MA_x) for oil extraction from oil sand[151]. In **Figure 6-6**, Yang and Duhamel obtained bitumen extraction efficiency of up to 100% using a block copolymer.

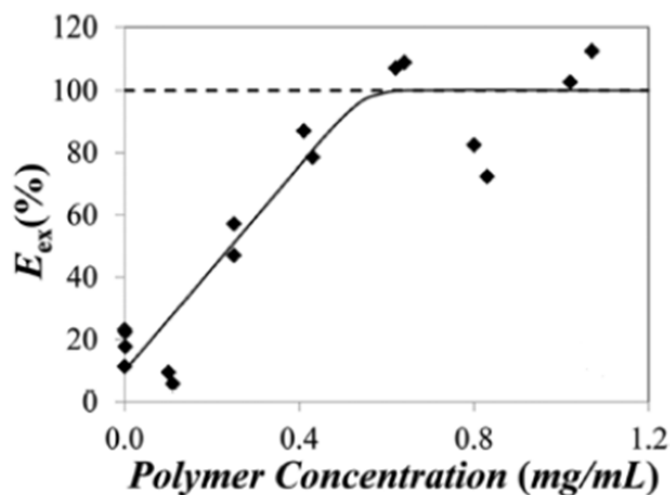


Figure 6-6: Extraction Efficiency as a function of PEG₁₁₃-b-PMEO₂MA₈₀ concentration when the extraction is conducted with 65 mg of toluene. Adapted with permission from [151]. Copyright (2015) American Chemical Society.

The maximum extraction was obtained at the concentration of 0.4mg/mL and greater as shown in **Figure 6-6**. Their method utilized a water-based extraction process using a thermoresponsive block polymer with the aid of toluene and THF as co-solvent.

In comparison to their results, within experimental error, we obtained a mean percent yield of approximately 34% in our preliminary trial. The starch nanoparticle utilized in this extraction process was unmodified. Thermos-responsively modified starch used by Zhang[153] for similar oil recovery work has been reported in the literature.

6.5 Conclusion

It can be concluded from the observed results that increasing starch concentration from 0.01wt% to 1wt% has an effect on the percent oil recovery from oil sand. This indicates that there could be a direct relationship between the starch solution concentrations from 0.01 wt% to 1wt % and the percent oil recovery from oil sands. These preliminary results show that the presence of octanol enhances the oil recovery from oil sands.

6.6 Limitation of study and Future Recommendations

The preliminary trial presented was limited to sampling in vials, the use of an organic solvent for extraction and bench-scale laboratory procedures. A larger-scale pilot plant operation, which models the extraction of mined oilsands in tumblers in the oilsands industry is recommended.

Chapter 7: Summary and Recommendations

7.1 Summary

The effects of HSNP and HOSNP starch nanoparticles on phase inversion and the stability of Pickering emulsions were investigated by the continuous addition of the dispersed phase. The dynamic oil-water interfacial tension was measured using the pendant drop method at varying starch concentrations in the aqueous phase while the contact angles were measured using the sessile drop method of the Axisymmetric Drop Shape Analysis-Profile (ADSA-P). Both types of starch nanoparticles (HSNP and HOSNP) were effective in delaying the phase inversion of emulsions from water-in-oil (W/O) type to oil-in-water (O/W) type. This delay in phase inversion was directly correlated with the concentration of the starch nanoparticles. The interfacial tension decreased as the drop aged at a given starch nanoparticle concentration. The contact angles for both types of starch nanoparticles were within the intermediate wettability range which confirmed the irreversible adsorption of starch nanoparticles at the oil/water interface leading to increased stability of the emulsions.

The stability of nanoclay stabilized water-in-oil emulsions formulated with various degrees of surfactant modification and its effect on the phase inversion of water-in-oil emulsion was investigated. CTAB adsorption to nanoclay was explored by studying how the presence of CTAB in an aqueous dispersion of nanoclay affects the critical volume fraction of water. CTAB was used to modify hydrophilic bentonite nanoclay (NC-Bt). Phase inversion experiments suggested that the modification brought about by the adsorption of CTAB at low concentrations improved the wettability of the nanoclay surface, thereby making it more hydrophobic, hence prolonging the phase inversion point. Not only did the CTAB prolong the phase inversion point, a mixture of CTAB/nanoclay combination equally delayed the phase inversion process, showing

a strong dependent relationship on the CTAB concentration ($R^2 = 0.9$). The adsorption of CTAB on nanoclay had a strong influence on the contact angle and the critical volume fraction of water where phase inversion took place. The modification of the nanoclay brought about by the adsorption of CTAB increased the three-phase contact angle (measured through the aqueous phase), thereby making it more hydrophobic, and prolonged the phase inversion point. CTAB alone and CTAB-modified nanoclay delayed the phase inversion process in a similar manner, showing a strong dependence on the CTAB concentration.

Although CTAB is known to favor O/W emulsions, in this phase inversion study, it was observed that CTAB initially favored W/O emulsion until the micelles were formed. This occurrence was seen for CTAB in both electrolyte, non-electrolyte medium and for nanoclay-CTAB hybrid systems. This behaviour, monitored by the critical volume fraction of the phase inversion of the emulsion peaked at the CMC region beyond which the trend was reversed. In the end, CTAB favored O/W emulsion. In the case of HSNP-CTAB solutions, O/W was favored before and after the CMC region although the net conductivity change around the CMC region was negligible.

The use of nanoparticles in oil sand recovery provides unique opportunities to develop economically and environmentally friendly oil sand extraction processes. The effects of starch nanoparticles (HSNPs) in oil recovery from oil sands was investigated using starch nanoparticles and octanol as the co-solvent. Increasing starch concentration from 0.01wt% to 1wt% seems to have an effect on the percent oil recovery from oil sand, suggesting a direct relationship between the starch solution concentrations from 0.01 wt% to 1wt % and the percent oil recovery from oil sands. The presence of octanol as a co-solvent also enhanced the oil recovery from oil sands.

Hence, these results support the significance of investigating the interfacial characteristics and behaviour of Pickering emulsions in the presence of naturally occurring nanoparticles.

7.2 Recommendations for Future work

Future studies are recommended to investigate the effect of temperature on phase inversion using thermo-responsive nanoparticles. Understanding the effect of temperature variability in stabilizing Pickering emulsion will further expand the applicability of the use of emulsion under different thermal conditions.

Additional studies is recommended to investigate the creaming of oil droplets and the settling behaviour of nanoparticles. Furthermore, additional research is recommended to investigate the pumping behaviour of starch solutions, especially for large-scale applications.

A future study on the hysteresis of the catastrophic inversion phenomenon of O/W to W/O emulsions is recommended with variation in oil volume fraction in the presence of starch and nanoclays as interfacial additives.

At 1wt% HSNP, the interfacial tension decreased as the drop ages. It is recommended that additional interfacial tension measurements should be conducted for the combination of CTAB-Oil, HSNP-Oil and CTAB/HSNP-Oil systems and investigate how to optimize the system to prevent frequent degradation of the drops to enhance the ability to run experiments for longer durations until steady state is achieved.

An extensive study of CTAB behavior at the CMC region is recommended to further probe the impact of micelle formation on the behavior of nanoparticles in phase inversion of Pickering emulsions.

Additional research is recommended to generate more data in order to further validate the observed direct relationship between starch nanoparticle concentrations and percent oil recovery from oil sands. The direct relationship was observed at low concentrations between 0.01 and 1 wt%. It will be interesting to investigate any possible relationship at different sets of concentrations. It is recommended that a lab-scale pilot plant is established to investigate the efficiency of commercial-grade starch nanoparticle on the removal of oil from oil sand. It is anticipated that these results will contribute to the available literature data on Pickering emulsion.

Letter of Copyright Permission

License agreements for Figure 2.1

PARTIES:

1. **Cambridge University Press** [CompanyName] (Licensor); and
2. **Sileola Ogunlaja** (Licensee).

Thank you for your recent permission request. Some permission requests for use of material published by the Licensor, such as this one, are now being facilitated by PLSclear.

Set out in this licence cover sheet (the **Licence Cover Sheet**) are the principal terms under which Licensor has agreed to license certain Licensed Material (as defined below) to Licensee. The terms in this Licence Cover Sheet are subject to the attached General Terms and Conditions, which together with this Licence Cover Sheet constitute the licence agreement (the **Licence**) between Licensor and Licensee as regards the Licensed Material. The terms set out in this Licence Cover Sheet take precedence over any conflicting provision in the General Terms and Conditions.

Free Of Charge Licence Terms

Licence Date: 20/01/2020

PLSclear Ref No: 32711

The Licensor

Company name: Cambridge University Press

Address: University Printing House

Shaftesbury Road

Cambridge

CB2 8BS

GB

The Licensee

Licensee Contact Name: Sileola Ogunlaja

Licensee Address: Chemical Engineering

University of Waterloo

Waterloo

N2L 3G1

Canada

Licensed Material

title: Colloidal Particles at Liquid Interfaces

ISBN: 9780521848466

publisher: Cambridge University Press

figure number & title / caption Figure 6.1

Are you requesting permission to reuse your own work?

No. I am NOT the author

page number 189

Are you using the content as a prop?

content will NOT be used as a prop

additional information Reuse in Thesis

reproduction colour Black and White

reproduction size Half page

positioning inside or later pages

will it be cropped No

full details of how it will be altered Figure title will be edited

For Use In Licensee's Publication(s)

usage type Book, Journal, Magazine or Academic Paper...-Thesis

estimated publication date January 23, 2020

language English

number of pages 241

publication title Effects of Nanoparticle Interfacial Additives on Phase

Inversion of Pickering Emulsion

type of document Thesis

Rights Granted

Exclusivity: Non-Exclusive

Format: Thesis

Language: English

Territory:

Duration: Lifetime of Licensee's Edition

Maximum Circulation: 0

License agreements for Figures 2.2 and 2.6



CONTRACTS-COPYRIGHT (shared) <Contracts-Copyright@rsc.org>

RE: Permission Request Form: Sileola Ogunlaja

to Sileola Ogunlaja

Dear Sileola

The Royal Society of Chemistry hereby grants permission for the use of the material specified below in the work described and in all subsequent editions of the work for distribution throughout the world, in all media including electronic and microfilm. You may use the material in conjunction with computer-based electronic and information retrieval systems, grant permissions for photocopying, reproductions and reprints, translate the material and to publish the translation, and authorize document delivery and abstracting and indexing services. The Royal Society of Chemistry is a signatory to the STM Guidelines on Permissions (available on request).

Please note that if the material specified below or any part of it appears with credit or acknowledgement to a third party then you must also secure permission from that third party before reproducing that material.

Please ensure that the published article carries a credit to The Royal Society of Chemistry in the following format:

[Original citation] – Reproduced by permission of The Royal Society of Chemistry

and that any electronic version of the work includes a hyperlink to the article on the Royal Society of Chemistry website.

Regards

Gill Cockhead
Contracts & Copyright Executive

Gill Cockhead
Contracts & Copyright Executive
Royal Society of Chemistry,
Thomas Graham House,
Science Park, Milton Road,
Cambridge, CB4 0WF, UK
Tel +44 (0) 1223 432134



Royal Society of Chemistry - License Terms and Conditions

Order Date	20-Jan-2020
Order license ID	1014450-1
ISSN	1744-6848
Type of Use	Republish in a thesis/dissertation
Publisher	ROYAL SOCIETY OF CHEMISTRY
Portion	Image/photo/illustration

LICENSED CONTENT

Publication Title	Soft matter	Country	United Kingdom of Great Britain and Northern Ireland
Author/Editor	Royal Society of Chemistry (Great Britain)	Rightsholder	Royal Society of Chemistry
Date	06/01/2005	Publication Type	e-Journal
Language	English	URL	http://www.rsc.org/Publishing/Journals/sm/index.asp

License agreements for Figure 2.3

The screenshot shows the RightsLink interface for a license. At the top, there are navigation tabs for 'My Orders', 'My Library', and 'My Profile', along with a welcome message for 'sogunlaj@uwaterloo.ca'. The main content area is titled 'License Details' and includes a description of the agreement between Sileola Ogunlaja and John Wiley and Sons. Below this, there are 'Print' and 'Copy' buttons. A detailed list of license information is provided, including the license number (4753221083700), date (Jan 20, 2020), publisher (John Wiley and Sons), publication (Wiley Books), title (Colloids), author (Laurier L. Schramm), date (Jun 11, 2019), pages (42), type of use (Dissertation/Thesis), requestor type (University/Academic), format (Print and electronic), portion (Figure/table), number of figures/tables (1), and the requestor's location (University of Waterloo, Waterloo, ON N2L 3G1, Canada, Attn: Sileola Ogunlaja).

License Number	4753221083700
License date	Jan 20, 2020
Licensed Content Publisher	John Wiley and Sons
Licensed Content Publication	Wiley Books
Licensed Content Title	Colloids
Licensed Content Author	Laurier L. Schramm
Licensed Content Date	Jun 11, 2019
Licensed Content Pages	42
Type of Use	Dissertation/Thesis
Requestor type	University/Academic
Format	Print and electronic
Portion	Figure/table
Number of figures/tables	1
Will you be translating?	No
Title of your thesis / dissertation	Effects of Nanoparticle Interfacial Additives on Phase Inversion of Pickering Emulsion
Expected completion date	Jan 2020
Expected size (number of pages)	
Original Wiley figure/table number(s)	Figure 1
Requestor Location	Sileola Ogunlaja University of Waterloo University of Waterloo Waterloo, ON N2L 3G1 Canada Attn: Sileola Ogunlaja

License agreements for Figure 2.5



RightsLink®



Home



Help



Email Support



Sileola Ogunlaja ▾

Solid Wettability from Surface Energy Components: Relevance to Pickering Emulsions

Author: Bernard P. Binks, John H. Clint

Publication: Langmuir

Publisher: American Chemical Society

Date: Feb 1, 2002



Copyright © 2002, American Chemical Society

PERMISSION/LICENSE IS GRANTED FOR YOUR ORDER AT NO CHARGE

This type of permission/license, instead of the standard Terms & Conditions, is sent to you because no fee is being charged for your order. Please note the following:

- Permission is granted for your request in both print and electronic formats, and translations.
 - If figures and/or tables were requested, they may be adapted or used in part.
 - Please print this page for your records and send a copy of it to your publisher/graduate school.
 - Appropriate credit for the requested material should be given as follows: "Reprinted (adapted) with permission from (COMPLETE REFERENCE CITATION). Copyright (YEAR) American Chemical Society." Insert appropriate information in place of the capitalized words.
 - One-time permission is granted only for the use specified in your request. No additional uses are granted (such as derivative works or other editions). For any other uses, please submit a new request.
- If credit is given to another source for the material you requested, permission must be obtained from that source.

License agreements for Figure 2.7



RightsLink®

My Orders

My Library

My Profile

Welcome sogunlaj@uwaterloo.ca [Log out](#) | [Help](#)

My Orders > Orders > All Orders

License Details

This Agreement between Sileola Ogunlaja ("You") and Elsevier ("Elsevier") consists of your license details and the terms and conditions provided by Elsevier and Copyright Clearance Center.

[Print](#)

[Copy](#)

License Number	4753161014862
License date	Jan 20, 2020
Licensed Content Publisher	Elsevier
Licensed Content Publication	Journal of Petroleum Science and Engineering
Licensed Content Title	Phase inversion and rheological behavior of emulsions stabilized by silica nanoparticles and nanoclay
Licensed Content Author	D. Slavova, S. Pollak, M. Petermann
Licensed Content Date	Jun 1, 2019
Licensed Content Volume	177
Licensed Content Issue	n/a
Licensed Content Pages	10
Type of Use	reuse in a thesis/dissertation
Portion	figures/tables/illustrations
Number of figures/tables/illustrations	1
Format	both print and electronic
Are you the author of this Elsevier article?	No
Will you be translating?	No
Title	Effects of Nanoparticle Interfacial Additives on Phase Inversion of Pickering Emulsion
Institution name	University of Waterloo
Expected presentation date	Jan 2020
Portions	Graphical Abstract
Requestor Location	Sileola Ogunlaja Chemical Engineering Dept. University of Waterloo

License agreements for Figure 6.6



RightsLink®



Home



Help



Email Support



Sileola Ogunlaja

Extraction of Oil from Oil Sands Using Thermoresponsive Polymeric Surfactants

Author: Bingqing Yang, Jean Duhamel

Publication: Applied Materials

Publisher: American Chemical Society

Date: Mar 1, 2015

Copyright © 2015, American Chemical Society



PERMISSION/LICENSE IS GRANTED FOR YOUR ORDER AT NO CHARGE

This type of permission/license, instead of the standard Terms & Conditions, is sent to you because no fee is being charged for your order. Please note the following:

- Permission is granted for your request in both print and electronic formats, and translations.
- If figures and/or tables were requested, they may be adapted or used in part.
- Please print this page for your records and send a copy of it to your publisher/graduate school.
- Appropriate credit for the requested material should be given as follows: "Reprinted (adapted) with permission from (COMPLETE REFERENCE CITATION). Copyright (YEAR) American Chemical Society." Insert appropriate information in place of the capitalized words.
- One-time permission is granted only for the use specified in your request. No additional uses are granted (such as derivative works or other editions). For any other uses, please submit a new request.

If credit is given to another source for the material you requested, permission must be obtained from that source.

References

- [1] B. Binks, "Particles as surfactants - similarities and differences," *Curr. Opin. Colloid Interface Sci.*, vol. 7, pp. 21–41, 2002.
- [2] V. B. Menon and D. T. Wasan, "Particle-Fluid Interactions With Application To Solidstabilized Emulsions," *Colloids and Surfaces*, vol. 19, pp. 89–105, 1986.
- [3] V. B. Menon and D. T. Wasan, "Characterization of oil-water interfaces containing finely divided solids with applications to the coalescence of water-in-oil Emulsions: A review," *Colloids and Surfaces*, vol. 29, no. 1, pp. 7–27, 1988.
- [4] V. B. Menon and D. T. Wasan, "Separation science and technology," *Sep. Sci. Technol.*, vol. 23, no. 12–13, p. 2131, 1990.
- [5] N. Yan and J. H. Masliyah, "Effect of pH on adsorption and desorption of clay particles at oil-water interface," *J. Colloid Interface Sci.*, vol. 181, no. 1, pp. 20–27, 1996.
- [6] H. Vatanparast, A. Javadi, and A. Bahramian, "Silica nanoparticles cationic surfactants interaction in water-oil system," *Colloids Surfaces A Physicochem. Eng. Asp.*, vol. 521, pp. 221–230, 2017.
- [7] D. Pradilla, S. Simon, and J. Sjöblom, "Mixed Interfaces of Asphaltenes and Model Demulsifiers, Part II: Study of Desorption Mechanisms at Liquid/Liquid Interfaces," *Energy and Fuels*, vol. 29, no. 9, pp. 5507–5518, 2015.
- [8] J. E. Park, D. R. Hickey, S. Jun, S. Kang, X. Hu, X. J. Chen, and S. J. Park, "Surfactant-Assisted Emulsion Self-Assembly of Nanoparticles into Hollow Vesicle-Like Structures and 2D Plates," *Adv. Funct. Mater.*, vol. 26, no. 43, pp. 7791–7798, 2016.
- [9] S. Levine and E. Sanford, "Stabilisation of emulsion droplets by fine powders," *Can. J. Chem. Eng.*, vol. 63, no. 2, pp. 258–268, 1985.
- [10] K. Kovalchuk, E. Riccardi, A. Mehandzhiyski, and B. A. Grimes, "Aggregates of poly-functional amphiphilic molecules in water and oil phases," *Colloid J.*, vol. 76, no. 5, pp. 564–575, 2014.
- [11] N. Yan, M. R. Gray, and J. H. Masliyah, "On water-in-oil emulsions stabilized by fine

- solids,” *Colloids Surfaces A Physicochem. Eng. Asp.*, vol. 193, no. 1–3, pp. 97–107, 2001.
- [12] W. Wang, Z. Zhou, K. Nandakumar, Z. Xu, and J. H. Masliyah, “Effect of charged colloidal particles on adsorption of surfactants at oil-water interface,” *J. Colloid Interface Sci.*, vol. 274, no. 2, pp. 625–630, 2004.
- [13] Y. Cui, M. Threlfall, and J. S. Van Duijneveldt, “Optimizing organoclay stabilized Pickering emulsions,” *J. Colloid Interface Sci.*, vol. 356, no. 2, pp. 665–671, 2011.
- [14] B. Z. Chowdhry, M. J. Snowden, S. A. Leharne, L. G. Torres, and R. Iturbe, “Preparation of o/w emulsions stabilized by solid particles and their characterization by oscillatory rheology,” *Colloids Surfaces A Physicochem. Eng. Asp.*, vol. 302, no. 1–3, pp. 439–448, 2007.
- [15] S. U. Pickering, “Emulsions,” *J. Chem. Soc.*, vol. 91, p. 2001, 1907.
- [16] B. P. Binks and R. Murakami, “Phase inversion of particle-stabilized materials from foams to dry water,” *Nat. Mater.*, vol. 5, p. 865, 2006.
- [17] T. N. Hunter, R. J. Pugh, G. V. Franks, and G. J. Jameson, “The role of particles in stabilising foams and emulsions,” *Adv. Colloid Interface Sci.*, vol. 137, no. 2, pp. 57–81, 2008.
- [18] L. L. Schramm, *Emulsions, Foams, and Suspensions: Fundamentals and Applications*. 2006.
- [19] S. Abdolbaghi, S. Pourmahdian, and Y. Saadat, “Preparation of poly(acrylamide)/nanoclay organic-inorganic hybrid nanoparticles with average size of ~250 nm via inverse Pickering emulsion polymerization,” *Colloid Polym. Sci.*, vol. 292, no. 5, pp. 1091–1097, 2014.
- [20] S. Tsuji and H. Kawaguchi, “Thermosensitive pickering emulsion stabilized by poly(N-isopropylacrylamide)-carrying particles,” *Langmuir*, vol. 24, no. 7, pp. 3300–3305, 2008.
- [21] P. Becher, *Emulsions: Theory and Practice*. New Jersey: Reinhold Publishing Corporation, 1957.
- [22] R. Pichot, F. Spyropoulos, and I. T. Norton, “Competitive adsorption of surfactants and hydrophilic silica particles at the oil-water interface: Interfacial tension and contact angle

- studies,” *J. Colloid Interface Sci.*, vol. 377, no. 1, pp. 396–405, 2012.
- [23] L. L. Schramm, “Colloids,” in *Kirk–Othmer Encyclopedia of Chemical Technology*, Online., New York: Wiley, 2003, p. 17.
- [24] B. P. Binks and S. O. Lumsdon, “Influence of particle wettability on the type and stability of surfactant-free emulsions,” *Langmuir*, vol. 16, no. 23, pp. 8622–8631, 2000.
- [25] B. P. Binks and T. S. Horozov, “Colloidal particles at liquid interfaces: An introduction,” in *Colloidal Particles at Liquid Interfaces*, B. P. Binks and T. S. Horozov, Eds. Cambridge University Press., 2006, pp. 1–74.
- [26] E. Dickinson, “Interfacial Particles in Emulsions,” 2012, no. June, pp. 1–52.
- [27] E. Dickinson, R. Ettelaie, T. Kostakis, and B. S. Murray, “Factors controlling the formation and stability of air bubbles stabilized by partially hydrophobic silica nanoparticles,” *Langmuir*, vol. 20, no. 20, pp. 8517–8525, 2004.
- [28] R. Lopetinsky, J. Masliyah, and Z. Xu, “Solid-Stabilized Emulsions: A Review in Colloidal Particles at Liquid Interfaces, B.P. Binks and T.S. Horozov (Eds.),” in *Colloidal Particles at Liquid Interfaces*, Cambridge University Press, 2006, p. 189.
- [29] L. Schramm, “Petroleum Emulsions: Basic Principles,” in *Advances in Chemistry*, Washington DC: American Chemical Society, 1992.
- [30] S. S. Elnashaie, F. Danafar, and H. Hashemipour, *Nanotechnology for chemical engineers*. 2016.
- [31] W. Li, L. Yu, G. Liu, J. Tan, S. Liu, and D. Sun, “Oil-in-water emulsions stabilized by Laponite particles modified with short-chain aliphatic amines,” *Colloids Surfaces A Physicochem. Eng. Asp.*, vol. 400, pp. 44–51, 2012.
- [32] R. Pal, “Modeling of Sedimentation and Creaming in Suspensions and Pickering Emulsions,” *Fluids*, vol. 4, no. 186, pp. 1–22, 2019.
- [33] W. Ramsden, “Separation of Solids in the Surface-Layers of Solutions and ‘Suspensions’ (Observations on Surface-Membranes, Bubbles, Emulsions, and Mechanical Coagulation). - Preliminary Account,” in *Royal Society of London*, 1904, vol. 72, pp. 156–164.
- [34] A. Boker, J. He, T. Emrick, and T. Russell, “Self-assembly of nanoparticles at interfaces,”

- Soft Matter*, vol. 3, no. 10, p. 1231, 2007.
- [35] T. S. Horozov and B. P. Binks, “Particle-stabilized emulsions: A bilayer or a bridging monolayer?,” *Angew. Chemie - Int. Ed.*, vol. 45, no. 5, pp. 773–776, 2006.
- [36] B. P. Binks and S. O. Lumsdon, “Stability of oil-in-water emulsions stabilised by silica particles,” *Phys. Chem. Chem. Phys.*, vol. 1, no. 12, pp. 3007–3016, 1999.
- [37] R. Kaegi, A. Voegelin, B. Sinnet, S. Zuleeg, H. Hagendorfer, M. Burkhardt, and H. Siegrist, “Behavior of metallic silver nanoparticles in a pilot wastewater treatment plant,” *Environ. Sci. Technol.*, vol. 45, no. 9, pp. 3902–3908, 2011.
- [38] Y. Chevalier and M. A. Bolzinger, “Emulsions stabilized with solid nanoparticles: Pickering emulsions,” *Colloids Surfaces A Physicochem. Eng. Asp.*, vol. 439, pp. 23–34, 2013.
- [39] A. D. Dinsmore, M. F. Hsu, M. G. Nikolaides, M. Marquez, A. R. Bausch, and D. A. Weitz, “Colloidosomes: Selectively Permeable Capsules Composed of Colloidal Particles,” *Science (80-.)*, vol. 298, no. 80, pp. 1006–1009, 2002.
- [40] B. P. Binks, “Colloidal Particles at a Range of Fluid-Fluid Interfaces,” *Langmuir*, vol. 33, no. 28, pp. 6947–6963, 2017.
- [41] R. J. Stokes and D. F. Evans, *Fundamentals of Interfacial Engineering*. New York: John Wiley & Sons, Inc, 1997.
- [42] M. Jawaid, A. el K. Qaiss, and R. Bouhfid, “Nanoclay Reinforced Polymer Composites : Natural Fibre/Nanoclay Hybrid Composites,” *Eng. Mater.*, no. July, p. 301, 2016.
- [43] L. L. Schramm, *Emulsions, Foams, and Suspensions: Fundamentals and Applications*. 2006.
- [44] B. Derjaguin and L. Landau, “Theory of the Stability of Strongly Charged Lyophobic Sols and of the Adhesion of Strongly Charged Particles in Solutions of Electrolytes,” *Inst. Colloid Electrochem.*, pp. 30–59, 1941.
- [45] E. J. W. Verwey and J. T. G. Overbeek, “Theory of the stability of lyophobic colloids,” *J. Colloid Interface Sci.*, vol. 10, no. 5, pp. 224–225, 1955.
- [46] D. Myers, *Surfaces, interfaces, and colloids: Principles and Applications*, Second., vol. 4.

New York, 1999.

- [47] Malvern, “Zeta potential: An Introduction in 30 minutes,” Worcestershire, 2011.
- [48] “Diagram showing Zeta potential: Retrieved from Particle Tech Lab website 11/12/2019.” [Online]. Available: <https://www.particletechlabs.com/analytical-testing/zeta-potential-analysis>.
- [49] J. Israelachvili, *Intermolecular and Surface Forces*, 3rd ed. Amsterdam: Academic Press, 2011.
- [50] N. P. Ashby and B. P. Binks, “Pickering emulsions stabilised by Laponite clay particles,” *Phys. Chem. Chem. Phys.*, vol. 2, no. 24, pp. 5640–5646, 2000.
- [51] B. P. Binks, “Particles as surfactants—similarities and differences,” *Curr. Opin. Colloid Interface Sci.*, vol. 7, no. 1–2, pp. 21–41, 2002.
- [52] S. Abend, N. Bonnke, U. Gutschner, and G. Lagaly, “Stabilization of emulsions by heterocoagulation of clay minerals and layered double hydroxides,” *Colloid Polym. Sci.*, vol. 276, no. 8, pp. 730–737, 1998.
- [53] S. Arditty, C. P. Whitby, B. P. Binks, V. Schmitt, and F. Leal-Calderon, “Some general features of limited coalescence in solid-stabilized emulsions,” *Eur. Phys. J. E*, vol. 11, no. 3, pp. 273–281, 2003.
- [54] B. P. Binks and S. O. Lumsdon, “Effects of oil type and aqueous phase composition on oil water mixtures containing particles of intermediate hydrophobicity,” *Phys. Chem. Chem. Phys.*, vol. 2, no. March, pp. 2959–2967, 2000.
- [55] B. P. Binks, J. H. Clint, and C. P. Whitby, “Rheological behavior of water-in-oil emulsions stabilized by hydrophobic bentonite particles,” *Langmuir*, vol. 21, no. 12, pp. 5307–5316, 2005.
- [56] I. Langmuir, “The constitution and fundamental properties of solids and liquids,” *J. Am. Chem. Soc.*, vol. 38, p. 102, 1916.
- [57] R. Aveyard, B. P. Binks, J. H. Clint, P. D. Fletcher, T. S. Horozov, B. Neumann, V. N. Paunov, J. Annesley, S. W. Botchway, D. Nees, A. W. Parker, A.D. Ward, and A. N. Burgess, “Measurement of long-range repulsive forces between charged particles at an oil-

- water interface,” *Phys. Rev. Lett.*, vol. 88, no. 24, pp. 2461021–2461024, 2002.
- [58] C. P. Whitby, F. E. Fischer, D. Fornasiero, and J. Ralston, “Shear-induced coalescence of oil-in-water Pickering emulsions,” *J. Colloid Interface Sci.*, vol. 361, no. 1, pp. 170–177, 2011.
- [59] B. P. Binks and J. H. Clint, “Solid wettability from surface energy components: Relevance to pickering emulsions,” *Langmuir*, vol. 18, no. 4, pp. 1270–1273, 2002.
- [60] N. Yan and J. H. Masliyah, “Characterization and demulsification of solids-stabilized oil-in-water emulsions Part 1. Partitioning of clay particles and preparation of emulsions,” *Colloids Surfaces A Physicochem. Eng. Asp.*, vol. 96, no. 3, pp. 229–242, 1995.
- [61] A. Ding, B. P. Binks, and W. A. Goedel, “Influence of particle hydrophobicity on particle-assisted wetting,” *Langmuir*, vol. 21, no. 4, pp. 1371–1376, 2005.
- [62] Levine, Samuel, Bowen, Bruce D., and Partridge, Susan J., “Stabilization of Emulsions by Fine Particles I. Partitioning of Particles Between Continuous Phase and Oil/Water Interface,” *Colloids and Surfaces*, vol. 38, pp. 325–343, 1989.
- [63] R. Aveyard, B. P. Binks, and J. H. Clint, “Emulsions Stabilised Solely by Colloidal Particles,” vol. 102, no. February, pp. 503–546, 2003.
- [64] B. P. Binks and S. O. Lumsdon, “Catastrophic Phase Inversion of Water-in-Oil Emulsions Stabilized by Hydrophobic Silica,” *Langmuir*, vol. 16, no. 6, pp. 2539–2547, 2002.
- [65] B. P. Binks and C. P. Whitby, “Silica Particle-Stabilized Emulsions of Silicone Oil and Water: Aspects of Emulsification,” *Langmuir*, vol. 20, no. 4, pp. 1130–1137, 2004.
- [66] R. Pal, “A simple model for the viscosity of pickering emulsions,” *Fluids*, vol. 3, no. 1, pp. 1–13, 2018.
- [67] W. Ramsden, “Separation of solids in the surface-layers of solutions and ‘suspensions’ (observations on surface-membranes, bubbles, emulsions, and mechanical coagulation).—Preliminary account,” *Proc. R. Soc. London*, vol. 72, no. 477–486, pp. 156–164, 1904.
- [68] T. Y. Jeon and J. S. Hong, “Stabilization of O/W emulsion with hydrophilic/hydrophobic clay particles,” *Colloid Polym. Sci.*, vol. 292, no. 11, pp. 2939–2947, 2014.
- [69] B. P. Binks and R. Murakami, “Phase inversion of particle-stabilized materials from

- foams to dry water,” *Nat. Mater.*, vol. 5, no. 11, pp. 865–869, 2006.
- [70] S. Melle, M. Lask, and G. G. Fuller, “Pickering emulsions with controllable stability,” *Langmuir*, vol. 21, no. 6, pp. 2158–2162, 2005.
- [71] B. P. Binks and J. A. Rodrigues, “Types of phase inversion of silica particle stabilized emulsions containing triglyceride oil,” *Langmuir*, vol. 19, no. 12, pp. 4905–4912, 2003.
- [72] B. P. Binks, *Modern Aspects of Emulsion Science*. Cambridge: The Royal Society of Chemistry, 1998.
- [73] D. Tambe, J. Paulis, and M. M. Sharma, “Factors Controlling the Stability of Colloid-Stabilized Emulsions,” *Journal of Colloid and Interface Science*, vol. 171, no. 2, pp. 463–469, 2002.
- [74] T. Young, *An Essay on the Cohesion of Fluids*, 95th ed. London: Phil. Trans. Royal Society of London, 1805.
- [75] N. Yan and J. H. Masliyah, “Effect of pH on Adsorption and Desorption of Clay Particles at Oil–Water Interface,” *J. Colloid Interface Sci.*, vol. 181, pp. 20–27, 1996.
- [76] J. . Quinn and D. . Sigloh, “Phase Inversion in the Mixing of Immiscible Liquids,” *Can. J. Chem. Eng.*, pp. 15–18, 1963.
- [77] D. Slavova, S. Pollak, and M. Petermann, “Phase inversion and rheological behavior of emulsions stabilized by silica nanoparticles and nanoclay,” *J. Pet. Sci. Eng.*, vol. 177, no. September 2018, pp. 624–633, 2019.
- [78] S. Chakraborty, B. Sahoo, I. Teraoka, and R. A. Gross, “Solution properties of starch nanoparticles in water and DMSO as studied by dynamic light scattering,” *Carbohydr. Polym.*, vol. 60, no. 4, pp. 475–481, 2005.
- [79] S. Bloembergen, I. J. McLennan, and D. I. Lee, “Specialty Biobased Monomers and Emulsion Polymers Derived from Starch,” *Adv. Coat. Fundam. Symp.*, pp. 1–19, 2010.
- [80] S. Bloembergen, M. P. Santos, P. Greenall, R. DeJong, J. Y. Shin, N. Jones, P. D. Fleming, M. K. Joyce, and D. I. Lee, “The effects of biolatex binders on the dynamic water retention properties of paper coating formulations,” in *The 46th ABTCP International Pulp and Paper Congress*, 2013, vol. 46, pp. 55–65.

- [81] Y. Zhang, M. F. Cunningham, N. M. B. Smeets, and M. A. Dubé, “Starch nanoparticle incorporation in latex-based adhesives,” *Eur. Polym. J.*, vol. 106, no. June, pp. 128–138, 2018.
- [82] M. Perez Herrera and T. Vasanthan, “Rheological characterization of gum and starch nanoparticle blends,” *Food Chem.*, vol. 243, no. September 2017, pp. 43–49, 2018.
- [83] S. Sinha Ray and M. Okamoto, “Polymer/layered silicate nanocomposites: A review from preparation to processing,” *Prog. Polym. Sci.*, vol. 28, no. 11, p. 1542, 2003.
- [84] J. K. Kim, P. A. Rühs, P. Fischer, and J. S. Hong, “Interfacial localization of nanoclay particles in oil-in-water emulsions and its reflection in interfacial moduli,” *Rheol. Acta*, vol. 52, pp. 327–335, 2013.
- [85] C. Li, Q. Liu, Z. Mei, J. Wang, J. Xu, and D. Sun, “Pickering emulsions stabilized by paraffin wax and Laponite clay particles,” *J. Colloid Interface Sci.*, vol. 336, no. 1, pp. 314–321, 2009.
- [86] A. Tsugita, S. Takemoto, and K. Mori, “Studies on O / W Emulsions Stabilized with Insoluble Montmorillonite-Organic Complexes Preparation of Emulsions Emulsification method . The standard Determination of emulsion stability . The Measurements of Emulsion Properties Differential scanning calorimetry,” *October*, vol. 95, no. 2, 1983.
- [87] S. Arditty, V. Schmitt, J. Giermanska-Kahn, and F. Leal-Calderon, “Materials based on solid-stabilized emulsions,” *J. Colloid Interface Sci.*, vol. 275, no. 2, pp. 659–664, 2004.
- [88] Y. Yan and J. H. Masliyah, “Solids-stabilized oil-in-water emulsions: Scavenging of emulsion droplets by fresh oil addition,” *Colloids Surfaces A Physicochem. Eng. Asp.*, vol. 75, no. C, pp. 123–132, 1993.
- [89] N. Berkowitz and J. G. Speight, “The oil sands of Alberta,” *Fuel*, vol. 54, no. 3, pp. 138–149, 1975.
- [90] R. J. Chalaturnyk, J. Don Scott, and B. Özüm, “Management of Oil Sands Tailings,” *Pet. Sci. Technol.*, vol. 20, no. 9–10, pp. 1025–1046, 2002.
- [91] A. B. Hande, “Accelerated Dewatering and Drying Treatment of Oil Sands Tailings by Electrical Resonant Auto-Transformer,” pp. 59–61, 2014.

- [92] J. Masliyah, Z. J. Zhou, Z. Xu, J. Czarnecki, and H. Hamza, “Understanding Water-Based Bitumen Extraction,” vol. 82, no. August, pp. 628–654, 2004.
- [93] L. J. Michot, I. Bihannic, K. Porsch, S. Maddi, C. Baravian, J. Mougel, and P. Levitz, “Phase diagrams of wyoming Na-montmorillonite clay. Influence of particle anisotropy,” *Langmuir*, vol. 20, no. 25, pp. 10829–10837, 2004.
- [94] W. J. Ganley and J. S. Van Duijneveldt, “Controlling clusters of colloidal platelets: Effects of edge and face surface chemistries on the behavior of montmorillonite suspensions,” *Langmuir*, vol. 31, no. 15, pp. 4377–4385, 2015.
- [95] Orion, “Thermo Scientific Orion Star Series Conductivity Meter Guide,” 2010.
- [96] V. Malhotra, R. Pal, and A. Saeed, “Catastrophic Phase Inversion of Emulsions Stabilized by Amphiphilic Nanoparticles,” *J. Nanofluids*, vol. 7, no. 1, pp. 30–37, 2018.
- [97] Ramsden. W, “Separation of Solids in the Surface-Layers of Solutions and ‘Suspensions’ (Observations on Surface-Membranes, Bubbles, Emulsions, and Mechanical Coagulation). -- Preliminary Account,” *Proc. R. Soc.*, vol. 72, p. 156, 1903.
- [98] S. U. Pickering, “S.U Pickering, Emulsions, *J. Chem. Soc.*91 (1907) 2001 - 2021,” *J. Chem. Soc.*, vol. 91, pp. 2001–2021, 1907.
- [99] S. Fujii, E. S. Read, B. P. Binks, and S. P. Armes, “Stimulus-responsive emulsifiers based on nanocomposite microgel particles,” *Adv. Mater.*, vol. 17, no. 8, pp. 1014–1018, 2005.
- [100] P. F. Noble, O. J. Cayre, R. G. Alargova, O. D. Velez, and V. N. Paunov, “Fabrication of ‘hairy’ colloidosomes with shells of polymeric microrods,” *J. Am. Chem. Soc.*, vol. 126, pp. 8092–8093, 2004.
- [101] A. Popadyuk, N. Popadyuk, I. Tarnavchyk, S. Voronov, and A. Voronov, “Colloidosomes from Peroxidized Pickering Emulsions,” *Int. J. Theor. Appl. Nanotechnol.*, vol. 3, pp. 20–27, 2015.
- [102] J. W. Kim, A. Fernández-Nieves, N. Dan, A. S. Utada, M. Marquez, and D. A. Weitz, “Colloidal assembly route for responsive colloidosomes with tunable permeability,” *Nano Lett.*, vol. 7, no. 9, pp. 2876–2880, 2007.
- [103] M. Rondon-Gonzalez, L. F. Madariaga, V. Sadtler, L. Choplin, L. Marquez, and J.-L.

- Salager, "Emulsion Catastrophic Inversion from Abnormal to Normal Morphology. 6. Effect of the Phase Viscosity on the Inversion Produced by Continuous Stirring," *Ind. Eng. Chem. Res.*, vol. 46, no. 11, pp. 3595–3601, 2007.
- [104] M. Rondón-González, V. Sadtler, L. Choplin, and J. L. Salager, "Emulsion inversion from abnormal to normal morphology by continuous stirring without internal phase addition. Effect of surfactant mixture fractionation at extreme water-oil ratio," *Colloids Surfaces A Physicochem. Eng. Asp.*, vol. 288, pp. 151–157, 2006.
- [105] S. Tsuji and H. Kawaguchi, "Self-Assembly of Poly (N -isopropylacrylamide) -Carrying Microspheres into Two-Dimensional Colloidal Arrays," *Langmuir*, vol. 21, no. 15, pp. 2434–2437, 2005.
- [106] R. Pal, "Viscous properties of polymer-thickened water-in-oil emulsions," *J. Appl. Polym. Sci.*, vol. 49, p. 65, 1993.
- [107] J. A. Holgado-Terriza, J. F. Gómez-Lopera, P. L. Luque-Escamilla, C. Atae-Allah, and M. A. Cabrerizo-Vílchez, "Measurement of ultralow interfacial tension with ADSA using an entropic edge-detector," *Colloids Surfaces A Physicochem. Eng. Asp.*, vol. 156, pp. 579–586, 1999.
- [108] M. A. Cabrerizo-Vílchez, Z. Policova, D. Y. Kwok, P. Chen, and A. W. Neumann, "The temperature dependence of the interfacial tension of aqueous human albumin solution/decane," *Colloids Surfaces B Biointerfaces*, vol. 5, pp. 1–9, 1995.
- [109] K. Sarikhani, R. Nasser, V. Lotocki, R. B. Thompson, C. B. Park, and P. Chen, "Effect of well-dispersed surface-modified silica nanoparticles on crystallization behavior of poly (lactic acid) under compressed carbon dioxide," *Polymer (Guildf.)*, vol. 98, pp. 100–109, 2016.
- [110] K. Sarikhani, K. Jeddi, R. B. Thompson, C. B. Park, and P. Chen, "Adsorption of surface-modified silica nanoparticles to the interface of melt poly(lactic acid) and supercritical carbon dioxide," *Langmuir*, vol. 31, no. 20, pp. 5571–5579, 2015.
- [111] H. Park, C. B. Park, C. Tzoganakis, K. H. Tan, and P. Chen, "Surface tension measurement of polystyrene melts in supercritical carbon dioxide," *Ind. Eng. Chem. Res.*, vol. 45, no. 5, pp. 1650–1658, 2006.

- [112] W. Ostwald, *Kolloid-Z*, vol. 6, no. 103, 1910.
- [113] J. Pinter and E. Wolfram, *Surface Phenomena in Enhanced Oil Recovery*, 1st Ed. Springer, 1981.
- [114] C. P. Whitby, D. Fornasiero, J. Ralston, L. Liggieri, and F. Ravera, “Properties of Fatty Amine – Silica Nanoparticle Interfacial Layers at the Hexane – Water Interface,” *J. Phys. Chem. C*, vol. 116, pp. 3050–3058, 2012.
- [115] K. Staszak, D. Wiczorek, and K. Michocka, “Effect of Sodium Chloride on the Surface and Wetting Properties of Aqueous Solutions of Cocamidopropyl Betaine,” *J. Surfactants Deterg.*, vol. 18, no. 2, pp. 321–328, 2014.
- [116] S. B. Ogunlaja, R. Pal, and K. Sarikhani, “Effects of starch nanoparticles on phase inversion of Pickering emulsions,” *Can. J. Chem. Eng.*, vol. 96, no. 5, pp. 1089–1097, 2018.
- [117] B. P. Binks, “Influence of Particle Wettability on the Type and Stability Binks,” *Am. Chem. Soc.*, vol. 16, no. 23, pp. 8622–8631, 2000.
- [118] S. Tunç, O. Duman, and B. Kanci, “Rheological measurements of Na-bentonite and sepiolite particles in the presence of tetradecyltrimethylammonium bromide, sodium tetradecyl sulfonate and Brij 30 surfactants,” *Colloids Surfaces A Physicochem. Eng. Asp.*, vol. 398, pp. 37–47, 2012.
- [119] M. Moosavi, “Bentonite clay as a natural remedy: A brief review,” *Iran. J. Public Health*, vol. 46, no. 9, pp. 1176–1183, 2017.
- [120] G. F. Perotti, H. S. Barud, Y. Messaddeq, S. J. L. Ribeiro, and V. R. L. Constantino, “Bacterial cellulose-laponite clay nanocomposites,” *Polymer (Guildf.)*, vol. 52, no. 1, pp. 157–163, 2011.
- [121] Sigma Aldrich, “Advanced Applications of Engineered Nanomaterials,” *Aldrich - Mater. Matters*, vol. 2, no. 1, pp. 1–15, 2007.
- [122] X. Jian, W. Xuebing, D. Bingyao, and L. Qingsheng, “Modification of montmorillonite by different surfactants and its use for the preparation of polyphenylene sulfide nanocomposites,” *High Perform. Polym.*, vol. 28, no. 5, pp. 618–629, 2016.

- [123] A. Tsugita, S. Takemoto, and K. Mori, "Studies on O/W Emulsions Stabilized with Insoluble Montmorillonite-Organic Complexes," *J. Colloid Interface Sci.*, vol. 95, no. 2, pp. 551–560, 1983.
- [124] Z. G. Cui, L. L. Yang, Y. Z. Cui, and B. P. Binks, "Effects of surfactant structure on the phase inversion of emulsions stabilized by mixtures of silica nanoparticles and cationic surfactant," *Langmuir*, vol. 26, no. 7, p. 4717, 2010.
- [125] B. H. Cipriano, S. R. Raghavan, and P. M. McGuiggan, "Surface tension and contact angle measurements of a hexadecyl imidazolium surfactant adsorbed on a clay surface," *Colloids Surfaces A Physicochem. Eng. Asp.*, vol. 262, no. 1–3, pp. 8–13, 2005.
- [126] A. Desmond, F. Desai, and K. Hayes, "Effect of cationic surfactants on organic liquid-water capillary pressure-saturation relationships," *Water Resour. Res.*, vol. 30, no. 2, pp. 333–342, 1994.
- [127] C. Jouany and P. Chassin, "Determination of the Surface Energy of Materials by Using Contact Angle Measurements," *Colloids and Surfaces*, vol. 27, pp. 289–303, 1987.
- [128] R. Pal, "A novel method to determine the thermal conductivity of interfacial layers surrounding the nanoparticles of a nanofluid," *Nanomaterials*, vol. 4, pp. 844–855, 2014.
- [129] M. H. Gabr, N. T. Phong, M. A. Abdelkareem, K. Okubo, K. Uzawa, I. Kimpara and T. Fujii, "Mechanical, thermal, and moisture absorption properties of nano-clay reinforced nano-cellulose biocomposites," *Cellulose*, vol. 20, pp. 819–826, 2013.
- [130] J. A. Bichard, "The research papers of John A. Bichard, 1957-1965 (AOSTRA technical publication series)," in *Oil Sands Composition and Behaviour Research*, Edmonton, Canada: Alberta Oil Sands Technology and Research Authority (1987), 1987.
- [131] K. L. Kasperski, "Review of research on aqueous extraction of bitumen from mined oil sands," Devon, Alberta, 2001.
- [132] "<https://economicdashboard.alberta.ca/>," *Government of Alberta*. .
- [133] Kobayashi K, "Forecasting supply and demand up to 2030," 2005.
- [134] A. T. Bell, "The Impact of Nanoscience on Heterogeneous Catalysis," *Sci. New Ser.*, vol. 299, no. 5613, pp. 1688–1691, 2003.

- [135] J. M. Perez, "Iron oxide nanoparticles: Hidden talent," *Nature*, vol. 2, no. September, pp. 535–536, 2007.
- [136] L. E. Foster, *Nanotechnology: Science, Innovation, and Opportunity*. Upper Saddle River, New Jersey: Prentice Hall PTR, 2005.
- [137] J. Zarkesh, R. Hashemi, M. Ghaedian, H. R. Khakdaman, S. J. Ahmadpanah, and S. Khadzhiev, "HRH: nano catalytic process to upgrade extra heavy crude/residual oils," in *19th world petroleum congress*, 2008.
- [138] R. Hashemi, N. N. Nassar, and P. Pereira Almao, "In situ upgrading of athabasca bitumen using multimetallic ultradispersed nanocatalysts in an oil sands packed-bed column: Part 1. Produced liquid quality enhancement," *Energy and Fuels*, vol. 28, no. 2, pp. 1338–1350, 2014.
- [139] R. Hashemi, N. N. Nassar, and P. Pereira Almao, "In situ upgrading of athabasca bitumen using multimetallic ultradispersed nanocatalysts in an oil sands packed-bed column: Part 2. Solid analysis and gaseous product distribution," *Energy and Fuels*, vol. 28, no. 2, pp. 1351–1361, 2014.
- [140] F. A. Z. a. Alatraktchi, Y. Zhang, and I. Angelidaki, "Nanomodification of the electrodes in microbial fuel cell: Impact of nanoparticle density on electricity production and microbial community," *Appl. Energy*, vol. 116, pp. 216–222, 2014.
- [141] B. Zhu, L. Fan, and P. Lund, "Breakthrough fuel cell technology using ceria-based multi-functional nanocomposites," *Appl. Energy*, vol. 106, pp. 163–175, 2013.
- [142] K. I. Winey and R. A. Vaia, "Polymer Nanocomposites," *MRS Bull.*, vol. 32, no. April, pp. 314–322, 2007.
- [143] M. Roy, J. K. Nelson, R. K. MacCrone, L. S. Schadler, C. W. Reed, R. Keefe, and W. Zenger, "Polymer nanocomposite dielectrics - The role of the interface," *IEEE Trans. Dielectr. Electr. Insul.*, vol. 12, no. 4, pp. 629–642, 2005.
- [144] T. Tanaka, M. Kozako, N. Fuse, and Y. Ohki, "Proposal of a multi-core model for polymer nanocomposite dielectrics," *IEEE Trans. Dielectr. Electr. Insul.*, vol. 12, no. 4, pp. 669–681, 2005.

- [145] J. M. Thomas, B. F. G. Johnson, R. Raja, G. Sankar, and P. A. Midgley, "High-performance nanocatalysts for single-step hydrogenations," *Acc. Chem. Res.*, vol. 36, no. 1, pp. 20–30, 2003.
- [146] T. F. Jaramillo, K. P. Jørgensen, J. Bonde, J. H. Nielsen, S. Hørch, and I. Chorkendorff, "Identification of active edge sites for electrochemical H₂ evolution from MoS₂ nanocatalysts," *Science (80)*, vol. 317, no. July, pp. 100–102, 2007.
- [147] S. H. Joo, J. Y. Park, C. K. Tsung, Y. Yamada, P. Yang, and G. A. Somorjai, "Thermally stable Pt/mesoporous silica core-shell nanocatalysts for high-temperature reactions," *Nat. Mater.*, vol. 8, no. 2, pp. 126–131, 2009.
- [148] F. Han, V. S. R. Kambala, M. Srinivasan, D. Rajarathnam, and R. Naidu, "Tailored titanium dioxide photocatalysts for the degradation of organic dyes in wastewater treatment: A review," *Appl. Catal. A Gen.*, vol. 359, no. 1–2, pp. 25–40, 2009.
- [149] H. Hildebrand, K. Mackenzie, and F. D. Kopinke, "Pd/Fe₃O₄ nano-catalysts for selective dehalogenation in wastewater treatment processes-Influence of water constituents," *Appl. Catal. B Environ.*, vol. 91, no. 1–2, pp. 389–396, 2009.
- [150] K. Xiangling and M. Ohadi, "Applications of micro and nano technologies in the oil and gas industry-overview of the recent progress," in *Abu Dhabi international petroleum exhibition and conference*, 2010.
- [151] B. Yang and J. Duhamel, "Extraction of Oil from Oil Sands Using Thermoresponsive Polymeric Surfactants," *Am. Chem. Soc.*, vol. 7, no. 10, pp. 5879–5889, 2015.
- [152] M. Shi, X. Liang, Y. Yan, H. Pan, and Y. Liu, "Influence of ethanol-water solvent and ultra-high pressure on the stability of amylose-n-octanol complex," *Food Hydrocoll.*, vol. 74, pp. 315–323, 2018.
- [153] Q. Zhang, "Thermoresponsive Starch Nanoparticles for Use in the Extraction of Oil from Oil Sands," 2018.

Appendix A

Table A 1: Physical and chemical properties of materials used-Hydrophilic bentonite nanoclay

Synonyms	Montmorillinite clay Bentonite Nanomer® PGV Nanomer® clay
Formula	Theoretical Formula for montmorillonite: $M^+_y(Al_{2-y}Mg_y)(Si_4)O_{10}(OH)_2 \cdot nH_2O$
Molecular weight	180.1 g/mol
CAS-No	1302-78-9
EC-No	215-108-5

Table A 2: Physical and chemical properties of materials used-Hexadecyl trimethyl ammonium bromide

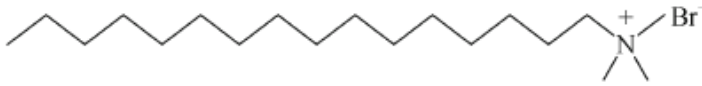
Synonyms	Cetrimonium bromide Palmityltrimethylammonium bromide Cetyltrimethylammonium bromide CTAB
Formula	$C_{19}H_{42}BrN$
Structure	
Molecular weight	364.45 g/mol
CAS-No	57-09-0
EC-No	200-311-3

Table A 3: Physical and chemical properties of materials used-White Mineral Oil 15

Synonyms	Oil A: White mineral oil (petroleum)
Product Code	PFWO15
Concentration	100% w/w
Density	0.85 kg/l (15 °C / 59 °F)
Kinematic Viscosity	15.00 cSt (40 °C / 104 °F) 3.43 cSt (100 °C / 212 °F)
CAS-No	8042-47-5

Table A 4: Physical and chemical properties of materials used-White Mineral Oil 35

Synonyms	Oil B: White mineral oil (petroleum)
Product Code	PFWO35
Concentration	100% w/w
Density	0.85 kg/l (15 °C / 59 °F)
Kinematic Viscosity	36.1 cSt (40 °C / 104 °F) 5.82 cSt (100 °C / 212 °F)
CAS-No	8042-47-5

Appendix B

Experimental Data

W/O to O/W Phase Inversion – Electrolyte (NaCl/Acticide) Medium

Hydrophilic Starch Nanoparticle (HSNP) Phase Inversion in Oil A

Blank/Oil A Emulsion

Oil (mL)	Water (mL)	k ($\mu\text{S}/\text{cm}$)	Volume Fraction (Water)
450	0	0	0.00
450	20	0	0.04
450	40	0	0.08
450	60	0	0.12
450	80	0	0.15
450	100	0	0.18
450	120	0	0.21
450	140	0	0.24
450	160	0	0.26
450	180	16.9	0.29
450	200	26	0.31
450	220	163.5	0.33
450	240	175.9	0.35
450	260	182.9	0.37
450	280	203.4	0.38
450	300	218.7	0.40
450	320	221.1	0.42
450	340	252.1	0.43
450	360	273.2	0.44
450	380	304	0.46
450	400	323	0.47
450	420	333	0.48
450	440	365	0.49
450	460	370	0.51
450	480	404	0.52
450	520	422	0.54
450	560	440	0.55

450	600	457	0.57
450	640	484	0.59
450	680	502	0.60
450	700	520	0.61
450	740	539	0.62
450	780	557	0.63
450	820	575	0.65
450	860	580	0.66
450	900	581	0.67
450	940	582	0.68
450	980	595	0.69
450	1020	605	0.69
450	1060	601	0.70
450	1100	614	0.71
450	1160	626	0.72
450	1220	643	0.73
450	1280	653	0.74
450	1340	671	0.75
450	1410	682	0.76
450	1480	693	0.77
450	1550	705	0.78

0.1wt% HSNP/Oil A Emulsion

Oil (mL)	Water (mL)	k ($\mu\text{S}/\text{cm}$)	Volume Fraction (Water)
450	0	0	0.00
450	20	0.04	0.04
450	40	0.05	0.08
450	60	0.07	0.12
450	80	0.19	0.15
450	100	0.13	0.18
450	120	0.14	0.21
450	140	0.53	0.24
450	160	0.63	0.26
450	180	0.53	0.29
450	200	2.33	0.31
450	220	1.9	0.33
450	240	1.87	0.35

450	260	44.5	0.37
450	280	4.19	0.38
450	300	28.72	0.40
450	320	25.22	0.42
450	340	29.5	0.43
450	360	51	0.44
450	380	202	0.46
450	400	259.9	0.47
450	420	354	0.48
450	440	385	0.49
450	460	395	0.51
450	480	407	0.52
450	500	416	0.53
450	520	427	0.54
450	540	437	0.55
450	560	452	0.55
450	580	457	0.56
450	620	477	0.58
450	660	502	0.59
450	700	522	0.61
450	740	541	0.62
450	780	556	0.63
450	820	569	0.65
450	860	579	0.66
450	910	596	0.67
450	960	612	0.68
450	1010	626	0.69
450	1060	643	0.70
450	1110	652	0.71
450	1160	670	0.72
450	1210	696	0.73
450	1260	706	0.74
450	1310	720	0.74
450	1370	733	0.75
450	1430	740	0.76
450	1490	746	0.77
450	1550	756	0.78
450	1610	764	0.78

0.2wt% HSNP/Oil A Emulsion

Oil (mL)	Water (mL)	k ($\mu\text{S}/\text{cm}$)	Volume Fraction (Water)
450	0	0	0.00
450	20	0	0.04
450	40	0	0.08
450	60	0.19	0.12
450	80	0.14	0.15
450	100	0.22	0.18
450	120	0.2	0.21
450	140	0.23	0.24
450	160	0.42	0.26
450	180	0.82	0.29
450	200	0.7	0.31
450	220	1.44	0.33
450	240	3.39	0.35
450	260	1.15	0.37
450	280	4.87	0.38
450	300	3.74	0.40
450	320	6.23	0.42
450	340	5.1	0.43
450	360	4.55	0.44
450	380	4.19	0.46
450	400	10.6	0.47
450	420	14.34	0.48
450	440	15.7	0.49
450	460	107.1	0.51
450	480	411	0.52
450	500	434	0.53
450	520	443	0.54
450	540	453	0.55
450	560	468	0.55
450	580	480	0.56
450	600	489	0.57
450	640	504	0.59
450	680	524	0.60
450	720	542	0.62

450	760	555	0.63
450	800	570	0.64
450	840	583	0.65
450	880	596	0.66
450	920	615	0.67
450	960	626	0.68
450	1000	636	0.69
450	1050	651	0.70
450	1100	663	0.71
450	1150	677	0.72
450	1200	689	0.73
450	1250	699	0.74
450	1300	710	0.74
450	1350	717	0.75
450	1400	729	0.76
450	1450	740	0.76
450	1500	748	0.77
450	1540	755	0.77
450	1580	761	0.78
450	1620	768	0.78

0.4wt% HSNP/Oil A Emulsion

Oil (mL)	Water (mL)	k ($\mu\text{S}/\text{cm}$)	Volume Fraction (Water)
450	0	0	0.00
450	20	0	0.04
450	40	0	0.08
450	60	0.03	0.12
450	80	0.03	0.15
450	100	0.03	0.18
450	120	0.04	0.21
450	140	0.07	0.24
450	160	0.13	0.26
450	180	0.39	0.29
450	200	0.96	0.31
450	220	1.14	0.33
450	240	1.77	0.35
450	260	3.4	0.37

450	280	0.85	0.38
450	300	0.76	0.40
450	320	1.12	0.42
450	340	1.43	0.43
450	360	0.73	0.44
450	380	0.62	0.46
450	400	0.82	0.47
450	420	1.31	0.48
450	440	0.83	0.49
450	460	3.15	0.51
450	480	3.21	0.52
450	500	4.71	0.53
450	520	4.56	0.54
450	540	6.96	0.55
450	560	1.64	0.55
450	580	2.46	0.56
450	600	5.55	0.57
450	620	7.62	0.58
450	640	499	0.59
450	660	515	0.59
450	680	518	0.60
450	700	530	0.61
450	720	541	0.62
450	760	562	0.63
450	820	577	0.65
450	860	595	0.66
450	900	611	0.67
450	940	630	0.68
450	980	643	0.69
450	1020	656	0.69
450	1060	673	0.70
450	1120	686	0.71
450	1160	703	0.72
450	1220	719	0.73
450	1280	733	0.74
450	1340	748	0.75
450	1400	761	0.76

1wt% HSNP/Oil A Emulsion

Oil (mL)	Water (mL)	k ($\mu\text{S}/\text{cm}$)	Volume Fraction (Water)
450	0	0	0.00
450	20	0	0.04
450	40	0.03	0.08
450	60	0.06	0.12
450	80	0.08	0.15
450	100	0.14	0.18
450	120	0.58	0.21
450	140	0.17	0.24
450	160	0.74	0.26
450	180	1.16	0.29
450	200	2.31	0.31
450	220	2.13	0.33
450	240	5.45	0.35
450	260	4.29	0.37
450	280	5.59	0.38
450	300	5.93	0.40
450	320	4.69	0.42
450	340	5.68	0.43
450	360	2.91	0.44
450	380	5.84	0.46
450	400	4.71	0.47
450	420	41.9	0.48
450	440	6.93	0.49
450	460	9.33	0.51
450	480	3.15	0.52
450	500	1.76	0.53
450	520	4.52	0.54
450	540	6.44	0.55
450	560	4.32	0.55
450	580	4.14	0.56
450	600	5.1	0.57
450	620	6.8	0.58
450	640	7.71	0.59
450	660	2.84	0.59
450	680	5.44	0.60

450	700	4.67	0.61
450	720	2.67	0.62
450	740	4.97	0.62
450	760	5.22	0.63
450	780	3.13	0.63
450	800	4.3	0.64
450	820	3.7	0.65
450	840	8.14	0.65
450	860	8.75	0.66
450	880	11.41	0.66
450	900	8.96	0.67
450	920	49.4	0.67
450	940	135.2	0.68
450	960	16.68	0.68
450	980	614	0.69
450	1000	644	0.69
450	1020	648	0.69
450	1040	655	0.70
450	1060	664	0.70
450	1080	669	0.71
450	1120	684	0.71
450	1160	697	0.72
450	1200	706	0.73
450	1240	718	0.73
450	1280	728	0.74
450	1320	739	0.75
450	1360	747	0.75
450	1400	758	0.76
450	1440	766	0.76
450	1480	775	0.77
450	1520	784	0.77
450	1560	791	0.78
450	1600	799	0.78
450	1640	803	0.78

2wt% HSNP/Oil A Emulsion

Oil (mL)	Water (mL)	k ($\mu\text{S}/\text{cm}$)	Volume Fraction (Water)
450	0	0	0.00
450	20	0	0.04
450	40	0.03	0.08
450	60	0.04	0.12
450	80	0.07	0.15
450	100	0.12	0.18
450	120	0.3	0.21
450	140	0.42	0.24
450	160	1.67	0.26
450	180	2.11	0.29
450	200	5.24	0.31
450	220	3.88	0.33
450	240	5.9	0.35
450	260	7.6	0.37
450	280	4.5	0.38
450	300	5.46	0.40
450	320	4.05	0.42
450	340	2.08	0.43
450	360	4.16	0.44
450	380	4.74	0.46
450	400	4.89	0.47
450	420	7.74	0.48
450	440	8.97	0.49
450	460	9.12	0.51
450	480	9.72	0.52
450	500	6.16	0.53
450	520	9.67	0.54
450	540	10.15	0.55
450	560	7.59	0.55
450	580	9.73	0.56
450	600	8.57	0.57
450	620	9.07	0.58
450	640	7.94	0.59
450	660	8.11	0.59

450	680	8.88	0.60
450	700	6.33	0.61
450	720	6.56	0.62
450	740	8.59	0.62
450	760	15.22	0.63
450	780	15.75	0.63
450	800	11.47	0.64
450	820	12.07	0.65
450	840	11	0.65
450	860	9.73	0.66
450	880	11.24	0.66
450	900	10.75	0.67
450	920	10.18	0.67
450	940	10.04	0.68
450	960	10.13	0.68
450	980	18.81	0.69
450	1000	13.24	0.69
450	1020	11.52	0.69
450	1040	12.53	0.70
450	1060	47	0.70
450	1080	637	0.71
450	1100	669	0.71
450	1120	676	0.71
450	1140	680	0.72
450	1180	693	0.72
450	1220	703	0.73
450	1260	710	0.74
450	1300	723	0.74
450	1340	735	0.75
450	1380	747	0.75
450	1420	756	0.76
450	1460	764	0.76
450	1500	774	0.77
450	1540	783	0.77
450	1580	791	0.78
450	1600	796	0.78
450	1620	798	0.78

Hydrophilic Starch Nanoparticle (HSNP) Phase Inversion in Oil B

Blank/Oil B Emulsion

Oil (mL)	Water (mL)	k ($\mu\text{S}/\text{cm}$)	Volume Fraction (Water)
450	0	0	0.00
450	20	0	0.04
450	40	0.05	0.08
450	60	0.11	0.12
450	80	0.16	0.15
450	100	1.07	0.18
450	120	14.69	0.21
450	140	26.44	0.24
450	160	29.88	0.26
450	180	142.2	0.29
450	200	174.2	0.31
450	220	208.8	0.33
450	240	231.6	0.35
450	260	246.6	0.37
450	280	263.5	0.38
450	300	282.7	0.40
450	320	288.9	0.42
450	360	325.4	0.44
450	400	362.9	0.47
450	440	377	0.49
450	480	403	0.52
450	540	441	0.55
450	600	486	0.57
450	690	502	0.61
450	780	572	0.63
450	880	608	0.66
450	980	631	0.69
450	1080	660	0.71
450	1180	681	0.72
450	1280	695	0.74
450	1380	710	0.75
450	1480	724	0.77
450	1580	732	0.78

0.1wt% HSNP/Oil B Emulsion

Oil (mL)	Water (mL)	k ($\mu\text{S}/\text{cm}$)	Volume Fraction (Water)
450	0	0	0.00
450	20	0	0.04
450	40	0	0.08
450	60	0.02	0.12
450	80	0.03	0.15
450	100	0.04	0.18
450	120	0.06	0.21
450	140	0.16	0.24
450	160	0.25	0.26
450	180	0.3	0.29
450	200	1.26	0.31
450	220	3.76	0.33
450	240	148.8	0.35
450	260	194.2	0.37
450	280	223.6	0.38
450	300	255.1	0.40
450	320	268.4	0.42
450	360	275.6	0.44
450	400	297.6	0.47
450	440	321	0.49
450	480	369	0.52
450	520	408	0.54
450	560	409	0.55
450	620	452	0.58
450	680	491	0.60
450	740	526	0.62
450	800	541	0.64
450	880	540	0.66
450	960	567	0.68
450	1040	595	0.70
450	1120	610	0.71
450	1200	618	0.73
450	1300	634	0.74
450	1400	681	0.76
450	1500	703	0.77

450	1600	718	0.78
-----	------	-----	------

0.2wt% HSNP/Oil B Emulsion

Oil (mL)	Water (mL)	k ($\mu\text{S}/\text{cm}$)	Volume Fraction (Water)
450	0	0	0.00
450	20	0	0.04
450	40	0	0.08
450	60	0	0.12
450	80	0	0.15
450	100	0	0.18
450	120	0.05	0.21
450	140	0.07	0.24
450	160	0.17	0.26
450	180	0.26	0.29
450	200	2.95	0.31
450	220	3.88	0.33
450	240	28.02	0.35
450	260	173.8	0.37
450	280	205.7	0.38
450	300	225.6	0.40
450	320	247.7	0.42
450	340	269.1	0.43
450	380	296	0.46
450	420	326	0.48
450	460	347	0.51
450	500	370	0.53
450	540	390	0.55
450	580	427	0.56
450	620	434	0.58
450	680	474	0.60
450	740	502	0.62
450	800	528	0.64
450	860	558	0.66
450	920	571	0.67
450	980	575	0.69
450	1040	595	0.70

450	1120	618	0.71
450	1200	639	0.73
450	1280	652	0.74
450	1360	672	0.75
450	1440	685	0.76
450	1520	706	0.77
450	1600	715	0.78

0.4wt% HSNP/Oil B Emulsion

Oil	Water	k ($\mu\text{S}/\text{cm}$)	Volume Fraction (Water)
450	0	0	0.00
450	20	0	0.04
450	40	0	0.08
450	60	0	0.12
450	80	0.05	0.15
450	100	0.06	0.18
450	120	0.06	0.21
450	140	0.86	0.24
450	160	1.05	0.26
450	180	1.56	0.29
450	200	1.54	0.31
450	220	2.28	0.33
450	240	2.6	0.35
450	260	2.98	0.37
450	280	3.65	0.38
450	300	209.6	0.40
450	320	232.5	0.42
450	340	256.2	0.43
450	360	273.9	0.44
450	380	294	0.46
450	400	315	0.47
450	440	342	0.49
450	480	365	0.52
450	520	389	0.54
450	560	412	0.55
450	600	433	0.57
450	640	453	0.59

450	680	470	0.60
450	740	495	0.62
450	800	518	0.64
450	860	516	0.66
450	920	539	0.67
450	980	540	0.69
450	1040	559	0.70
450	1100	578	0.71
450	1180	603	0.72
450	1260	626	0.74
450	1340	650	0.75
450	1420	659	0.76
450	1520	682	0.77
450	1620	712	0.78

1wt% HSNP/Oil B Emulsion

Oil (mL)	Water (mL)	k ($\mu\text{S}/\text{cm}$)	Volume Fraction (Water)
450	0	0	0.00
450	20	0	0.04
450	40	0.03	0.08
450	60	0.11	0.12
450	80	0.15	0.15
450	100	0.29	0.18
450	120	0.2	0.21
450	140	0.22	0.24
450	160	0.26	0.26
450	180	0.29	0.29
450	200	0.57	0.31
450	220	0.73	0.33
450	240	0.63	0.35
450	260	0.55	0.37
450	280	1.11	0.38
450	300	1.68	0.40
450	320	1.7	0.42
450	340	2.53	0.43
450	360	5.47	0.44

450	380	7.62	0.46
450	400	10.11	0.47
450	420	13.92	0.48
450	440	8.15	0.49
450	460	56.4	0.51
450	480	61.4	0.52
450	500	67.9	0.53
450	520	62.8	0.54
450	540	62.3	0.55
450	560	55	0.55
450	580	117.1	0.56
450	600	373	0.57
450	620	395	0.58
450	640	411	0.59
450	660	425	0.59
450	700	454	0.61
450	740	474	0.62
450	780	489	0.63
450	820	512	0.65
450	860	531	0.66
450	900	552	0.67
450	940	580	0.68
450	1000	597	0.69
450	1060	623	0.70
450	1120	634	0.71
450	1200	664	0.73
450	1280	692	0.74
450	1360	687	0.75
450	1440	700	0.76
450	1500	724	0.77

2wt% HSNP/Oil B Emulsion

Oil (mL)	Water (mL)	k ($\mu\text{S}/\text{cm}$)	Volume Fraction (Water)
450	0	0	0.00
450	20	0	0.04
450	40	0	0.08

450	60	0	0.12
450	80	0.04	0.15
450	100	0.05	0.18
450	120	0.06	0.21
450	140	0.08	0.24
450	160	0.1	0.26
450	180	0.15	0.29
450	200	0.27	0.31
450	220	0.39	0.33
450	240	0.45	0.35
450	260	0.42	0.37
450	280	1.75	0.38
450	300	2.54	0.40
450	320	3.96	0.42
450	340	4.94	0.43
450	360	8.45	0.44
450	380	9.31	0.46
450	400	5.32	0.47
450	420	5.94	0.48
450	440	8.15	0.49
450	460	11.31	0.51
450	480	11.5	0.52
450	500	16.45	0.53
450	520	46.2	0.54
450	540	59.9	0.55
450	560	60	0.55
450	580	59.6	0.56
450	600	60	0.57
450	620	300	0.58
450	640	338	0.59
450	660	351	0.59
450	680	354	0.60
450	700	372	0.61
450	740	392	0.62
450	780	417	0.63
450	820	435	0.65
450	860	458	0.66
450	900	467	0.67
450	940	485	0.68
450	1000	517	0.69

450	1060	545	0.70
450	1120	565	0.71
450	1200	592	0.73
450	1280	620	0.74
450	1360	645	0.75
450	1440	652	0.76
450	1540	676	0.77
450	1640	700	0.78

Hydrophobic Starch Nanoparticle (HOSNP) Phase Inversion in Oil A

Blank/Oil A Emulsion

Oil (mL)	Water (mL)	k ($\mu\text{S}/\text{cm}$)	Volume Fraction (Water)
450	0	0	0.00
450	20	0	0.04
450	40	0	0.08
450	60	0	0.12
450	80	0	0.15
450	100	0	0.18
450	120	0	0.21
450	140	0	0.24
450	160	0	0.26
450	180	16.9	0.29
450	200	26	0.31
450	220	163.5	0.33
450	240	175.9	0.35
450	260	182.9	0.37
450	280	203.4	0.38
450	300	218.7	0.40
450	320	221.1	0.42
450	340	252.1	0.43
450	360	273.2	0.44
450	380	304	0.46
450	400	323	0.47
450	420	333	0.48
450	440	365	0.49

450	460	370	0.51
450	480	404	0.52
450	520	422	0.54
450	560	440	0.55
450	600	457	0.57
450	640	484	0.59
450	680	502	0.60
450	700	520	0.61
450	740	539	0.62
450	780	557	0.63
450	820	575	0.65
450	860	580	0.66
450	900	581	0.67
450	940	582	0.68
450	980	595	0.69
450	1020	605	0.69
450	1060	601	0.70
450	1100	614	0.71
450	1160	626	0.72
450	1220	643	0.73
450	1280	653	0.74
450	1340	671	0.75
450	1410	682	0.76
450	1480	693	0.77
450	1550	705	0.78

0.1wt% HOSNP/Oil A Emulsion

Oil (mL)	Water (mL)	k ($\mu\text{S}/\text{cm}$)	Volume Fraction (Water)
450	0	0	0.00
450	20	0	0.04
450	40	0	0.08
450	60	0	0.12
450	80	0.03	0.15
450	100	0.06	0.18
450	120	0.15	0.21
450	140	3.26	0.24
450	160	2.68	0.26

450	180	4.21	0.29
450	200	6.09	0.31
450	220	7.75	0.33
450	240	6.53	0.35
450	260	7.51	0.37
450	280	8.59	0.38
450	300	8.95	0.40
450	320	12.76	0.42
450	340	17.99	0.43
450	360	19.27	0.44
450	380	21.05	0.46
450	400	24.89	0.47
450	420	24.93	0.48
450	440	351	0.49
450	460	384	0.51
450	480	391	0.52
450	500	413	0.53
450	520	431	0.54
450	545	450	0.55
450	570	471	0.56
450	620	501	0.58
450	670	530	0.60
450	720	559	0.62
450	770	583	0.63
450	820	607	0.65
450	870	628	0.66
450	920	646	0.67
450	970	666	0.68
450	1020	684	0.69
450	1070	701	0.70
450	1140	723	0.72
450	1210	740	0.73
450	1290	759	0.74
450	1370	779	0.75
450	1450	797	0.76
450	1520	811	0.77

0.2wt% HOSNP/Oil A Emulsion

Oil (mL)	Water (mL)	k ($\mu\text{S}/\text{cm}$)	Volume Fraction (Water)
450	0	0	0.00
450	20	0	0.04
450	40	0	0.08
450	60	0	0.12
450	80	0.1	0.15
450	100	1.91	0.18
450	120	3.41	0.21
450	140	3.95	0.24
450	160	4.58	0.26
450	180	5.34	0.29
450	200	6.46	0.31
450	220	7.67	0.33
450	240	8.61	0.35
450	260	12.04	0.37
450	280	14.36	0.38
450	300	16.46	0.40
450	320	18.78	0.42
450	340	19.89	0.43
450	360	19.47	0.44
450	380	21.29	0.46
450	400	295.6	0.47
450	420	336	0.48
450	440	355	0.49
450	460	373	0.51
450	480	395	0.52
450	505	417	0.53
450	530	435	0.54
450	555	455	0.55
450	580	473	0.56
450	600	487	0.57
450	640	510	0.59
450	680	532	0.60
450	720	553	0.62
450	780	581	0.63
450	840	610	0.65
450	900	632	0.67
450	960	657	0.68

450	1020	678	0.69
450	1100	704	0.71
450	1180	728	0.72
450	1260	750	0.74
450	1340	771	0.75
450	1420	790	0.76
450	1500	807	0.77
450	1490	837	0.77
450	1500	838	0.77

0.4wt% HOSNP/Oil A Emulsion

Oil (mL)	Water (mL)	k ($\mu\text{S}/\text{cm}$)	Volume Fraction (Water)
450	0	0	0.00
450	20	0.11	0.04
450	40	0.19	0.08
450	60	1.45	0.12
450	80	1.73	0.15
450	100	2.95	0.18
450	120	4.82	0.21
450	140	6.05	0.24
450	160	6.69	0.26
450	180	8.33	0.29
450	200	9.31	0.31
450	220	10.96	0.33
450	240	12.29	0.35
450	260	13.47	0.37
450	280	14.42	0.38
450	300	14.47	0.40
450	320	14.98	0.42
450	340	15.06	0.43
450	360	14.03	0.44
450	380	14.32	0.46
450	400	14.72	0.47
450	420	16.34	0.48
450	440	17.01	0.49
450	460	19.49	0.51
450	480	18.84	0.52

450	500	19.85	0.53
450	520	19.06	0.54
450	540	17.9	0.55
450	560	19.8	0.55
450	580	17.58	0.56
450	600	22.17	0.57
450	620	16.22	0.58
450	640	22.95	0.59
450	660	16.79	0.59
450	680	13.22	0.60
450	700	316	0.61
450	720	384	0.62
450	740	410	0.62
450	760	441	0.63
450	780	458	0.63
450	800	476	0.64
450	820	491	0.65
450	840	505	0.65
450	860	519	0.66
450	880	532	0.66
450	900	545	0.67
450	925	560	0.67
450	950	573	0.68
450	975	585	0.68
450	1000	596	0.69
450	1040	611	0.70
450	1080	627	0.71
450	1120	641	0.71
450	1180	661	0.72
450	1240	681	0.73
450	1300	699	0.74
450	1360	715	0.75
450	1440	736	0.76
450	1520	754	0.77

0.6wt% HOSNP/Oil A Emulsion

Oil (mL)	Water (mL)	k ($\mu\text{S}/\text{cm}$)	Volume Fraction (Water)
450	0	0	0.00
450	20	0	0.04
450	40	0	0.08
450	60	0	0.12
450	80	0	0.15
450	100	0.63	0.18
450	120	0.71	0.21
450	140	2.49	0.24
450	160	3.48	0.26
450	180	4.17	0.29
450	200	4.75	0.31
450	220	5.62	0.33
450	240	9.15	0.35
450	260	10.66	0.37
450	280	7.88	0.38
450	300	10.83	0.40
450	320	8.09	0.42
450	340	9.38	0.43
450	360	10.49	0.44
450	380	10.74	0.46
450	400	12.41	0.47
450	420	12.56	0.48
450	440	10.78	0.49
450	460	10.64	0.51
450	480	12.41	0.52
450	500	11.25	0.53
450	520	11.19	0.54
450	540	9.75	0.55
450	560	5.98	0.55
450	580	10.76	0.56
450	600	11.75	0.57
450	620	11.48	0.58
450	640	11.98	0.59
450	660	5.19	0.59

450	680	4.97	0.60
450	700	5.41	0.61
450	720	4.53	0.62
450	740	8.28	0.62
450	760	7.41	0.63
450	780	8.77	0.63
450	800	13.79	0.64
450	820	19.05	0.65
450	840	354	0.65
450	860	397	0.66
450	880	425	0.66
450	900	448	0.67
450	920	470	0.67
450	940	487	0.68
450	965	504	0.68
450	990	522	0.69
450	1015	538	0.69
450	1040	551	0.70
450	1080	571	0.71
450	1120	588	0.71
450	1160	603	0.72
450	1220	625	0.73
450	1280	644	0.74
450	1340	662	0.75
450	1420	684	0.76
450	1500	704	0.77

0.8wt% HOSNP/Oil A Emulsion

Oil (mL)	Water (mL)	k ($\mu\text{S}/\text{cm}$)	Volume Fraction (Water)
450	0	0	0.00
450	20	0	0.04
450	40	0	0.08
450	60	0	0.12
450	80	0.74	0.15
450	100	1.62	0.18
450	120	2.29	0.21
450	140	4.46	0.24

450	160	3.4	0.26
450	180	7.46	0.29
450	200	7.22	0.31
450	220	9.83	0.33
450	240	11.23	0.35
450	260	11.84	0.37
450	280	12.45	0.38
450	300	13.47	0.40
450	320	12.67	0.42
450	340	11.63	0.43
450	360	10.95	0.44
450	380	10.59	0.46
450	400	7.37	0.47
450	420	8.85	0.48
450	440	10.36	0.49
450	460	8.38	0.51
450	480	10.42	0.52
450	500	10.01	0.53
450	520	8.75	0.54
450	540	8.57	0.55
450	560	8.51	0.55
450	580	9.63	0.56
450	600	9.97	0.57
450	620	10.39	0.58
450	640	10.58	0.59
450	660	9.94	0.59
450	680	10.68	0.60
450	700	10.8	0.61
450	720	11.83	0.62
450	740	11.61	0.62
450	760	10.58	0.63
450	780	12.73	0.63
450	800	12.21	0.64
450	820	10.63	0.65
450	840	13.51	0.65
450	860	12.64	0.66
450	880	352	0.66
450	900	390	0.67
450	920	417	0.67
450	940	440	0.68

450	960	458	0.68
450	980	475	0.69
450	1000	492	0.69
450	1025	509	0.69
450	1050	524	0.70
450	1075	539	0.70
450	1100	552	0.71
450	1140	569	0.72
450	1180	586	0.72
450	1220	601	0.73
450	1260	616	0.74
450	1320	636	0.75
450	1380	655	0.75
450	1440	672	0.76
450	1500	687	0.77

1wt% HOSNP/Oil A Emulsion

Oil (mL)	Water (mL)	k ($\mu\text{S}/\text{cm}$)	Volume Fraction (Water)
450	0	0	0.00
450	20	1.28	0.04
450	40	1.55	0.08
450	60	2.23	0.12
450	80	2.37	0.15
450	100	2.04	0.18
450	120	2.06	0.21
450	140	4.37	0.24
450	160	3.09	0.26
450	180	1.64	0.29
450	200	2.09	0.31
450	220	4.7	0.33
450	240	2.63	0.35
450	260	3.06	0.37
450	280	4.91	0.38
450	300	6.58	0.40
450	320	3.15	0.42
450	340	4.22	0.43
450	360	7.45	0.44

450	380	4.08	0.46
450	400	6.78	0.47
450	420	4.64	0.48
450	440	2.51	0.49
450	460	5.95	0.51
450	480	5.2	0.52
450	500	5.18	0.53
450	520	3.07	0.54
450	540	6.56	0.55
450	560	4.27	0.55
450	580	6.88	0.56
450	600	4.79	0.57
450	620	4.65	0.58
450	640	5.25	0.59
450	660	4.1	0.59
450	680	4.57	0.60
450	700	4.21	0.61
450	720	6.48	0.62
450	740	4.95	0.62
450	760	4.1	0.63
450	780	3.97	0.63
450	800	4.46	0.64
450	820	4.57	0.65
450	840	5.22	0.65
450	860	6.56	0.66
450	880	6.23	0.66
450	900	6.72	0.67
450	920	6.92	0.67
450	940	8.04	0.68
450	960	9	0.68
450	980	9.26	0.69
450	1000	360	0.69
450	1020	389	0.69
450	1045	416	0.70
450	1070	430	0.70
450	1095	451	0.71
450	1120	468	0.71
450	1160	496	0.72
450	1200	514	0.73
450	1240	537	0.73

450	1300	563	0.74
450	1360	587	0.75
450	1420	610	0.76
450	1480	634	0.77
450	1520	649	0.77

2wt% HOSNP/Oil A Emulsion

Oil (mL)	Water (mL)	k ($\mu\text{S}/\text{cm}$)	Volume Fraction (Water)
450	0	0	0.00
450	20	0	0.04
450	40	0	0.08
450	60	0	0.12
450	80	0	0.15
450	100	0.66	0.18
450	120	3.42	0.21
450	140	5.71	0.24
450	160	6	0.26
450	180	6.68	0.29
450	200	7.43	0.31
450	220	8.47	0.33
450	240	9.86	0.35
450	260	9.25	0.37
450	280	10.32	0.38
450	300	9.92	0.40
450	320	9.66	0.42
450	340	8.77	0.43
450	360	9.08	0.44
450	380	9.89	0.46
450	400	8.85	0.47
450	420	8.44	0.48
450	440	7.96	0.49
450	460	8.09	0.51
450	480	7.94	0.52
450	500	7.73	0.53
450	520	7.68	0.54
450	540	9.19	0.55
450	560	8.63	0.55

450	580	8.87	0.56
450	600	8.06	0.57
450	620	4.69	0.58
450	640	7.24	0.59
450	660	7.53	0.59
450	680	7.35	0.60
450	700	7.18	0.61
450	720	7.03	0.62
450	740	9.95	0.62
450	760	5.5	0.63
450	780	6.59	0.63
450	800	7.56	0.64
450	820	7.17	0.65
450	840	7.7	0.65
450	860	7.59	0.66
450	880	6.91	0.66
450	900	6.32	0.67
450	920	5.82	0.67
450	940	7.83	0.68
450	960	6.24	0.68
450	980	5.35	0.69
450	1000	5.86	0.69
450	1020	6.33	0.69
450	1040	6.72	0.70
450	1060	7.18	0.70
450	1080	7.36	0.71
450	1100	8.07	0.71
450	1120	8.28	0.71
450	1140	8.68	0.72
450	1160	8.78	0.72
450	1180	376	0.72
450	1200	404	0.73
450	1220	425	0.73
450	1240	441	0.73
450	1260	456	0.74
450	1285	471	0.74
450	1310	481	0.74
450	1350	502	0.75
450	1390	518	0.76
450	1450	538	0.76

450	1510	556	0.77
-----	------	-----	------

Hydrophilic Starch Nanoparticle (HSNP): CTAB Variations Phase Inversion in Oil A

CTAB in Oil A Emulsion

Blank Emulsion

Oil (mL)	Water (mL)	k ($\mu\text{S}/\text{cm}$)	Volume Fraction (Water)
450	0	0	0.00
450	10	0	0.02
450	20	0	0.04
450	30	0	0.06
450	40	0	0.08
450	50	0	0.10
450	60	0	0.12
450	70	0	0.13
450	80	0	0.15
450	90	0	0.17
450	100	0	0.18
450	110	0	0.20
450	120	0	0.21
450	130	4.67	0.22
450	140	31.3	0.24
450	150	11.88	0.25
450	160	7.97	0.26
450	170	11.92	0.27
450	180	56.4	0.29
450	190	36.3	0.30
450	200	49.2	0.31
450	210	34.2	0.32
450	220	143.9	0.33
450	230	231.8	0.34

450	240	268.6	0.35
450	250	280.7	0.36
450	260	288.2	0.37
450	270	296.6	0.38
450	280	308	0.38
450	290	318	0.39
450	300	325	0.40
450	325	343	0.42
450	350	351	0.44
450	375	382	0.45
450	400	409	0.47
450	425	440	0.49
450	450	462	0.50
450	475	491	0.51
450	500	507	0.53
450	525	533	0.54
450	550	542	0.55
450	575	565	0.56
450	600	581	0.57
450	650	621	0.59
450	700	662	0.61
450	750	688	0.63
450	800	715	0.64
450	850	725	0.65
450	900	751	0.67
450	950	758	0.68
450	1000	775	0.69
450	1050	800	0.70
450	1100	807	0.71
450	1150	814	0.72
450	1200	820	0.73
450	1250	831	0.74
450	1350	857	0.75
450	1450	871	0.76
450	1550	939	0.78

0.01wt% CTAB/Oil A Emulsion

Oil (mL)	Water (mL)	k ($\mu\text{S}/\text{cm}$)	Volume Fraction (Water)
450	0	0	0.00
450	10	0	0.02
450	20	0	0.04
450	30	0	0.06
450	40	0	0.08
450	50	0	0.10
450	60	0	0.12
450	70	0	0.13
450	80	0	0.15
450	90	0	0.17
450	100	0	0.18
450	110	0	0.20
450	120	0	0.21
450	130	0	0.22
450	140	0	0.24
450	150	0	0.25
450	160	0	0.26
450	170	0	0.27
450	180	0	0.29
450	190	0.06	0.30
450	200	0.2	0.31
450	210	0.05	0.32
450	220	0.06	0.33
450	230	0.08	0.34
450	240	0.05	0.35
450	250	0.05	0.36
450	260	0.06	0.37
450	270	0.61	0.38
450	280	2.36	0.38
450	290	1.74	0.39
450	300	5.41	0.40
450	310	241.8	0.41
450	325	264.9	0.42
450	350	277	0.44
450	375	311	0.45

450	400	345	0.47
450	425	353	0.49
450	450	378	0.50
450	475	396	0.51
450	500	409	0.53
450	525	416	0.54
450	550	429	0.55
450	575	446	0.56
450	600	461	0.57
450	650	490	0.59
450	700	517	0.61
450	750	543	0.63
450	800	566	0.64
450	850	588	0.65
450	900	609	0.67
450	950	627	0.68
450	1000	647	0.69
450	1050	662	0.70
450	1100	679	0.71
450	1150	694	0.72
450	1200	710	0.73
450	1250	723	0.74
450	1300	734	0.74
450	1350	752	0.75
450	1400	763	0.76
450	1450	773	0.76
450	1500	785	0.77
450	1550	797	0.78

0.02wt% CTAB/Oil A Emulsion

Oil (mL)	Water (mL)	k ($\mu\text{S}/\text{cm}$)	Volume Fraction (Water)
450	0	0	0.00
450	10	0	0.02
450	20	0	0.04
450	30	0	0.06
450	40	0	0.08
450	50	0	0.10

450	60	0	0.12
450	70	0	0.13
450	80	0	0.15
450	90	0	0.17
450	100	0	0.18
450	110	0	0.20
450	120	0	0.21
450	130	0	0.22
450	140	0	0.24
450	150	0	0.25
450	160	0	0.26
450	170	0	0.27
450	180	0	0.29
450	190	0	0.30
450	200	0	0.31
450	210	0.11	0.32
450	220	0.19	0.33
450	230	0	0.34
450	240	0.45	0.35
450	250	0.23	0.36
450	260	0.4	0.37
450	270	0.13	0.38
450	280	0.31	0.38
450	290	0.94	0.39
450	300	1.13	0.40
450	310	1.27	0.41
450	325	2.69	0.42
450	350	10.23	0.44
450	375	250.4	0.45
450	400	280.5	0.47
450	425	303	0.49
450	450	322	0.50
450	475	343	0.51
450	500	362	0.53
450	525	380	0.54
450	550	397	0.55
450	575	417	0.56
450	600	433	0.57
450	650	466	0.59
450	700	503	0.61

450	750	532	0.63
450	800	558	0.64
450	850	580	0.65
450	900	600	0.67
450	950	622	0.68
450	1000	640	0.69
450	1050	660	0.70
450	1100	679	0.71
450	1150	697	0.72
450	1200	710	0.73
450	1250	727	0.74
450	1300	741	0.74
450	1350	753	0.75
450	1400	768	0.76
450	1450	777	0.76
450	1500	781	0.77
450	1550	786	0.78

0.03wt% CTAB/Oil A Emulsion

Oil (mL)	Water (mL)	k ($\mu\text{S}/\text{cm}$)	Volume Fraction (Water)
450	0	0	0.00
450	10	0	0.02
450	20	0	0.04
450	30	0	0.06
450	40	0	0.08
450	50	0	0.10
450	60	0	0.12
450	70	0	0.13
450	80	0	0.15
450	90	0	0.17
450	100	0	0.18
450	110	0	0.20
450	120	0	0.21
450	130	0	0.22
450	140	0	0.24
450	150	0	0.25
450	160	0	0.26

450	170	0	0.27
450	180	0	0.29
450	190	0	0.30
450	200	0	0.31
450	210	0	0.32
450	220	0	0.33
450	230	0	0.34
450	240	0	0.35
450	250	0.03	0.36
450	260	0.08	0.37
450	270	0.09	0.38
450	280	0.05	0.38
450	290	0.04	0.39
450	300	0.05	0.40
450	325	0.11	0.42
450	350	6.46	0.44
450	375	4.02	0.45
450	400	258.2	0.47
450	425	279.2	0.49
450	450	310	0.50
450	475	329	0.51
450	500	341	0.53
450	525	357	0.54
450	550	379	0.55
450	575	393	0.56
450	600	407	0.57
450	650	433	0.59
450	700	458	0.61
450	750	481	0.63
450	800	508	0.64
450	850	534	0.65
450	900	554	0.67
450	950	574	0.68
450	1000	592	0.69
450	1050	610	0.70
450	1100	626	0.71
450	1150	644	0.72
450	1200	659	0.73
450	1250	673	0.74
450	1300	686	0.74

450	1350	701	0.75
450	1400	714	0.76
450	1450	725	0.76
450	1500	738	0.77
450	1550	750	0.78

0.04wt% CTAB/Oil A Emulsion

Oil (mL)	Water (mL)	k ($\mu\text{S}/\text{cm}$)	Volume Fraction (Water)
450	0	0	0.00
450	10	0	0.02
450	20	0	0.04
450	30	0	0.06
450	40	0	0.08
450	50	0	0.10
450	60	0	0.12
450	70	0	0.13
450	80	0	0.15
450	90	0	0.17
450	100	0	0.18
450	110	0	0.20
450	120	0	0.21
450	130	0	0.22
450	140	0	0.24
450	150	0	0.25
450	160	0	0.26
450	170	0	0.27
450	180	0	0.29
450	190	0	0.30
450	200	0	0.31
450	210	0	0.32
450	220	0	0.33
450	230	0.09	0.34
450	240	0.33	0.35

450	250	0.51	0.36
450	260	0.63	0.37
450	270	0.49	0.38
450	280	1.17	0.38
450	290	1.33	0.39
450	300	1.58	0.40
450	310	2.15	0.41
450	325	3.3	0.42
450	350	5.47	0.44
450	375	6.77	0.45
450	400	10.84	0.47
450	425	284.2	0.49
450	450	301	0.50
450	475	318	0.51
450	500	346	0.53
450	525	364	0.54
450	550	383	0.55
450	575	400	0.56
450	600	419	0.57
450	650	450	0.59
450	700	479	0.61
450	750	506	0.63
450	800	529	0.64
450	850	552	0.65
450	900	576	0.67
450	950	596	0.68
450	1000	616	0.69
450	1050	634	0.70
450	1100	654	0.71
450	1150	670	0.72
450	1200	690	0.73
450	1250	705	0.74
450	1300	719	0.74
450	1350	733	0.75
450	1400	746	0.76
450	1450	758	0.76
450	1500	770	0.77
450	1550	783	0.78

0.05wt% CTAB/Oil A Emulsion

Oil (mL)	Water (mL)	k ($\mu\text{S}/\text{cm}$)	Volume Fraction (Water)
450	0	0	0.00
450	10	0	0.02
450	20	0	0.04
450	30	0	0.06
450	40	0	0.08
450	50	0	0.10
450	60	0	0.12
450	70	0	0.13
450	80	0	0.15
450	90	0	0.17
450	100	0	0.18
450	110	0	0.20
450	120	0	0.21
450	130	0	0.22
450	140	0	0.24
450	150	0	0.25
450	160	0	0.26
450	170	0	0.27
450	180	0	0.29
450	190	0	0.30
450	200	0	0.31
450	210	0	0.32
450	220	0	0.33
450	230	0	0.34
450	240	0	0.35
450	250	0.04	0.36
450	260	0.33	0.37
450	270	0.53	0.38
450	280	0.56	0.38
450	290	0.65	0.39
450	300	3.55	0.40
450	325	5.96	0.42
450	350	6.01	0.44
450	375	3.5	0.45
450	400	6.19	0.47

450	425	7.64	0.49
450	450	296.7	0.50
450	475	322	0.51
450	500	342	0.53
450	525	361	0.54
450	550	380	0.55
450	575	397	0.56
450	600	414	0.57
450	650	446	0.59
450	700	475	0.61
450	750	502	0.63
450	800	529	0.64
450	850	552	0.65
450	900	574	0.67
450	950	595	0.68
450	1000	615	0.69
450	1050	633	0.70
450	1100	649	0.71
450	1150	665	0.72
450	1200	681	0.73
450	1250	696	0.74
450	1300	711	0.74
450	1350	724	0.75
450	1400	737	0.76
450	1450	755	0.76
450	1500	767	0.77
450	1550	778	0.78

0.25wt% CTAB/Oil A Emulsion

Oil (mL)	Water (mL)	k ($\mu\text{S}/\text{cm}$)	Volume Fraction (Water)
450	0	0	0.00
450	10	0	0.02
450	20	0	0.04
450	30	0	0.06
450	40	0	0.08
450	50	0	0.10
450	60	0	0.12

450	70	0	0.13
450	80	0	0.15
450	90	0	0.17
450	100	0	0.18
450	110	0	0.20
450	120	0	0.21
450	130	0	0.22
450	140	0	0.24
450	150	0	0.25
450	160	0	0.26
450	170	0	0.27
450	180	0	0.29
450	190	0	0.30
450	200	0.07	0.31
450	210	0.13	0.32
450	220	0.14	0.33
450	230	0.28	0.34
450	240	0.32	0.35
450	250	0.46	0.36
450	260	0.69	0.37
450	270	0.89	0.38
450	280	1.87	0.38
450	290	2.17	0.39
450	300	2.57	0.40
450	315	4.51	0.41
450	325	4.85	0.42
450	350	3.87	0.44
450	375	6.18	0.45
450	400	13.24	0.47
450	425	293	0.49
450	450	320	0.50
450	475	346	0.51
450	500	369	0.53
450	525	390	0.54
450	550	411	0.55
450	575	430	0.56
450	600	449	0.57
450	650	483	0.59
450	700	516	0.61
450	750	546	0.63

450	800	576	0.64
450	850	602	0.65
450	900	627	0.67
450	950	651	0.68
450	1000	672	0.69
450	1050	695	0.70
450	1100	713	0.71
450	1150	732	0.72
450	1200	749	0.73
450	1250	767	0.74
450	1300	782	0.74
450	1350	796	0.75
450	1400	809	0.76
450	1450	823	0.76
450	1500	839	0.77
450	1550	851	0.78

0.5wt% CTAB/Oil A Emulsion

Oil (mL)	Water (mL)	k ($\mu\text{S}/\text{cm}$)	Volume Fraction (Water)
450	0	0	0.00
450	10	0	0.02
450	20	0	0.04
450	30	0	0.06
450	40	0	0.08
450	50	0	0.10
450	60	0	0.12
450	70	0	0.13
450	80	0	0.15
450	90	0	0.17
450	100	0	0.18
450	110	0	0.20
450	120	0	0.21
450	130	0	0.22
450	140	0	0.24
450	150	0	0.25
450	160	0.05	0.26
450	170	0.19	0.27

450	180	0.56	0.29
450	190	0.72	0.30
450	200	0.75	0.31
450	210	1.59	0.32
450	220	1.84	0.33
450	230	1.93	0.34
450	240	2.59	0.35
450	250	3.09	0.36
450	260	3.16	0.37
450	270	4.28	0.38
450	280	5.59	0.38
450	290	9.74	0.39
450	300	22.67	0.40
450	315	271.2	0.41
450	325	301	0.42
450	350	334	0.44
450	375	367	0.45
450	400	393	0.47
450	425	418	0.49
450	450	443	0.50
450	475	463	0.51
450	500	485	0.53
450	525	505	0.54
450	550	525	0.55
450	575	540	0.56
450	600	557	0.57
450	625	576	0.58
450	650	593	0.59
450	675	610	0.60
450	700	626	0.61
450	750	655	0.63
450	800	682	0.64
450	850	710	0.65
450	900	734	0.67
450	950	756	0.68
450	1000	781	0.69
450	1050	801	0.70
450	1100	821	0.71
450	1150	840	0.72
450	1200	859	0.73

450	1250	875	0.74
450	1300	891	0.74
450	1350	908	0.75
450	1400	923	0.76
450	1450	937	0.76
450	1500	949	0.77
450	1550	964	0.78

1 wt% HSNP : CTAB in Oil A Emulsion

1wt% HSNP + 0.02wt% CTAB/Oil A Emulsion

Oil (mL)	Water (mL)	k ($\mu\text{S}/\text{cm}$)	Volume Fraction (Water)
450	0	0	0.00
450	10	0	0.02
450	20	0	0.04
450	30	0	0.06
450	40	0	0.08
450	50	0	0.10
450	60	0	0.12
450	70	0	0.13
450	80	0	0.15
450	90	0.08	0.17
450	100	0.11	0.18
450	110	0.79	0.20
450	120	1.42	0.21
450	130	2.13	0.22
450	140	4.43	0.24
450	150	2.75	0.25
450	160	2.26	0.26
450	170	4.8	0.27
450	180	29.49	0.29
450	190	8.45	0.30
450	200	9.21	0.31
450	210	9.02	0.32

450	220	10.32	0.33
450	230	11.52	0.34
450	240	9.3	0.35
450	250	10.63	0.36
450	270	12.74	0.38
450	290	13.32	0.39
450	310	12.09	0.41
450	330	16.72	0.42
450	350	17.98	0.44
450	370	17.3	0.45
450	390	18.59	0.46
450	410	25.7	0.48
450	430	29.51	0.49
450	450	18.9	0.50
450	470	22.35	0.51
450	490	21.23	0.52
450	510	21.41	0.53
450	530	337	0.54
450	550	368	0.55
450	570	388	0.56
450	595	412	0.57
450	620	432	0.58
450	670	465	0.60
450	720	498	0.62
450	770	524	0.63
450	820	550	0.65
450	870	572	0.66
450	920	594	0.67
450	970	616	0.68
450	1020	637	0.69
450	1070	655	0.70
450	1120	674	0.71
450	1170	692	0.72
450	1220	707	0.73
450	1270	724	0.74
450	1320	739	0.75
450	1370	753	0.75
450	1420	765	0.76

1wt% HSNP + 0.02wt% CTAB/Oil A Emulsion

Oil (mL)	Water (mL)	k ($\mu\text{S}/\text{cm}$)	Volume Fraction (Water)
450	0	0	0.00
450	10	0	0.02
450	20	0	0.04
450	30	0	0.06
450	40	0	0.08
450	50	0	0.10
450	60	0	0.12
450	70	0	0.13
450	80	0	0.15
450	90	0	0.17
450	100	0	0.18
450	110	0	0.20
450	120	0	0.21
450	130	0.05	0.22
450	140	0.12	0.24
450	150	0.33	0.25
450	160	0.72	0.26
450	170	0.63	0.27
450	180	0.73	0.29
450	190	0.85	0.30
450	200	1.7	0.31
450	210	2.69	0.32
450	220	4.29	0.33
450	230	5.71	0.34
450	240	4.1	0.35
450	250	4.59	0.36
450	260	6.31	0.37
450	270	6.58	0.38
450	290	8.22	0.39
450	300	7.18	0.40
450	320	12.21	0.42
450	340	17.09	0.43
450	360	19.14	0.44
450	380	17.69	0.46
450	400	17.91	0.47
450	420	25.63	0.48

450	440	39.4	0.49
450	460	17.9	0.51
450	480	84.4	0.52
450	500	35.8	0.53
450	520	36.4	0.54
450	540	23.9	0.55
450	560	36.8	0.55
450	580	327	0.56
450	600	350	0.57
450	620	368	0.58
450	645	386	0.59
450	670	404	0.60
450	695	420	0.61
450	745	452	0.62
450	795	480	0.64
450	845	506	0.65
450	895	530	0.67
450	945	555	0.68
450	995	576	0.69
450	1045	597	0.70
450	1095	617	0.71
450	1145	636	0.72
450	1195	653	0.73
450	1245	672	0.73
450	1295	687	0.74
450	1345	703	0.75
450	1395	714	0.76
450	1410	724	0.76

1wt% HSNP + 0.03wt% CTAB/Oil A Emulsion

Oil (mL)	Water (mL)	k ($\mu\text{S}/\text{cm}$)	Volume Fraction (Water)
450	0	0	0.00
450	10	0	0.02
450	20	0	0.04
450	30	0	0.06
450	40	0	0.08
450	50	0	0.10

450	60	0	0.12
450	70	0	0.13
450	80	0	0.15
450	90	0	0.17
450	100	0.09	0.18
450	110	0.01	0.20
450	120	0	0.21
450	130	0.06	0.22
450	140	0.12	0.24
450	150	0.16	0.25
450	160	0.1	0.26
450	170	0.32	0.27
450	180	0.55	0.29
450	190	3.29	0.30
450	200	2.28	0.31
450	210	4.29	0.32
450	220	3.51	0.33
450	230	4.01	0.34
450	240	6.72	0.35
450	250	4.8	0.36
450	260	5.34	0.37
450	270	4.51	0.38
450	280	3.36	0.38
450	290	8.47	0.39
450	310	8.37	0.41
450	330	9.43	0.42
450	350	10.74	0.44
450	370	10.82	0.45
450	390	16.18	0.46
450	410	20.79	0.48
450	430	25.57	0.49
450	450	23.01	0.50
450	470	32.4	0.51
450	490	21.46	0.52
450	510	34.3	0.53
450	530	38.1	0.54
450	550	40.9	0.55
450	570	358	0.56
450	590	373	0.57
450	610	394	0.58

450	630	409	0.58
450	655	423	0.59
450	680	438	0.60
450	705	453	0.61
450	755	480	0.63
450	805	507	0.64
450	855	530	0.66
450	905	556	0.67
450	955	579	0.68
450	1005	601	0.69
450	1055	623	0.70
450	1105	643	0.71
450	1155	663	0.72
450	1205	681	0.73
450	1255	698	0.74
450	1305	713	0.74
450	1355	731	0.75
450	1405	746	0.76
450	1455	761	0.76

1wt% HSNP + 0.04wt% CTAB/Oil A Emulsion

Oil (mL)	Water (mL)	k ($\mu\text{S}/\text{cm}$)	Volume Fraction (Water)
450	0	0	0.00
450	10	0	0.02
450	20	0	0.04
450	30	0	0.06
450	40	0	0.08
450	50	0	0.10
450	60	0	0.12
450	70	0	0.13
450	80	0	0.15
450	90	0	0.17
450	100	0	0.18
450	110	0	0.20
450	120	0	0.21
450	130	0.02	0.22
450	140	0.04	0.24

450	150	0.07	0.25
450	160	0.05	0.26
450	170	0.06	0.27
450	180	0.12	0.29
450	190	0.14	0.30
450	200	0.19	0.31
450	210	0.21	0.32
450	220	0.2	0.33
450	230	0.45	0.34
450	240	0.6	0.35
450	250	0.52	0.36
450	260	0.52	0.37
450	270	1.05	0.38
450	280	0.86	0.38
450	290	1.57	0.39
450	300	1.64	0.40
450	310	3.15	0.41
450	330	3.78	0.42
450	350	6.35	0.44
450	370	16.48	0.45
450	390	19.45	0.46
450	410	15.31	0.48
450	430	24.56	0.49
450	450	19.3	0.50
450	470	14.1	0.51
450	490	17.3	0.52
450	510	24.54	0.53
450	530	27.23	0.54
450	550	25.35	0.55
450	570	33	0.56
450	590	350	0.57
450	610	370	0.58
450	630	385	0.58
450	650	400	0.59
450	670	411	0.60
450	695	431	0.61
450	720	449	0.62
450	745	465	0.62
450	795	494	0.64
450	845	517	0.65

450	895	552	0.67
450	945	575	0.68
450	995	597	0.69
450	1045	617	0.70
450	1095	637	0.71
450	1145	652	0.72
450	1195	669	0.73
450	1245	690	0.73
450	1295	707	0.74
450	1345	722	0.75
450	1395	735	0.76
450	1445	749	0.76

1wt% HSNP + 0.05wt% CTAB/Oil A Emulsion

Oil (mL)	Water (mL)	k ($\mu\text{S}/\text{cm}$)	Volume Fraction (Water)
450	0	0	0.00
450	10	0	0.02
450	20	0	0.04
450	30	0	0.06
450	40	0	0.08
450	50	0	0.10
450	60	0	0.12
450	70	0	0.13
450	80	0	0.15
450	90	0	0.17
450	100	0	0.18
450	110	0	0.20
450	120	0.04	0.21
450	130	0.04	0.22
450	140	0.03	0.24
450	150	0.04	0.25
450	160	0.05	0.26
450	170	0.23	0.27
450	180	1.34	0.29
450	190	2.49	0.30
450	200	4.47	0.31
450	210	3.39	0.32

450	220	5.17	0.33
450	230	4.3	0.34
450	240	9.89	0.35
450	250	4.14	0.36
450	260	9.72	0.37
450	270	7.15	0.38
450	280	6.39	0.38
450	290	6.4	0.39
450	300	3.04	0.40
450	325	6.44	0.42
450	350	8.9	0.44
450	375	10.1	0.45
450	400	27.7	0.47
450	425	32.9	0.49
450	450	29.09	0.50
450	475	37.3	0.51
450	550	32.5	0.55
450	575	346	0.56
450	600	371	0.57
450	625	389	0.58
450	650	406	0.59
450	675	423	0.60
450	700	437	0.61
450	750	464	0.63
450	800	494	0.64
450	850	514	0.65
450	900	536	0.67
450	950	558	0.68
450	1000	579	0.69
450	1050	597	0.70
450	1100	619	0.71
450	1150	637	0.72
450	1200	654	0.73
450	1250	670	0.74
450	1300	687	0.74
450	1350	702	0.75
450	1400	716	0.76
450	1450	732	0.76

1wt% HSNP + 0.25wt% CTAB/Oil A Emulsion

Oil (mL)	Water (mL)	k ($\mu\text{S}/\text{cm}$)	Volume Fraction (Water)
450	0	0	0.00
450	10	0	0.02
450	20	0	0.04
450	30	0	0.06
450	40	0	0.08
450	50	0	0.10
450	60	0	0.12
450	70	0	0.13
450	80	0	0.15
450	90	0	0.17
450	100	0	0.18
450	110	0	0.20
450	120	0.03	0.21
450	130	0.05	0.22
450	140	0.16	0.24
450	150	0.28	0.25
450	160	0.43	0.26
450	170	0.57	0.27
450	180	0.72	0.29
450	190	1.26	0.30
450	200	1.24	0.31
450	210	1.56	0.32
450	220	1.81	0.33
450	230	2.75	0.34
450	240	2.57	0.35
450	250	3.49	0.36
450	260	4.54	0.37
450	270	5.2	0.38
450	280	3.28	0.38
450	290	3.59	0.39
450	300	6.4	0.40
450	310	9.44	0.41
450	325	7.22	0.42
450	350	14.64	0.44
450	375	17.17	0.45
450	400	35.3	0.47

450	425	345	0.49
450	450	374	0.50
450	475	402	0.51
450	500	427	0.53
450	525	451	0.54
450	550	475	0.55
450	575	496	0.56
450	600	516	0.57
450	625	535	0.58
450	650	570	0.59
450	700	604	0.61
450	750	634	0.63
450	800	663	0.64
450	850	688	0.65
450	900	714	0.67
450	950	738	0.68
450	1000	758	0.69
450	1050	779	0.70
450	1100	798	0.71
450	1150	820	0.72
450	1200	838	0.73
450	1250	854	0.74
450	1300	873	0.74
450	1350	888	0.75
450	1400	903	0.76
450	1450	917	0.76

1wt% HSNP + 0.5wt% CTAB/Oil A Emulsion

Oil (mL)	Water (mL)	k ($\mu\text{S}/\text{cm}$)	Volume Fraction (Water)
450	0	0	0.00
450	10	0	0.02
450	20	0	0.04
450	30	0	0.06
450	40	0	0.08
450	50	0	0.10
450	60	0.06	0.12
450	70	0.07	0.13

450	80	0.18	0.15
450	90	0.32	0.17
450	100	0.54	0.18
450	110	0.4	0.20
450	120	0.47	0.21
450	130	0.52	0.22
450	140	0.82	0.24
450	150	1.38	0.25
450	160	1.62	0.26
450	170	1.88	0.27
450	180	3.97	0.29
450	190	2.8	0.30
450	200	3.04	0.31
450	210	4.24	0.32
450	220	4.54	0.33
450	230	6.66	0.34
450	240	8.83	0.35
450	250	8.81	0.36
450	260	15.33	0.37
450	270	19.58	0.38
450	280	16.53	0.38
450	290	297.5	0.39
450	300	333	0.40
450	310	352	0.41
450	325	376	0.42
450	350	408	0.44
450	375	437	0.45
450	400	463	0.47
450	425	485	0.49
450	450	509	0.50
450	475	531	0.51
450	500	566	0.53
450	525	584	0.54
450	550	602	0.55
450	575	620	0.56
450	600	637	0.57
450	625	657	0.58
450	650	674	0.59
450	675	689	0.60
450	700	705	0.61

450	725	720	0.62
450	750	734	0.63
450	775	748	0.63
450	800	761	0.64
450	850	789	0.65
450	900	813	0.67
450	950	836	0.68
450	1000	856	0.69
450	1050	879	0.70
450	1100	899	0.71
450	1150	920	0.72
450	1200	940	0.73
450	1250	957	0.74
450	1300	977	0.74
450	1350	993	0.75
450	1400	1007	0.76
450	1450	1027	0.76

Appendix C

Experimental Data

W/O to O/W Phase Inversion – Non-Electrolyte Medium

Hydrophilic Starch Nanoparticle (SNP) Phase Inversion (water)

0.1wt% SNP in MilliQ/Oil Emulsion

Oil (mL)	Water (mL)	Volume Fraction (Water)	k ($\mu\text{S}/\text{cm}$)
450	0	0.00	0.00
450	10	0.02	0.00
450	20	0.04	0.06
450	30	0.06	0.05
450	40	0.08	0.07
450	50	0.10	0.05
450	60	0.12	0.15
450	70	0.13	0.49
450	80	0.15	0.21
450	90	0.17	0.54
450	100	0.18	0.73
450	110	0.20	0.68
450	120	0.21	0.54
450	130	0.22	0.44
450	140	0.24	1.16
450	150	0.25	0.45
450	160	0.26	0.69
450	170	0.27	0.16
450	180	0.29	0.35
450	190	0.30	0.46
450	200	0.31	0.14
450	210	0.32	0.04
450	220	0.33	0.64
450	230	0.34	0.07
450	240	0.35	0.06
450	250	0.36	0.05
450	260	0.37	0.05
450	270	0.38	0.06
450	280	0.38	0.07
450	290	0.39	0.06

450	300	0.40	0.08
450	310	0.41	0.30
450	320	0.42	1.34
450	330	0.42	0.36
450	340	0.43	1.19
450	350	0.44	0.47
450	360	0.44	0.27
450	370	0.45	0.46
450	380	0.46	1.74
450	390	0.46	0.31
450	400	0.47	1.03
450	410	0.48	0.97
450	420	0.48	3.77
450	430	0.49	3.96
450	440	0.49	4.11
450	460	0.51	4.15
450	480	0.52	4.32
450	500	0.53	4.44
450	550	0.55	4.68
450	600	0.57	4.95
450	700	0.61	5.32
450	800	0.64	5.71
450	900	0.67	6.08
450	1000	0.69	6.35
450	1100	0.71	6.63
450	1200	0.73	6.90
450	1300	0.74	7.07
450	1400	0.76	7.25
450	1500	0.77	7.49
450	1600	0.78	7.66

0.2wt% SNP in MilliQ/Oil Emulsion

Oil (mL)	Water (mL)	Volume Fraction (Water)	k ($\mu\text{S}/\text{cm}$)
450	0	0.00	0.00
450	10	0.02	0.00
450	20	0.04	0.00
450	30	0.06	0.00
450	40	0.08	0.12
450	50	0.10	0.06

450	60	0.12	0.05
450	70	0.13	0.06
450	80	0.15	0.26
450	90	0.17	0.56
450	100	0.18	2.48
450	110	0.20	2.60
450	120	0.21	4.80
450	130	0.22	1.81
450	140	0.24	2.16
450	150	0.25	0.08
450	160	0.26	0.35
450	170	0.27	1.52
450	180	0.29	0.09
450	190	0.30	0.46
450	200	0.31	0.30
450	210	0.32	0.19
450	220	0.33	0.20
450	230	0.34	0.15
450	240	0.35	14.08
450	250	0.36	15.60
450	260	0.37	17.14
450	270	0.38	17.86
450	280	0.38	17.72
450	290	0.39	17.93
450	300	0.40	18.09
450	310	0.41	18.05
450	320	0.42	18.18
450	330	0.42	18.16
450	340	0.43	17.95
450	350	0.44	18.22
450	360	0.44	18.20
450	370	0.45	18.02
450	380	0.46	18.15
450	390	0.46	18.20
450	400	0.47	18.14
450	410	0.48	17.95
450	420	0.48	17.99
450	430	0.49	2.47
450	440	0.49	5.79
450	450	0.50	6.21
450	460	0.51	6.26
450	470	0.51	6.42
450	480	0.52	6.56

450	490	0.52	6.77
450	500	0.53	6.85
450	550	0.55	7.47
450	600	0.57	7.97
450	650	0.59	8.43
450	700	0.61	8.92
450	800	0.64	9.68
450	900	0.67	10.35
450	1000	0.69	11.01
450	1100	0.71	11.49
450	1200	0.73	11.93
450	1300	0.74	12.40
450	1400	0.76	12.79
450	1500	0.77	13.25
450	1600	0.78	13.56

0.4wt% SNP in MilliQ/Oil Emulsion

Oil (mL)	Water (mL)	Volume Fraction (Water)	k ($\mu\text{S}/\text{cm}$)
450	0	0.00	0.00
450	10	0.02	0.04
450	20	0.04	0.07
450	30	0.06	0.07
450	40	0.08	0.10
450	50	0.10	0.12
450	60	0.12	0.13
450	70	0.13	0.14
450	80	0.15	0.13
450	90	0.17	0.12
450	100	0.18	0.22
450	110	0.20	1.04
450	120	0.21	1.79
450	130	0.22	5.32
450	140	0.24	0.41
450	150	0.25	1.27
450	160	0.26	9.62
450	170	0.27	23.07
450	180	0.29	27.88
450	190	0.30	29.36
450	200	0.31	30.30

450	210	0.32	30.90
450	220	0.33	31.20
450	230	0.34	31.90
450	240	0.35	32.60
450	250	0.36	32.20
450	260	0.37	33.70
450	270	0.38	33.80
450	280	0.38	33.60
450	290	0.39	33.50
450	300	0.40	33.70
450	310	0.41	33.80
450	320	0.42	33.90
450	330	0.42	33.80
450	340	0.43	34.00
450	350	0.44	34.10
450	360	0.44	34.20
450	370	0.45	34.21
450	380	0.46	34.31
450	390	0.46	34.66
450	400	0.47	34.47
450	410	0.48	34.48
450	420	0.48	34.38
450	430	0.49	33.90
450	440	0.49	34.10
450	450	0.50	34.00
450	460	0.51	34.10
450	470	0.51	34.10
450	480	0.52	33.90
450	490	0.52	32.10
450	500	0.53	33.90
450	550	0.55	12.68
450	600	0.57	13.89
450	650	0.59	14.79
450	700	0.61	15.63
450	800	0.64	17.18
450	900	0.67	18.37
450	1000	0.69	19.16
450	1100	0.71	20.30
450	1200	0.73	21.20
450	1300	0.74	21.88
450	1400	0.76	22.62
450	1500	0.77	23.29
450	1600	0.78	24.06

1wt% SNP in MilliQ/Oil Emulsion

Oil (mL)	Water (mL)	Volume Fraction (Water)	k ($\mu\text{S}/\text{cm}$)
450	0	0.00	0.00
450	10	0.02	0.00
450	20	0.04	0.18
450	30	0.06	0.61
450	40	0.08	1.02
450	50	0.10	1.97
450	60	0.12	0.52
450	70	0.13	0.23
450	80	0.15	0.48
450	90	0.17	1.84
450	100	0.18	1.87
450	110	0.20	1.21
450	120	0.21	0.36
450	130	0.22	1.15
450	140	0.24	5.90
450	150	0.25	6.17
450	160	0.26	1.20
450	170	0.27	1.36
450	180	0.29	3.31
450	190	0.30	2.49
450	200	0.31	2.08
450	210	0.32	2.20
450	220	0.33	0.73
450	230	0.34	25.62
450	240	0.35	18.39
450	250	0.36	27.78
450	260	0.37	27.04
450	270	0.38	31.01
450	280	0.38	52.90
450	290	0.39	57.70
450	300	0.40	62.40
450	310	0.41	62.70
450	320	0.42	63.40
450	330	0.42	56.20
450	340	0.43	52.00
450	350	0.44	59.10

450	360	0.44	60.60
450	370	0.45	62.10
450	380	0.46	61.90
450	390	0.46	58.80
450	400	0.47	60.30
450	410	0.48	63.40
450	420	0.48	64.50
450	430	0.49	63.80
450	440	0.49	64.20
450	460	0.51	63.80
450	480	0.52	66.10
450	500	0.53	63.80
450	550	0.55	64.50
450	600	0.57	63.40
450	650	0.59	61.44
450	700	0.61	62.80
450	750	0.63	63.60
450	800	0.64	63.42
450	850	0.65	63.91
450	900	0.67	63.28
450	950	0.68	63.86
450	1000	0.69	33.40
450	1050	0.70	36.00
450	1100	0.71	38.10
450	1200	0.73	39.90
450	1300	0.74	41.30
450	1400	0.76	42.80
450	1500	0.77	43.50
450	1600	0.78	44.80

2wt% SNP in MilliQ/Oil Emulsion

Oil (mL)	Water (mL)	Volume Fraction (Water)	k ($\mu\text{S}/\text{cm}$)
450	0	0.00	0.00
450	10	0.02	0.00
450	20	0.04	0.22
450	30	0.06	0.25
450	40	0.08	0.29
450	50	0.10	0.27

450	60	0.12	0.33
450	70	0.13	0.40
450	80	0.15	0.38
450	90	0.17	1.06
450	100	0.18	1.19
450	110	0.20	1.57
450	120	0.21	1.52
450	130	0.22	0.53
450	140	0.24	0.97
450	150	0.25	0.83
450	160	0.26	1.22
450	170	0.27	0.67
450	180	0.29	1.55
450	190	0.30	0.63
450	200	0.31	0.52
450	210	0.32	0.63
450	220	0.33	0.56
450	230	0.34	0.57
450	240	0.35	1.11
450	250	0.36	0.90
450	260	0.37	0.86
450	270	0.38	0.85
450	280	0.38	1.08
450	290	0.39	2.06
450	300	0.40	3.05
450	310	0.41	2.63
450	320	0.42	2.01
450	330	0.42	2.14
450	340	0.43	3.06
450	350	0.44	2.85
450	360	0.44	2.82
450	370	0.45	2.98
450	380	0.46	3.48
450	390	0.46	4.25
450	400	0.47	4.79
450	410	0.48	2.69
450	420	0.48	2.94
450	430	0.49	2.68
450	440	0.49	3.09
450	450	0.50	2.17
450	460	0.51	2.28
450	470	0.51	3.65
450	480	0.52	3.17

450	490	0.52	26.63
450	500	0.53	28.96
450	510	0.53	30.20
450	520	0.54	31.40
450	530	0.54	32.40
450	540	0.55	33.50
450	560	0.55	35.30
450	580	0.56	36.50
450	600	0.57	37.80
450	650	0.59	40.60
450	700	0.61	43.50
450	750	0.63	45.90
450	800	0.64	48.10
450	850	0.65	50.10
450	900	0.67	52.00
450	1000	0.69	55.10
450	1100	0.71	58.40
450	1200	0.73	61.40
450	1300	0.74	64.30
450	1400	0.76	66.70
450	1500	0.77	67.60
450	1600	0.78	70.00

HSNP:Nanoclay Phase Inversion (Water)

1wt% SNP-1wt% CLAY - 80:20 (Bentonite Clay/MilliQ/Oil) Emulsion

Oil (mL)	Water (mL)	Volume Fraction (Water)	k ($\mu\text{S}/\text{cm}$)
450	0	0.00	0.00
450	10	0.02	0.00
450	20	0.04	0.02
450	30	0.06	0.05
450	40	0.08	0.07
450	50	0.10	0.22
450	60	0.12	0.41
450	70	0.13	0.38
450	80	0.15	0.36
450	90	0.17	0.23
450	100	0.18	0.50

450	110	0.20	0.38
450	120	0.21	0.37
450	130	0.22	0.26
450	140	0.24	0.33
450	150	0.25	0.46
450	160	0.26	0.94
450	170	0.27	1.18
450	180	0.29	1.96
450	190	0.30	2.58
450	200	0.31	5.17
450	210	0.32	4.62
450	220	0.33	4.06
450	230	0.34	0.45
450	240	0.35	6.55
450	250	0.36	9.96
450	260	0.37	7.62
450	270	0.38	7.82
450	280	0.38	28.80
450	290	0.39	35.20
450	300	0.40	30.52
450	310	0.41	30.33
450	320	0.42	36.44
450	330	0.42	63.10
450	340	0.43	61.90
450	350	0.44	71.90
450	360	0.44	76.80
450	370	0.45	71.04
450	380	0.46	78.80
450	390	0.46	71.94
450	400	0.47	80.00
450	420	0.48	75.60
450	440	0.49	83.50
450	460	0.51	83.50
450	480	0.52	83.60
450	500	0.53	83.40
450	550	0.55	83.00
450	600	0.57	80.58
450	650	0.59	30.80
450	700	0.61	42.10
450	750	0.63	39.60
450	800	0.64	41.20
450	850	0.65	42.80
450	900	0.67	44.70

1wt% SNP-1wt% CLAY - 50:50 (Bentonite Clay/MilliQ/Oil) Emulsion

Oil (mL)	Water (mL)	Volume Fraction (Water)	k ($\mu\text{S}/\text{cm}$)
450	0	0.00	0.00
450	10	0.02	0.00
450	20	0.04	1.29
450	30	0.06	0.36
450	40	0.08	0.49
450	50	0.10	0.70
450	60	0.12	0.43
450	70	0.13	0.75
450	80	0.15	0.18
450	90	0.17	0.46
450	100	0.18	0.50
450	110	0.20	1.07
450	120	0.21	2.99
450	130	0.22	0.66
450	140	0.24	3.03
450	150	0.25	0.60
450	160	0.26	0.28
450	170	0.27	1.06
450	180	0.29	4.18
450	190	0.30	1.30
450	200	0.31	3.07
450	210	0.32	0.74
450	220	0.33	7.07
450	230	0.34	4.36
450	240	0.35	59.70
450	250	0.36	94.60
450	260	0.37	72.50
450	270	0.38	114.80
450	280	0.38	154.70
450	290	0.39	159.10
450	300	0.40	160.60
450	310	0.41	160.80
450	320	0.42	160.5
450	330	0.42	159.80
450	340	0.43	158.50
450	350	0.44	159.40

450	360	0.44	159.60
450	370	0.45	158.60
450	380	0.46	154.10
450	390	0.46	158.10
450	400	0.47	157.60
450	420	0.48	153.28
450	440	0.49	153.70
450	460	0.51	158.90
450	480	0.52	59.70
450	500	0.53	61.70
450	550	0.55	66.00
450	600	0.57	71.20
450	650	0.59	75.10
450	700	0.61	78.30
450	750	0.63	81.40
450	800	0.64	84.30
450	850	0.65	87.00
450	900	0.67	89.60

1wt% SNP-1wt% CLAY - 20:80 (Bentonite Clay/MilliQ/Oil) Emulsion

Oil (mL)	Water (mL)	Volume Fraction (Water)	k ($\mu\text{S}/\text{cm}$)
450	0	0.00	0.04
450	10	0.02	0.09
450	20	0.04	0.18
450	30	0.06	0.29
450	40	0.08	0.34
450	50	0.10	0.37
450	60	0.12	0.45
450	70	0.13	1.02
450	80	0.15	0.60
450	90	0.17	0.48
450	100	0.18	1.26
450	110	0.20	0.18
450	120	0.21	0.20
450	130	0.22	0.23
450	140	0.24	0.23
450	150	0.25	0.34
450	160	0.26	0.38
450	170	0.27	1.26

450	180	0.29	0.64
450	190	0.30	1.08
450	200	0.31	1.24
450	210	0.32	6.13
450	220	0.33	27.35
450	230	0.34	49.00
450	240	0.35	106.20
450	250	0.36	155.30
450	260	0.37	178.90
450	270	0.38	231.80
450	280	0.38	230.60
450	290	0.39	230.30
450	300	0.40	231.10
450	310	0.41	59.50
450	320	0.42	62.3
450	330	0.42	64.00
450	340	0.43	65.60
450	350	0.44	67.70
450	360	0.44	71.40
450	370	0.45	72.91
450	380	0.46	74.70
450	390	0.46	76.10
450	400	0.47	77.70
450	420	0.48	81.20
450	440	0.49	84.00
450	460	0.51	87.00
450	480	0.52	90.10
450	500	0.53	92.30
450	550	0.55	97.90
450	600	0.57	104.30
450	650	0.59	111.20
450	700	0.61	115.90
450	750	0.63	120.60
450	800	0.64	125.30
450	850	0.65	129.40
450	900	0.67	133.20

Nanoclay Phase Inversion (Water)

1wt% Bentonite Clay/MilliQ/Oil Emulsion

Oil (mL)	Water (mL)	Volume Fraction (Water)	k ($\mu\text{S}/\text{cm}$)
450	0	0.00	0.00
450	10	0.02	0.00
450	20	0.04	0.00
450	30	0.06	0.36
450	40	0.08	0.21
450	50	0.10	0.23
450	60	0.12	0.27
450	70	0.13	0.34
450	80	0.15	0.40
450	90	0.17	0.52
450	100	0.18	0.85
450	110	0.20	1.17
450	120	0.21	1.93
450	130	0.22	4.40
450	140	0.24	5.26
450	150	0.25	38.40
450	160	0.26	40.80
450	170	0.27	42.80
450	180	0.29	46.50
450	190	0.30	52.60
450	200	0.31	56.7
450	220	0.33	59
450	240	0.35	62.8
450	260	0.37	66
450	280	0.38	70.6
450	300	0.40	74.4
450	350	0.44	83.8
450	400	0.47	92.2
450	450	0.50	100.1
450	500	0.53	106.4
450	550	0.55	113
450	600	0.57	118.9
450	650	0.59	124.6
450	700	0.61	129.5
450	750	0.63	134.2
450	800	0.64	138.5

450	900	0.67	142.8
450	1000	0.69	146.6
450	1100	0.71	153.4
450	1200	0.73	160
450	1300	0.74	165.5
450	1400	0.76	171.1
450	1500	0.77	175.6
450	1600	0.78	179.8
450	1700	0.79	185.3

0.5wt% Bentonite Clay/MilliQ/Oil Emulsion

Oil (mL)	Water (mL)	Volume Fraction (Water)	k ($\mu\text{S}/\text{cm}$)
450	0	0.00	0
450	10	0.02	0
450	20	0.04	0
450	30	0.06	0
450	40	0.08	0
450	50	0.10	8.81
450	60	0.12	8.75
450	70	0.13	11.32
450	80	0.15	10.3
450	90	0.17	15.12
450	100	0.18	13.71
450	110	0.20	11.24
450	120	0.21	11.51
450	130	0.22	14.48
450	140	0.24	8.24
450	150	0.25	13.49
450	160	0.26	14.59
450	170	0.27	12.24
450	180	0.29	14.5
450	190	0.30	36.2
450	200	0.31	38.3
450	210	0.32	40.3
450	220	0.33	43.3
450	230	0.34	44.6
450	240	0.35	46
450	250	0.36	47.1

450	260	0.37	48.9
450	270	0.38	50.4
450	280	0.38	51.8
450	290	0.39	53.3
450	310	0.41	56.3
450	330	0.42	59
450	350	0.44	61.8
450	370	0.45	64.6
450	390	0.46	67
450	420	0.48	71.2
450	470	0.51	77.2
450	520	0.54	83.3
450	570	0.56	88.3
450	620	0.58	93.1
450	670	0.60	97.5
450	720	0.62	101.3
450	770	0.63	104.8
450	820	0.65	108.3
450	870	0.66	111.6
450	920	0.67	114.8
450	970	0.68	117

2.5wt% Bentonite Clay/MilliQ/Oil Emulsion

Oil (mL)	Water (mL)	Volume Fraction (Water)	k ($\mu\text{S}/\text{cm}$)
450	0	0.00	0
450	10	0.02	0.64
450	20	0.04	1.43
450	30	0.06	2.29
450	40	0.08	2.75
450	50	0.10	2.7
450	60	0.12	3.7
450	70	0.13	1.66
450	80	0.15	4.2
450	90	0.17	5.85
450	100	0.18	7.98
450	110	0.20	13.65
450	120	0.21	6.82
450	130	0.22	24.9
450	140	0.24	37.9

450	150	0.25	125.1
450	160	0.26	132
450	170	0.27	145.80
450	180	0.29	156.2
450	190	0.30	166.1
450	200	0.31	172.8
450	210	0.32	192
450	220	0.33	198.7
450	230	0.34	210.4
450	240	0.35	215.3
450	250	0.36	219.6
450	260	0.37	223.8
450	270	0.38	229.4
450	280	0.38	235.2
450	300	0.40	249.3
450	320	0.42	264.1
450	340	0.43	274.9
450	360	0.44	285.8
450	380	0.46	299
450	400	0.47	313
450	450	0.50	339
450	500	0.53	364
450	550	0.55	387
450	600	0.57	413
450	650	0.59	431
450	700	0.61	452
450	750	0.63	468
450	800	0.64	484
450	850	0.65	502
450	900	0.67	515

5wt% Bentonite Clay/MilliQ/Oil Emulsion

Oil (mL)	Water (mL)	Volume Fraction (Water)	k ($\mu\text{S}/\text{cm}$)
450	0	0.00	0
450	10	0.02	0
450	20	0.04	0
450	30	0.06	3.89
450	40	0.08	0
450	50	0.10	0

450	60	0.12	0
450	70	0.13	0
450	80	0.15	3.09
450	90	0.17	3.38
450	100	0.18	3.58
450	110	0.20	8.02
450	120	0.21	3.19
450	130	0.22	14.99
450	140	0.24	159.2
450	150	0.25	163.2
450	160	0.26	175.7
450	170	0.27	179.5
450	180	0.29	185.1
450	190	0.30	198.5
450	200	0.31	229.8
450	210	0.32	224.3
450	220	0.33	237.6
450	230	0.34	240.8
450	240	0.35	253.9
450	250	0.36	262.1
450	260	0.37	268.4
450	270	0.38	281.9
450	280	0.38	290.4
450	300	0.40	302
450	320	0.42	315
450	340	0.43	336
450	360	0.44	352
450	380	0.46	365
450	400	0.47	378
450	450	0.50	416
450	500	0.53	439
450	550	0.55	465
450	600	0.57	492
450	650	0.59	518
450	700	0.61	540
450	750	0.63	559
450	800	0.64	577
450	850	0.65	593
450	900	0.67	612

CTAB Phase Inversion (Water)

0.01wt% CTAB/MilliQ/Oil Emulsion

Oil (mL)	Water (mL)	Volume Fraction (Water)	k ($\mu\text{S}/\text{cm}$)
450	0	0.00	0.00
450	10	0.02	0.00
450	20	0.04	0.00
450	30	0.06	0.00
450	40	0.08	1.00
450	60	0.12	0.05
450	70	0.13	0.06
450	80	0.15	0.05
450	90	0.17	0.06
450	100	0.18	0.06
450	110	0.20	0.11
450	120	0.21	0.16
450	130	0.22	0.12
450	140	0.24	0.78
450	150	0.25	0.08
450	160	0.26	0.67
450	170	0.27	0.15
450	180	0.29	0.12
450	190	0.30	0.50
450	200	0.31	0.77
450	210	0.32	0.38
450	220	0.33	1.04
450	230	0.34	1.64
450	240	0.35	0.3
450	250	0.36	1.41
450	260	0.37	2.52
450	270	0.38	2.51
450	280	0.38	2.09
450	290	0.39	2.08
450	300	0.40	2.05
450	310	0.41	2.36
450	320	0.42	1.82

450	330	0.42	1.36
450	340	0.43	0.85
450	350	0.44	1.36
450	360	0.44	1.45
450	370	0.45	0.34
450	380	0.46	0.6
450	390	0.46	0.39
450	400	0.47	0.69
450	410	0.48	0.75
450	420	0.48	0.85
450	430	0.49	0.6
450	440	0.49	5.39
450	450	0.50	5.65
450	460	0.51	5.8
450	470	0.51	5.91
450	480	0.52	6.06
450	490	0.52	6.23
450	500	0.53	6.38
450	520	0.54	6.75
450	540	0.55	6.94
450	560	0.55	7.18
450	580	0.56	7.42
450	600	0.57	7.66
450	650	0.59	8.22
450	700	0.61	8.83
450	800	0.64	10.03
450	900	0.67	10.94
450	1000	0.69	12.06
450	1100	0.71	12.97
450	1200	0.73	13.9
450	1300	0.74	14.66
450	1400	0.76	15.46
450	1500	0.77	16.19
450	1600	0.78	16.7

0.02wt% CTAB/MilliQ/Oil Emulsion

Oil (mL)	Water (mL)	Volume Fraction (Water)	k ($\mu\text{S}/\text{cm}$)
450	0	0.00	0.00
450	10	0.02	0.16
450	20	0.04	0.14
450	30	0.06	0.05
450	40	0.08	0.07
450	50	0.10	0.11
450	60	0.12	0.14
450	70	0.13	0.16
450	80	0.15	0.17
450	90	0.17	0.11
450	100	0.18	0.21
450	110	0.20	0.15
450	120	0.21	0.15
450	130	0.22	0.13
450	140	0.24	0.14
450	150	0.25	0.21
450	160	0.26	0.16
450	170	0.27	0.27
450	180	0.29	0.22
450	190	0.30	0.2
450	200	0.31	0.26
450	210	0.32	0.13
450	220	0.33	0.11
450	230	0.34	0.13
450	240	0.35	0.16
450	250	0.36	0.19
450	260	0.37	0.16
450	270	0.38	0.31
450	280	0.38	0.22
450	290	0.39	0.26
450	300	0.40	0.31
450	310	0.41	0.14
450	320	0.42	0.1
450	330	0.42	0.2
450	340	0.43	0.47

450	350	0.44	0.28
450	360	0.44	0.49
450	370	0.45	0.39
450	380	0.46	0.4
450	390	0.46	0.68
450	400	0.47	0.49
450	410	0.48	0.39
450	420	0.48	0.37
450	430	0.49	0.8
450	440	0.49	0.68
450	450	0.50	0.58
450	460	0.51	0.78
450	470	0.51	7.37
450	480	0.52	7.73
450	490	0.52	8.01
450	500	0.53	8.24
450	520	0.54	8.63
450	540	0.55	9.07
450	560	0.55	9.53
450	580	0.56	9.98
450	600	0.57	10.39
450	650	0.59	11.52
450	700	0.61	12.6
450	750	0.63	13.58
450	800	0.64	14.58
450	900	0.67	16.45
450	1000	0.69	18.28
450	1100	0.71	19.95
450	1200	0.73	21.48
450	1300	0.74	22.91
450	1400	0.76	24.2
450	1500	0.77	25.41
450	1600	0.78	26.47

0.03wt% CTAB/MilliQ/Oil Emulsion

Oil (mL)	Water (mL)	Volume Fraction (Water)	k ($\mu\text{S}/\text{cm}$)
450	0	0.00	0.00
450	10	0.02	0.07
450	20	0.04	0.09
450	30	0.06	0.11
450	40	0.08	0.12
450	50	0.10	0.19
450	60	0.12	0.20
450	70	0.13	0.23
450	80	0.15	0.20
450	90	0.17	0.23
450	100	0.18	0.23
450	110	0.20	0.24
450	120	0.21	0.13
450	130	0.22	0.20
450	140	0.24	0.19
450	150	0.25	0.14
450	160	0.26	0.19
450	170	0.27	0.21
450	180	0.29	0.34
450	190	0.30	0.15
450	200	0.31	0.19
450	210	0.32	0.18
450	220	0.33	0.23
450	230	0.34	0.22
450	240	0.35	0.31
450	250	0.36	0.41
450	260	0.37	0.33
450	270	0.38	0.36
450	280	0.38	0.65
450	290	0.39	0.43
450	300	0.40	0.45
450	310	0.41	0.62
450	320	0.42	0.63
450	330	0.42	0.91
450	340	0.43	0.68

450	350	0.44	0.69
450	360	0.44	0.69
450	370	0.45	0.72
450	380	0.46	0.64
450	390	0.46	0.7
450	400	0.47	0.67
450	410	0.48	0.59
450	420	0.48	0.75
450	430	0.49	0.76
450	440	0.49	1.21
450	450	0.50	1.13
450	460	0.51	1.24
450	470	0.51	1.13
450	480	0.52	1.32
450	490	0.52	11.5
450	500	0.53	11.91
450	520	0.54	12.64
450	540	0.55	13.32
450	560	0.55	14
450	580	0.56	14.61
450	600	0.57	15.28
450	650	0.59	16.85
450	700	0.61	18.43
450	750	0.63	19.97
450	800	0.64	21.42
450	900	0.67	24.29
450	1000	0.69	26.87
450	1100	0.71	29.39
450	1200	0.73	31.7
450	1300	0.74	33.8
450	1400	0.76	35.7
450	1500	0.77	37.5
450	1600	0.78	39.1

0.04wt% CTAB/MilliQ/Oil Emulsion

Oil (mL)	Water (mL)	Volume Fraction (Water)	k ($\mu\text{S}/\text{cm}$)
450	0	0.00	0.00
450	10	0.02	0.02
450	20	0.04	0.06
450	30	0.06	0.07
450	40	0.08	0.09
450	50	0.10	0.10
450	60	0.12	0.12
450	70	0.13	0.12
450	80	0.15	0.23
450	90	0.17	0.24
450	100	0.18	0.20
450	110	0.20	0.16
450	120	0.21	0.26
450	130	0.22	0.27
450	140	0.24	0.37
450	150	0.25	0.16
450	160	0.26	0.23
450	170	0.27	0.18
450	180	0.29	0.22
450	190	0.30	0.29
450	200	0.31	0.22
450	210	0.32	0.25
450	220	0.33	0.29
450	230	0.34	0.3
450	240	0.35	0.32
450	250	0.36	0.44
450	260	0.37	0.57
450	270	0.38	0.46
450	280	0.38	0.42
450	290	0.39	0.43
450	300	0.40	0.54
450	310	0.41	0.72
450	320	0.42	0.77
450	330	0.42	0.83
450	340	0.43	0.62

450	350	0.44	0.78
450	360	0.44	0.79
450	370	0.45	0.86
450	380	0.46	0.91
450	390	0.46	0.88
450	400	0.47	1.06
450	410	0.48	1.44
450	420	0.48	1.43
450	430	0.49	1.65
450	440	0.49	1.52
450	450	0.50	1.49
450	460	0.51	1.69
450	470	0.51	1.41
450	480	0.52	2.34
450	490	0.52	8.84
450	500	0.53	14.46
450	520	0.54	15.55
450	540	0.55	16.57
450	560	0.55	17.45
450	580	0.56	18.34
450	600	0.57	19.25
450	650	0.59	21.37
450	700	0.61	23.49
450	750	0.63	25.5
450	800	0.64	27.5
450	900	0.67	31.4
450	1000	0.69	34.8
450	1100	0.71	38.1
450	1200	0.73	41.1
450	1300	0.74	43.9
450	1400	0.76	46.5
450	1500	0.77	48.9
450	1600	0.78	51.2

0.05wt% CTAB/MilliQ/Oil Emulsion

Oil (mL)	Water (mL)	Volume Fraction (Water)	k ($\mu\text{S}/\text{cm}$)
450	0	0.00	0.00
450	10	0.02	0.01
450	20	0.04	0.03
450	30	0.06	0.19
450	40	0.08	0.20
450	50	0.10	0.14
450	60	0.12	0.22
450	70	0.13	0.37
450	80	0.15	0.35
450	90	0.17	0.23
450	100	0.18	0.26
450	110	0.20	0.30
450	120	0.21	0.25
450	130	0.22	0.25
450	140	0.24	0.31
450	150	0.25	0.26
450	160	0.26	0.41
450	170	0.27	0.24
450	180	0.29	0.41
450	190	0.30	0.34
450	200	0.31	0.36
450	210	0.32	0.37
450	220	0.33	0.51
450	230	0.34	0.42
450	240	0.35	0.50
450	250	0.36	0.49
450	260	0.37	0.74
450	270	0.38	0.58
450	280	0.38	0.73
450	290	0.39	0.79
450	300	0.40	0.81
450	310	0.41	0.84
450	320	0.42	0.89
450	330	0.42	1.06
450	340	0.43	0.69

450	350	0.44	0.61
450	360	0.44	1.07
450	370	0.45	0.73
450	380	0.46	0.90
450	390	0.46	0.98
450	400	0.47	1.01
450	410	0.48	1.13
450	420	0.48	1.27
450	430	0.49	1.54
450	440	0.49	1.31
450	450	0.50	1.59
450	460	0.51	1.51
450	470	0.51	16.89
450	480	0.52	17.70
450	490	0.52	18.31
450	500	0.53	18.95
450	520	0.54	20.05
450	540	0.55	21.13
450	560	0.55	22.24
450	580	0.56	23.28
450	600	0.57	24.36
450	650	0.59	27.03
450	700	0.61	29.60
450	750	0.63	32.10
450	800	0.64	34.50
450	900	0.67	39.10
450	1000	0.69	43.30
450	1100	0.71	47.40
450	1200	0.73	51.50
450	1300	0.74	54.40
450	1400	0.76	57.30
450	1500	0.77	59.80
450	1600	0.78	61.90

0.25wt% CTAB/MilliQ/Oil Emulsion

Oil (mL)	Water (mL)	Volume Fraction (Water)	k ($\mu\text{S}/\text{cm}$)
450	0	0.00	0.00
450	10	0.02	0.02
450	20	0.04	0.10
450	30	0.06	0.09
450	40	0.08	0.08
450	50	0.10	0.21
450	60	0.12	0.22
450	70	0.13	0.34
450	80	0.15	0.56
450	90	0.17	0.58
450	100	0.18	0.51
450	110	0.20	0.60
450	120	0.21	0.90
450	130	0.22	0.50
450	140	0.24	0.80
450	150	0.25	0.69
450	160	0.26	0.84
450	170	0.27	0.46
450	180	0.29	0.53
450	190	0.30	0.65
450	200	0.31	0.72
450	210	0.32	0.93
450	220	0.33	1.04
450	230	0.34	1.29
450	240	0.35	1.30
450	250	0.36	1.37
450	260	0.37	1.82
450	270	0.38	2.01
450	280	0.38	3.30
450	290	0.39	4.31
450	300	0.40	6.87
450	310	0.41	34.80
450	320	0.42	37.50
450	330	0.42	39.90
450	340	0.43	42.20

450	350	0.44	44.00
450	360	0.44	47.40
450	370	0.45	49.10
450	380	0.46	51.00
450	390	0.46	52.70
450	400	0.47	54.40
450	410	0.48	56.20
450	420	0.48	58.30
450	430	0.49	59.80
450	440	0.49	61.70
450	460	0.51	64.80
450	480	0.52	67.80
450	500	0.53	70.70
450	550	0.55	77.00
450	600	0.57	83.00
450	650	0.59	88.50
450	700	0.61	93.90
450	800	0.64	103.60
450	900	0.67	111.90
450	1000	0.69	119.60
450	1100	0.71	126.70
450	1200	0.73	132.40
450	1300	0.74	137.90
450	1400	0.76	143.30
450	1500	0.77	148.10
450	1600	0.78	152.40

0.5wt% CTAB/MilliQ/Oil Emulsion

Oil (mL)	Water (mL)	Volume Fraction (Water)	k ($\mu\text{S}/\text{cm}$)
450	0	0.00	0.00
450	10	0.02	0.18
450	20	0.04	0.35
450	30	0.06	0.36
450	40	0.08	0.28
450	50	0.10	0.46
450	60	0.12	0.60

450	70	0.13	0.41
450	80	0.15	0.57
450	90	0.17	0.49
450	100	0.18	0.38
450	110	0.20	0.43
450	120	0.21	0.53
450	130	0.22	0.62
450	140	0.24	0.64
450	150	0.25	0.55
450	160	0.26	0.73
450	170	0.27	1.09
450	180	0.29	1.28
450	190	0.30	1.11
450	200	0.31	1.25
450	210	0.32	1.01
450	220	0.33	0.88
450	230	0.34	1.75
450	240	0.35	1.94
450	250	0.36	1.55
450	260	0.37	1.01
450	270	0.38	2.26
450	280	0.38	2.21
450	290	0.39	2.42
450	300	0.40	3.37
450	310	0.41	2.20
450	320	0.42	2.18
450	330	0.42	66.80
450	340	0.43	71.80
450	350	0.44	75.90
450	360	0.44	79.30
450	370	0.45	82.40
450	380	0.46	85.40
450	390	0.46	88.50
450	400	0.47	91.50
450	420	0.48	97.10
450	440	0.49	102.20
450	460	0.51	106.70
450	480	0.52	111.20
450	500	0.53	115.80
450	550	0.55	125.40

450	600	0.57	134.60
450	650	0.59	143.20
450	700	0.61	151.50
450	750	0.63	159.50
450	800	0.64	166.40
450	900	0.67	179.60
450	1000	0.69	190.40
450	1100	0.71	200.80

Nanoclay/CTAB Phase Inversion (Water)

1wt% Nanoclay/0.01wt% CTAB/MilliQ/Oil Emulsion

Oil (mL)	Water (mL)	Volume Fraction (Water)	k ($\mu\text{S}/\text{cm}$)
450	0	0.00	0.00
450	10	0.02	0.22
450	20	0.04	0.97
450	30	0.06	1.84
450	40	0.08	1.41
450	50	0.10	1.04
450	60	0.12	1.07
450	70	0.13	1.83
450	80	0.15	1.52
450	90	0.17	1.22
450	100	0.18	1.52
450	110	0.20	2.52
450	120	0.21	3.77
450	130	0.22	3.99
450	140	0.24	3.33
450	150	0.25	3.71
450	160	0.26	4.45
450	170	0.27	5.04
450	180	0.29	5.37
450	190	0.30	5.11
450	200	0.31	5.91
450	210	0.32	5.29
450	220	0.33	57.1

450	230	0.34	58.8
450	240	0.35	62.5
450	250	0.36	69.4
450	270	0.38	75.1
450	290	0.39	86.2
450	310	0.41	91.5
450	360	0.44	100.2
450	410	0.48	110.8
450	460	0.51	120.2
450	510	0.53	131.7
450	560	0.55	138.1
450	610	0.58	146.5
450	660	0.59	152.5
450	710	0.61	158.6
450	760	0.63	164.2
450	810	0.64	169.5
450	860	0.66	174.7
450	910	0.67	179.5

1wt% Nanoclay/0.02wt% CTAB/MilliQ/Oil Emulsion

Oil (mL)	Water (mL)	Volume Fraction (Water)	k ($\mu\text{S}/\text{cm}$)
450	0	0.00	0.04
450	10	0.02	0.97
450	20	0.04	1.27
450	30	0.06	1.95
450	40	0.08	2.20
450	50	0.10	1.49
450	60	0.12	1.53
450	70	0.13	1.62
450	80	0.15	1.42
450	90	0.17	1.76
450	100	0.18	1.98
450	110	0.20	2.64
450	120	0.21	2.75
450	130	0.22	3.36
450	140	0.24	3.21

450	150	0.25	3.44
450	160	0.26	4.27
450	170	0.27	4.10
450	180	0.29	4.01
450	190	0.30	4.92
450	200	0.31	5.19
450	210	0.32	5.4
450	220	0.33	5.26
450	230	0.34	5.5
450	240	0.35	61.7
450	250	0.36	72.8
450	260	0.37	79.5
450	270	0.38	81.3
450	280	0.38	85.4
450	300	0.40	90.4
450	320	0.42	102.3
450	340	0.43	106.5
450	360	0.44	113.6
450	380	0.46	117.6
450	430	0.49	128.2
450	480	0.52	139.3
450	530	0.54	148.5
450	580	0.56	156.3
450	630	0.58	164.1
450	680	0.60	171.1
450	730	0.62	177.2
450	780	0.63	183.4
450	830	0.65	189.01
450	880	0.66	194.4

1wt% Nanoclay/0.03wt% CTAB/MilliQ/Oil Emulsion

Oil (mL)	Water (mL)	Volume Fraction (Water)	k ($\mu\text{S}/\text{cm}$)
450	0	0.00	0.06
450	10	0.02	0.32
450	20	0.04	1.25
450	30	0.06	1.05
450	40	0.08	2.03

450	50	0.10	1.78
450	60	0.12	1.67
450	70	0.13	1.92
450	80	0.15	2.16
450	90	0.17	2.66
450	100	0.18	2.63
450	110	0.20	2.49
450	120	0.21	3.15
450	130	0.22	3.29
450	140	0.24	3.37
450	150	0.25	4.93
450	160	0.26	4.59
450	170	0.27	4.67
450	180	0.29	5.56
450	190	0.30	4.74
450	200	0.31	5.49
450	210	0.32	5.29
450	220	0.33	4.88
450	230	0.34	4.48
450	240	0.35	5.65
450	250	0.36	6.18
450	260	0.37	6.06
450	270	0.38	7.99
450	280	0.38	81.6
450	290	0.39	93.8
450	300	0.40	99
450	320	0.42	102.8
450	340	0.43	106.2
450	360	0.44	118.5
450	410	0.48	128.2
450	460	0.51	141.3
450	510	0.53	151.6
450	560	0.55	161.4
450	610	0.58	170
450	660	0.59	178.2
450	710	0.61	185.3
450	760	0.63	191.9
450	810	0.64	199
450	860	0.66	204.9
450	910	0.67	210.2

1wt% Nanoclay/0.04wt% CTAB/MilliQ/Oil Emulsion

Oil (mL)	Water (mL)	Volume Fraction (Water)	k ($\mu\text{S}/\text{cm}$)
450	0	0.00	0.00
450	10	0.02	0.75
450	20	0.04	2.06
450	30	0.06	2.55
450	40	0.08	2.12
450	50	0.10	2.14
450	60	0.12	2.58
450	70	0.13	2.63
450	80	0.15	2.81
450	90	0.17	2.79
450	100	0.18	3.36
450	110	0.20	2.66
450	120	0.21	3.52
450	130	0.22	3.98
450	140	0.24	4.18
450	150	0.25	3.75
450	160	0.26	5.91
450	170	0.27	5.53
450	180	0.29	5.60
450	190	0.30	6.51
450	200	0.31	7.34
450	210	0.32	8.59
450	220	0.33	6.33
450	230	0.34	7.82
450	240	0.35	8.8
450	250	0.36	10.21
450	260	0.37	9.11
450	270	0.38	12.11
450	280	0.38	8.42
450	290	0.39	10.3
450	300	0.40	99.1
450	310	0.41	105.4
450	330	0.42	115.4
450	350	0.44	121.7
450	370	0.45	127.8

450	420	0.48	133.6
450	470	0.51	147.7
450	520	0.54	159.9
450	570	0.56	171.3
450	620	0.58	181.8
450	670	0.60	190.7
450	720	0.62	199.5
450	770	0.63	206.3
450	820	0.65	214.43
450	870	0.66	222.23

1wt% Nanoclay/0.05wt% CTAB/MilliQ/Oil Emulsion

Oil (mL)	Water (mL)	Volume Fraction (Water)	k ($\mu\text{S}/\text{cm}$)
450	0	0.00	0.00
450	10	0.02	0.00
450	20	0.04	0.44
450	30	0.06	0.71
450	40	0.08	0.85
450	50	0.10	1.22
450	60	0.12	1.35
450	70	0.13	1.85
450	80	0.15	2.73
450	90	0.17	3.00
450	100	0.18	3.84
450	110	0.20	3.67
450	120	0.21	4.48
450	130	0.22	5.48
450	140	0.24	5.84
450	150	0.25	5.71
450	160	0.26	5.19
450	170	0.27	6.19
450	180	0.29	5.80
450	190	0.30	5.38
450	200	0.31	8.18
450	210	0.32	4.81
450	220	0.33	8.37

450	230	0.34	5.33
450	240	0.35	8.82
450	250	0.36	11.36
450	260	0.37	10.12
450	270	0.38	9.27
450	280	0.38	11.16
450	290	0.39	12.68
450	300	0.40	7.87
450	310	0.41	9.67
450	320	0.42	106.8
450	330	0.42	119.4
450	350	0.44	128.8
450	370	0.45	136.1
450	420	0.48	149.8
450	470	0.51	162.9
450	520	0.54	174.6
450	570	0.56	185.9
450	620	0.58	196.9
450	670	0.60	205.7
450	720	0.62	214.4
450	770	0.63	222.9
450	820	0.65	230.8
450	870	0.66	238
450	920	0.67	244.6

1wt% Nanoclay/0.1wt% CTAB/MilliQ/Oil Emulsion

Oil (mL)	Water (mL)	Volume Fraction (Water)	k ($\mu\text{S}/\text{cm}$)
450	0	0.00	0.00
450	10	0.02	0.89
450	20	0.04	1.27
450	30	0.06	1.84
450	40	0.08	3.90
450	50	0.10	4.60
450	60	0.12	5.84
450	70	0.13	4.51
450	80	0.15	4.58

450	90	0.17	6.11
450	100	0.18	5.84
450	110	0.20	11.56
450	120	0.21	12.03
450	130	0.22	13.30
450	140	0.24	11.03
450	150	0.25	11.40
450	160	0.26	12.87
450	170	0.27	15.11
450	180	0.29	13.60
450	190	0.30	13.28
450	200	0.31	15.32
450	210	0.32	18.76
450	220	0.33	14.89
450	230	0.34	20.13
450	240	0.35	16.48
450	250	0.36	23.1
450	260	0.37	29.13
450	270	0.38	38.2
450	280	0.38	42.2
450	290	0.39	58.5
450	300	0.40	62.4
450	310	0.41	64.4
450	320	0.42	69.3
450	330	0.42	178.4
450	340	0.43	185.1
450	350	0.44	192.3
450	370	0.45	203.9
450	390	0.46	213.5
450	410	0.48	222
450	460	0.51	242.1
450	510	0.53	261.4
450	560	0.55	278.2
450	610	0.58	293.7
450	660	0.59	308
450	710	0.61	320
450	760	0.63	333
450	810	0.64	345
450	860	0.66	354